This is to certify that the

dissertation entitled

QUANTIFICATION OF THE LOCOMOTION OF GAITED HORSES

presented by

Molly Christine Nicodemus

has been accepted towards fulfillment
of the requirements for

PHD degree in Animal Science

Christine Stelly
Major professor

Date 11-22-00

QUANTIFICATION OF THE LOCOMOTION OF GAITED HORSES

By

Molly Christine Nicodemus

A DISSERTATION

Submitted to
Michigan State University
in partial fulfillment of the requirements
for the degree of

DOCTOR OF PHILOSOPHY

Department of Animal Science

2000

ABSTRACT

QUANTIFICATION OF THE LOCOMOTION OF GAITED HORSES

By

Molly Christine Nicodemus

The majority of equine kinematic studies have utilized two-dimensional analysis since the horse's limbs have evolved to move primarily in the sagittal plane. However, in horse breeds noted for their limbs moving outside of the sagittal plane, such as the Peruvian Paso, three-dimensional analysis of the joints is necessary.

Experiment I

The Application of Virtual Markers to a Joint Coordinate System for Equine Three-Dimensional Joint Motion. Earlier equine three-dimensional studies applying a joint coordinate system (JCS) encountered errors in the data due to marker displacement and visibility. This study presented a targeting scheme for the carpus and fetlock that met the requirements for developing a JCS while addressing marker problems. With this targeting scheme, an additional set of three-dimensional markers called virtual markers was applied to the forelimb. The earlier problems were minimized, and results compared favorably with previous equine studies of the walk.

Experiment II

Comparison of a Joint Coordinate System versus Multi-Planar Analysis. Multi-planar analysis (MPA) is more commonly used in equine three-dimensional kinematic

analysis, and therefore, this study compared JCS and MPA measurements of the Peruvian Paso walk. The Peruvian Paso "termino", a characteristic outward motion of the forelimbs during the swing phase, gave an ideal opportunity to study out-of-sagittal plane joint motion. MPA was found to be appropriate for flexion/extension when corrections were made for the angle of travel of the horse. The MPA abduction error at the carpus was a function of axial rotation and flexion when the antebrachial segment was vertical to the ground, and adduction/abduction error at the fetlock occurred as a result of metacarpal rotation when the pastern segment was horizontally aligned along the MPA x-axis. Adduction/abduction differences were attributed to the JCS axis moving with the horse's anatomy during locomotion while the MPA axis was static.

Experiment III

Three-Dimensional Motion of the Carpus and Fetlock in the Forelimb of the Missouri Fox Trotter. Three-dimensional kinematic analysis using a JCS was applied to the Missouri Fox Trotter to describe the carpal and fetlock joint motion of the flat walk and fox trot. Although velocity was faster at the fox trot, stride length and ranges of joint motions were similar between gaits. At both gaits, the carpus extended, abducted, and externally rotated during stance and flexed, abducted, and internally rotated during swing. The fetlock demonstrated a single peak of extension during stance and a double peak of flexion during swing with peak external rotation occurring around the first peak of flexion. The velocity, diagonal step duration, stride and stance durations, peak carpal external rotation, and the adduction/abduction joint patterns were different between gaits.

DEDICATION

I dedicate this dissertation to my parents. This dissertation is a product of our shared love for horses. From giving me my first horse to driving across several states to watch me compete at an intercollegiate horse show, your continued support has helped me reach my dreams. All that I have achieved is because of you.

ACKNOWLEDGEMENTS

First, I would like to extend my appreciation for all the patience, support, and guidance from my graduate committee: Dr. Robert Bowker, Dr. Susan Holcombe, and Dr. Brian Nielsen. A special thanks to my advisors, Dr. Hilary Clayton and Dr. Christine Corn. Your willingness to explore new areas and to share in my enthusiasm for my project is greatly appreciated.

I am eternally grateful to Joel Lanovaz for being such a patient and thought provoking teacher, and the graduate students of the McPhail Lab for going out of their way to assist in my project. This research would not have been possible without the Mary Anne McPhail Endowment. I would like to recognize and thank the following students for their help with data collection and analysis: Sara Blechinger, Anna Brookhouse, Niki Cilli, Audrey Fletcher, Jenni Himebaugh, Kristen Slater, Jacki Svetkovich, Katie Swartz, and Diane Ursu. Your excitement for the gaited horse brought new life to my project!

A personal thanks to my office-mates and all of the other graduate students, faculty, and staff of the Animal Science Department for all of their help, support, and friendship through my graduate program.

Finally, I would like to give my deepest thanks to the gaited horse community including the Michigan Fox Trotter Association and Los Grandes Peruvian Paso Horse Club for their support and enthusiasm for my project. A special recognition to the Bulmer, Byerly, Ostrom, and Potter families for the donation of their horses to my project. Your love for your horses was an inspiration for the development of this gaited

horse research program. I hope that you will learn as much from this dissertation as I have learned from you. I dedicate my continued research of the gaited horse to your "four-legged" family members. May this research help in their long and healthy lives.

TABLE OF CONTENTS

Table 5.1.
and fox tro

Table 5.2.
adductor.
Fox Trotte

Table 5.3.
motions of

LIST OF TABLES

Figure
betwee
% of st

Figure

Figure

Figure
and me
coordi

Figure
proxim
joint co

Figure
used as
to estab

Figure
relative

Figure
relative

Figure
angle re

Figure
relative

Figure
angle m

Figure
angle r

Figure
during

Figure
and fro

TABLE OF FIGURES

Figure 4.
GCS for

Figure 4.
stride an
axis with

Figure 4.
stride an
axis with

Figure 4.
GCS for

Figure 5

Figure 5
rotation

Figure 5
rotation

Figure 5
rotation

Figure 5
rotation

Figure 6
that crea

LIST OF APPENDIX A FIGURES

Figure
marke

Figure
of the

Figure
of the

Figure
and th

Figure
axes a

Figur
and th

Figur
and th

Figure
adsor

Figure
adsor

Figure
adsor

Figur
adsor

Figur
adsor

Figur
adsor

Figur
adsor

Figur
adsor

Figur
ads

Figur
ads

Figur
ads

Figur
ads

Figur
ads

Figur
ads

LIST OF APPENDIX C FIGURES

Figure
adduct

Figure
adduct

Figure
adduct

Figure
adduct

Figure
adduct

Figure
adduc

Figure
adduc

Figur
adduc

Figur
adduc

CHAPTER I

GENERAL INTRODUCTION AND OBJECTIVES

Locomotion, the act of moving from one place to another, is achieved by cycling the limbs back and forth in a variety of patterns called gaits. Each gait is defined by the sequence and timing of the movements. Horses are particularly versatile in terms of their gait repertoire. Gait analysis is applied to measure and describe the kinematics, the movements of the body, and the kinetics, the forces creating the movements. Human curiosity concerning the movement of the horse has been evident for many years. The American photographer Eadweard Muybridge made a breakthrough in 1877 when he provided photographic evidence of the existence of a suspension (airborne) phase in the gait of the trotting horse. He went on to take thousands of sequential photographs of people and animals engaged in various activities (Muybridge 1899). Muybridge's recordings were later applied to determine the footfall sequences for normal equine gait (Clayton 1989).

Over the years the technology used for gait analysis has evolved beyond simply documenting footfall sequences to applying gait analysis for clinical and performance evaluation. The mechanics of the walk, trot, canter, and gallop have been extensively studied, but the application of gait analysis to exotic equine gaits, such as the fox trot and paso gaits, is limited. Knowledge of the kinematics of these gaits as measured in the following chapters will assist in the evaluation of a horse's level of training and performance, in the detection of pathological gait, and in assessing the response to surgical or medical therapy.

breeds

steppin

each hi

The w

two fee

mother

walk (I

suspens

classifie

suspens

1957).

charact

quicker

as the sp

risk of m

ground c

joint flex

The decr

term exce

Gaited horses perform a range of gaits that are not performed by the non-gaited breeds. The gaited horse breeds have the ability to replace the trot with various four-beat stepping gaits described as non-walking stepping gaits. A four-beat gait is one in which each limb contacts the ground separately. A stepping gait lacks a period of suspension. The walk is a lateral sequence, stepping gait with a regular four-beat rhythm and at least two feet supporting the body at one time (Speirs 1997). The walk is described as "the mother of gaits" since the non-walking stepping gaits are considered variations of the walk (Imus 1995).

In contrast to the stepping gaits, the trot, pace, canter, and gallop have a suspension phase, a period where the horse is in flight. Gaits with a suspension phase are classified as leaping gaits. In contrast to the stepping gaits, the leaping gaits use the suspension phase to assist in increasing the speed of the gait (Clayton 1994; Leach *et al.* 1987).

Although the non-walking stepping gaits and the walk share similar characteristics, some of the kinematic variables must change in order to produce the quicker four-beat stepping gait. Humans demonstrated an increased range of joint motion as the speed increased at the walk (Mann 1975). This increased joint flexion reduces the risk of musculoskeletal damage by alternating the increased impact forces associated with ground contact at a higher speed (Hershman and Nicholas 1995). Furthermore, increased joint flexion may also act as a mechanism for increasing the inverted pendulum effect. The decrease in limb height due to flexion increases the upward centrifugal force, and in turn, exceeds the downward gravitational force. This ratio is described as the Froude

number. A

ground and

In

fetlock fle

speed of

the distal

flexion.

attribute

applicat

anterior

humans

flexion

studied

distal

when

forelim

stride

gaits. I

characte

underst

adducto

number. As the Froude number exceeds 1.0, the horse limbs are more apt to fly off the ground and increase stride turnover (Gray 1968).

In horses, van Weeren *et al.* (1993) reported an increase in maximal carpal and fetlock flexion and hind limb translational motion as Standardbred trotters increase the speed of the trot from 6 to 9 m/s. In humans, increased flexion is coupled with rotation of the distal limb joints. Maximal internal rotation of the knee occurs at 15° to 45° of flexion. Maximal external rotation occurs at 60° to 90° of flexion. Internal rotation is attributed to the application of an anterior force and external rotation results from the application of a posterior force. The amount of rotational force and the stability of the anterior and posterior cruciate ligaments determine the amount of coupled rotation in humans (Mann 1980).

Without the benefit of a suspension phase, the gaited horse may utilize increased flexion and coupled rotation to produce a faster four-beat gait though this has not been studied scientifically. Although axial rotation and abduction/adduction are limited in the distal joints of the equine limb, a noted exception is the "termino" motion that occurs when the Peruvian Paso performs the paso gaits. Termino is characterized by the forelimbs of the horse swinging outward from the shoulder during the swing phase of the stride (Harris 1993). This movement is a desirable characteristic of the Peruvian Paso's gaits, but is regarded as a defect in other breeds. Analysis of these unique gait characteristics, as described in the following chapters, will assist in the further understanding of the mechanisms of the non-walking stepping gaits.

These unique characteristics of the gaited horse, such as the additional adduction/abduction and axial rotation, create difficulties for measuring joint motion

using tradi

either two-

axial rotat

multi-plan

(Soutas-L

standard

using a p

these tec

flexion a

extreme

were fu

using traditional kinematic analysis techniques. Axial rotation can not be measured using either two-dimensional analysis or multi-planar analysis. Furthermore, the effects of axial rotation and flexion on frontal plane measurements of human joint motion using multi-planar analysis have found distortion in the adduction/abduction measurements (Soutas-Little *et al.* 1987). Therefore, in the studies described in this dissertation, standard gait analysis techniques were adapted to measure three-dimensional analysis using a joint coordinate system that produced acceptable accuracy. The availability of these techniques facilitated measurement of such gait characteristics as coupling of flexion and axial rotation. The termino motion of the Peruvian Paso was studied as an extreme example of motion occurring outside of the sagittal plane. These techniques were further applied to the gaits of the Missouri Fox Trotter.

The objectiv

1) To develo

repeatable p

2. To comp

system vers

3) To meas

and for tro

The objectives of this study were:

1) To develop a virtual marker methodology that creates an anatomically meaningful and repeatable joint coordinate system.

2) To compare the three-dimensional joint motion measured using a joint coordinate system versus multi-planar analysis using the Peruvian Paso.

3) To measure the three-dimensional carpal and fetlock joint motion during the flat walk and fox trot of the Missouri Fox Trotter.

Hypothesis:

The first chapter of this dissertation describes the development of a reliable and repeatable methodology for the establishment of a joint coordinate system for equine three-dimensional motion analysis. In the later chapters, the methodology was applied to test the following hypotheses:

1) The measured values of abduction/adduction and flexion/extension of the carpal and fetlock joints are different when measured with an anatomically-based joint coordinate system versus multi-planar analysis.

2) The three-dimensional joint motion measured for the flat walk and fox trot demonstrates characteristics unique to each gait and different from the kinematics measured in earlier studies for the walk and trot.

History

T

paintings

performa

stepping

stepping

carvings

1995). F

discover

pattern w

a running

the East

D

flourishe

that perfo

that perfo

suspensio

Chaucer's

Wife of B

CHAPTER II

GENERAL REVIEW OF THE LITERATURE

History of the Gaited Horse

The 55 million-year history of the horse has been documented through drawings, paintings, sculptures, and stories. Unlike modern day art that demonstrates the horse performing the trot, earlier artistic accounts show the horse performing a non-walking stepping gait. Evidence for the existence of gaited horses that performed a four-beat stepping gait other than the walk can be traced as far back as the Ice Age. Ancient ice carvings discovered in France depict a lateral stepping gait similar to the amble (Imus 1995). Hipparion equid fossil footprints, dating from 3.5 million years ago, were discovered in 1979 in Tanzania under volcanic acid. Comparisons of the fossil footfall pattern with contemporary gait patterns determined the Hipparion equid was performing a running walk (Budiansky 1997). The flying horse of Kansu, a bronze horse statue of the Eastern Han Dynasty (25 AD-220 AD), displays the racking gait (Ensminger 1977).

During the middle ages in Western Europe, the Palfrey, an ambling saddle horse, flourished among the royalty and society people. Wealthy individuals bred for horses that performed a smooth, easy riding gait. The Palfrey was a very refined, elegant horse that performed a fast, ground covering walking gait that lacked the jarring motion of the suspension phase while still maintaining speeds comparable to the trot and pace. Chaucer's *Canterbury Tales* makes references to the Palfrey when he writes about the Wife of Bath, "Upon an Amblere easily she sat" (Imus 1995). However, the longer

distances tr

led to the n

The

were poor

the same t

conquering

horses. T

Conquista

Indians.

and the p

along, bu

T

plantatio

since w

rows of

(Linus 1

current

1999),

taking

looking

distances traveled by coaches called for horses with greater speed and strength and this led to the rise of the trotting horse (Imus 1995).

The English began to settle the Americas in the 17th century. Most of the settlers were poor so the horses they brought over the oceans were grade trotting horses. Around the same time as the English settlers arrived, the Spanish military were actively conquering America as they rode north through Mexico on their majestic Spanish gaited horses. The Conquistadors traveled through America battling the Native Indians. If the Conquistadors lost a battle, their horses were left to run wild or were captured by the Indians. Gradually, these gaited horses were bred with the grade horses of the Indians and the poor English settlers. Some of the genetic traits of the gaited horses were passed along, but over time these gaits were seen less frequently (Imus 1995).

The popularity of the gaited horse returned to America with the growth of plantation farming. Plantation owners bred horses that could perform a ground-covering stride while moving at a smooth, comfortable gait. The horses were ridden between the rows of crops as the owners observed the conditions of the crops and work of the slaves (Imus 1995). The further rise in the popularity of the gaited horse is attributed to the current growth in "baby boomers," the population that is aged fifty and older (Pascoe 1999). As this population ages while maintaining financial security, older adults are taking up horseback riding. Unlike the younger riders, this older adult population is looking for a smooth, easy riding horse (Imus 1995).

Defining the Gaited Horse

What defines a horse as being gaited? A gaited horse is one that has the ability to perform non-walking stepping gaits that can reach speeds equivalent to the trot or the pace (Imus 1995). The trot is a two-beat gait in which a diagonal pair of legs move synchronously. Diagonal stance is followed by a suspension (airborne) phase, a period when all four hooves are off the ground. The pace is similar to the trot, but instead of the diagonal limb pairs moving synchronously, movements of the lateral limb pairs are synchronized. Due to the presence of suspension phases, the trot and pace are defined as leaping gaits. This is in contrast to the stepping gaits that lack a period of suspension.

The most common stepping gait is the walk, which is performed by both gaited and non-gaited horses. The walk is described as "the mother of gaits" since the other four-beat gaits are considered variations of the walk (Imus 1995). The most obvious difference between the walk and the non-walking stepping gaits is the speed of progression, which is faster in the non-walking stepping gaits. However, stylistic differences between breeds (e.g. animation and head nod) play a role in defining the gaits, in addition to the temporal characteristics.

The footfall sequence of the walk is left hind limb (LH)- left forelimb (LF)- right hind limb (RH)- right forelimb (RF) and the footfalls occur in a regular four-beat rhythm. Regularity is defined kinematically as the footfalls being spaced evenly in time so that limb motions are 90° out of phase and the duty factor of each limb is 25% (Hildebrand 1978). The regularity of the footfalls of the gait classifies the walk as a square gait, as opposed to a gait that shows lateral or diagonal couplets.

A symmetrical gait is one in which the left and right sides move 180° out of phase (Hildebrand 1965) so that the interval between the left footfall and right footfall is equal to the interval between the right footfall and left footfall in both the fore and hind limb pairs (Hildebrand 1978). The walk, trot, pace, fox trot, rack, slow gait, paso gaits, and running walk are all symmetrical gaits. The timing and sequence of the limb movements of symmetrical gaits can be described using two kinematic variables: the hind limb stance duration and the lateral advanced placement, both expressed as a percentage of stride duration (Hildebrand 1965).

The non-walking stepping gaits can be classified according to the rhythm of the footfalls. The rhythm may be regular, irregular with lateral couplets, or irregular with diagonal couplets. The rhythm affects the duration of the limb support phases of the stride. Horses performing a regular (or square) four-beat gait spend equal amounts of time in diagonal and lateral support phases (Imus 1995). Besides the walk, other square gaits include the flat walk, rack, tolt, flying pace, paso llano, and paso largo.

In a true lateral gait, movements of the lateral pairs of limbs are synchronized. The pace is usually described as a lateral gait in which the lateral support phase is followed by a period of suspension. At racing speed, however, pacers have been shown to dissociate the movements of the lateral limb pairs so that contact of the hind limb precedes that of the lateral forelimb by 3-10% of the stride duration. Thus, ground contact of the lateral limb pair occurs as a lateral couplet (Wilson *et al.* 1988). This dissociation of the pacing lateral limb pairs so that the hind limb makes contact before the ipsilateral forelimb creates a lateral footfall sequence similar to the walk and non-walking stepping gaits. A lateral stepping gait also demonstrates an irregular rhythm with lateral

couplets bu

occurs whe

of 10-20%

include the

Ilmus 1995

the stride a

In a

synchrono

by the dis

couplets.

15% of t

hind lim

foorfall

diagona

ground

before

associ

racing

creati

groun

displa

latera

couplets but differs from the pace by not having a period of suspension. A lateral couplet occurs when the hind footfall is followed by the ipsilateral fore footfall after an interval of 10-20% of the stride (Hildebrand 1965). Four-beat stepping gaits with lateral couplets include the broken pace, slow gait, amble, running walk, sobreandado, and single foot (Imus 1995). During these gaits the hind footfall precedes the fore footfall by 10-15% of the stride duration (Hildebrand 1965).

In a true diagonal gait, movements of the diagonal limb pairs occur synchronously. Similar to the modified lateral gait, the modified diagonal gait is created by the dissociation of diagonal limb pairs, resulting in an irregular rhythm with diagonal couplets. Diagonal couplets occur when the diagonal limb movements dissociate by 10-15% of the stride duration with the forelimb making contact just prior to the diagonal hind limb (Hildebrand 1978).

The trot is described as a diagonal gait, though even at slow speeds the diagonal footfalls may occur slightly asynchronously (Clayton 1994; Holstrom *et al.* 1994). The diagonal advanced placement is defined as being positive when the hind hoof contacts the ground before the diagonal fore hoof and negative when the fore hoof contacts the ground before the diagonal hind hoof. A positive diagonal advanced placement has been associated with good quality of the trot in warmblood horses (Holstrom *et al.* 1994). At racing speeds the trot demonstrates a marked dissociation of the diagonal limb pairs creating diagonal couplets (Drevemo *et al.* 1980) with the fore hoof contacting the ground before the diagonal hind hoof, which is a negative diagonal advanced displacement. This dissociation of the diagonal limb pair at the racing trot creates a lateral footfall sequence (LH, LF, RH, RF) that resembles the walk and the non-walking

stepping gaits. The fox trot is an example of a four-beat stepping gait with diagonal couplets (Imus 1995).

Changing the Speed

To increase speed, horses use transitions between gaits combined with changes of stride length and stride duration within each gait. Leach *et al.* (1987) studied the changes in stride length and stride duration in relation to speed. In general, an increase in speed was associated with reducing stride duration by increasing stride length. Shortening the stride duration is achieved as a result of reductions in stance duration and overlap and an increase in the duration of the suspension phase. The suspension phase is a large contributor to maintaining and increasing the speed of the gait at the trot (Clayton 1998), canter (Clayton 1994), and gallop (Leach *et al.* 1987). The non-walking stepping gaits, which do not show a suspension phase, are performed at speeds equivalent to the trot while maintaining a stepping sequence (Imus 1995). The mechanisms by which this is achieved have not been investigated in detail.

The non-gaited horse initially increases speed by walking faster, which is achieved by a combination of lengthening the stride and increasing the stride rate. At a certain walking speed there is a transition to the trot. In ponies, the walk-trot transition occurs at a speed range of 1.5 to 2.2 m/s (Hoyt and Taylor 1981). Gait transitions may occur as a means of improving energetic and metabolic efficiency (Hoyt and Taylor 1981) or as a means of changing the forces on the limbs (Taylor 1985; Niki *et al.* 1984). Vertical ground reaction forces increase at the walk-trot transition and decrease at the trot-canter transition. This decrease in forces is attributed to changes in limb movement

patterns (Rubin and Lanyon 1982). The transition from canter to gallop occurs more gradually as the diagonal limb pair (leading hind and trailing fore) become more dissociated with the hind limb making contact prior to the diagonal forelimb. The hind limb propulsive forces then act to lift the forelimbs, thus reducing forelimb forces (Pratt 1983).

The gallop usually has one suspension phase in each stride. The speed of the gallop increases in correspondence to stride length, but anatomically the horse reaches a maximum stride length (Hiraga *et al.* 1994). Velocity is increased further by cycling the limbs more rapidly to increase the stride rate. However, at maximum stride length and stride rate, some horses add another suspension phase to the gallop sequence. This occurs between lift off of the leading hind limb and contact of the trailing forelimb. A few horses even add a very short third suspension phase between the stance phases of the two forelimbs (Deuel *et al.* 1986; Rooney 1998).

The gaited horse does not make a distinct transition from the walk to a non-walking stepping gait. Instead, there is a gradual adjustment of the timing of the limb movements. Hildebrand (1965) describes the gaits of the gaited horse as a continuum that does not show distinct boundaries between the non-walking stepping gaits. Therefore, the arbitrary boundaries of non-walking stepping gaits form a gait continuum in which breed and style contribute to the differentiation between gaits.

Gaited horses continue to perform stepping gaits at speeds equivalent to those performed at the trot of the non-gaited horses (Hildebrand 1965). The Tennessee Walking horse, for example, maintains the footfall pattern of the walk at speeds up to 20 miles per hour (Harris 1993). The Missouri Fox Trotter can travel long distances at a relatively fast

fox trot without tiring. This apparent energetic efficiency is why the U.S. Forest Service selected these horses for use by their park rangers (Ridings and Bradbury 1976). The lack of a transition to the trot in gaited horses may indicate that the non-walking stepping gaits are more energetically efficient or that they create lower forces on the limbs.

The mechanics utilized for increasing the speed of the non-walking stepping gaits involves adjusting the stride length and stride frequency. Slight adjustments in the footfall timing of the various non-walking stepping gaits have also been recognized as a factor for influencing the speed of the gait (Imus 1995).

Understanding the Gaited Horse

So why is it important to understand the mechanics of the non-walking stepping gaits and the similarities and differences between these gaits and other equine gaits? The answer to this question relates both to understanding and judging performance and to the detection of pathological gaits. For lameness evaluations, the trot is the gait of choice due to its rhythmic, symmetric nature, combined with the fact that the forces on the limbs are higher than during the walk. Clinicians observe the symmetry of the gait from left to right, the motion of the head, withers and croup, and the rhythmic sound of the two-beat gait (Pasquini *et al.* 1995; Adams 1975). Most veterinarians have a very limited knowledge of the mechanics of the non-walking stepping gaits. Judging the soundness of the non-walking stepping gaits according to the criteria used at the walk or trot is not appropriate and may limit the detection of lameness problems specific to the breed.

Even though the walk and non-walking stepping gaits share similar gait characteristics, the horse performing a non-walking stepping gait protracts and retracts

the limbs more rapidly so the footfalls occur at a quicker rate than the walk. Therefore, the horse must change the temporal variables in order to produce the quicker four-beat gait. The head, neck and croup movements also differ between the walk and the non-walking stepping gaits and these differences cause confusion between normal and pathological gaits. Clinicians rely heavily on the head nodding to indicate forelimb lameness during lameness evaluations (Speirs 1997). However, a sound gaited horse performing the fox trot or the running walk will naturally display a head nod (Imus 1995).

Biomechanical Analysis of Gaited Horses

Ground Reaction Force Analysis. Kinetic analysis describes the forces that cause movement. In the past several years equine kinetic analysis has focused on the collection of force plate data to describe the ground reaction force (GRF) pattern of sound horses and the effects of lameness on gait symmetry.

Each gait has a typical force profile. In the walk, the vertical GRF is higher in the forelimbs than the hind limbs, which reflects the distribution of the body weight. At a constant walking velocity, the fore and hind limbs have approximately equal braking and propulsive impulses, changing from braking to propulsion at 50% of stance in the forelimb and 45% in the hind limb. During walking vertical force curves for both the fore and hind limbs demonstrate two peaks: the first is higher in the forelimbs and the second is higher in the hind limbs (Merkens *et al.* 1985). The two peaks become more distinct at higher walking velocities (Khumsap *et al.* in press).

During the trot, the vertical GRF curve has a single peak, the amplitude of which is higher in the forelimb than the hind limb. Both the fore and hind limbs have higher vertical forces at the trot than the walk. As for the longitudinal forces at the trot, the braking impulse is larger in the forelimbs, while the hind limbs provide more propulsion (Merkens *et al.* 1993).

In the canter, the trailing forelimb has the highest vertical GRF with a magnitude of 1.5 times the horse's body weight. The trailing fore and trailing hind limbs contribute more to propulsion than the leading limbs. The diagonal limb pair (leading hind limb and trailing fore limb) provide more braking, while the leading forelimb has the highest braking forces (Merkens *et al.* 1993).

Two-Dimensional Kinematic Analysis. Kinematic analysis provides a graphical record of the movements of the horse's limbs during locomotion. Hildebrand (1965) originally took on the role of objectively classifying the spectrum of gaits performed by various species including horses. The temporal characteristics of the symmetrical gaits were displayed on a graph in which the x-axis represented the percent of stride duration that each hind foot was on the ground and the y-axis represented percent of stride duration by which the fore foot footfall followed the ipsilateral hind footfall. Fourty-four possible limb support sequences of various symmetrical gaits made up the superimposed grid system from which he proposed a scheme of names for equine symmetrical gaits (Figure 2.1).

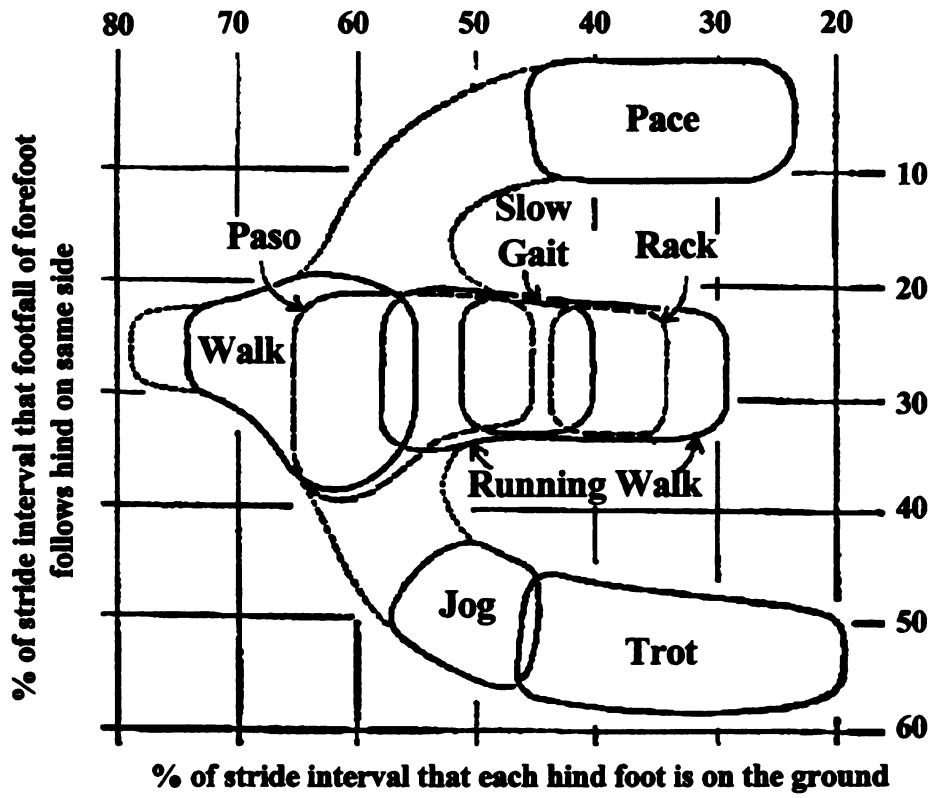

Figure 2.1. Hildebrand's graph (1965) demonstrating the distinction between various gaits according to hind limb stance duration and % of stride interval that footfall of forefoot follows hind on same side.

Hildebrand's graph was based on data describing the symmetrical gaits of sixty-eight horses performing the pace, trot, walk, paso gait, slow gait, rack, running walk, and variations of these basic symmetrical gaits (Figure 2.1). On the vertical axis, the paso gait, rack, running walk, and slow gait fell within the same region as the walk and mid-way between the regions occupied by the pace and the trot. On the horizontal axis, the walk and the paso gait have overlapping areas on the graph, but with the walk having a relatively longer hind stance duration than the paso gaits.

Both the trot and pace have a relatively large range of percentage of stride that each hind limb is on the ground. This range is attributed to the large speed variation within these gaits; at slower speeds the hind limbs are on the ground longer than at faster speeds. The stepping gaits represent a wide range of percentages of stride that each hind limb is on the ground with the running walk having the greatest range. Along the horizontal axis, areas of overlap between the different stepping gaits represent the fact that these gaits form a continuum rather than having distinct boundaries between them. The interval by which the forelimb follows the hind limb on the same side falls within the range of 20-40% of the stride for the stepping gaits with the walk having the greatest range. The stepping gaits lie between the trot at 45-60% and the pace at 0-10% dissociation.

Through graphing the various symmetrical gaits based on temporal measurements, Hildebrand developed a classification scheme based on these temporal gait characteristics. He concluded that the boundaries between the gaits are not distinct. Instead the gaits are more like a continuum, with different gaits being arbitrarily separated by styles within the breed (Hildebrand 1965). These breed styles play a major role in the distinction between the symmetrical gaits. The following are examples of stylistic differences between breeds: the head nod and an extreme overstriding (the hind limb showing a large amount of over-tracking relative to the forelimb on the same side) separates the running walk from the rack; the termino (lateral motion of the forelimb during the swing phase) separates the gait of the Peruvian Paso from the Paso Fino (Hildebrand 1965).

T

implies th

side by 10

bipedal su

horse swi

support an

running w

rhythmic

may swi

(1993) n

Walkon

time sp

Tenne

while

follow

diagr

leng

angl

The running walk is described as a stepping gait with lateral couplets, which implies that ground contact of the hind limb precedes that of the forelimb on the same side by 10-20% of the stride (Hildebrand 1965) and the primary support phase is lateral bipedal support. If the percentage of lateral support becomes too great, however, the horse switches to a pace. On the other hand, some horses spend less time in lateral support and slightly more time in a diagonal support while still technically performing a running walk by maintaining other gait characteristics such as hind limb overreach and a rhythmic head nod. If the percentage of diagonal support becomes too great, some horses may switch to a fox trot, which is not as common in a purebred Tennessee Walker. Slade (1993) measured sixty-four conformational traits in the Tennessee Walker, Icelandic, and Walkony horse, then made correlations between the measured traits and the percentage of time spent in lateral and diagonal support sequences during the running walk. The Tennessee Walker and Icelandic horses were found to have a more lateral running walk while the Walkony horses had a more diagonal running walk (Slade 1993). The following eight conformational characteristics were related to the degree of lateral or diagonal support of the running walk: rear cannon length, pelvis length, hip to hock length, neck length, stifle joint angle, hip joint angle, shoulder joint angle, and hock joint angle.

Just as kinematic analysis assisted in the further understanding of the running walk and the gait characteristics unique to different breeds performing these gaits, the mechanics of the fox trot have been explored using high speed cinematography. Clayton and Bradbury (1995) measured the temporal characteristics, including footfall and limb support sequences and classified the fox trot as a fast, lateral sequence, four-beat gait

with diagonal couplets. The support sequences consisted of 60.6% of the stride duration spent in diagonal support, 21.7% in lateral support, and 17.8% in tripedal support.

Along with describing the normal timing of the stepping gaits, kinematic analysis can detect defects in the gait. Clayton (1995) measured the stride kinematics of the collected, medium, and extended walks. Only one horse out of the six highly-trained dressage horses had a regular four-beat rhythm during all of these types of walk. Four of the horses displayed lateral couplets with irregularities evident more often in the medium and extended walks. Temporal measurements of the half pirouette at the walk indicated that horses performing this movement displayed irregularities in the rhythm. These irregularities were associated with a shorter interval between footfalls of the outside forelimb and inside hind limb and a longer interval between footfalls of the inside hind limb and inside forelimb. The absence of forward motion in the half pirouette causes instability in the horse's balance, and the horse compensates for this by using a longer tripedal support and substituting a period of quadripedal support for bipedal support (Hodson *et al.* 1998).

Three-Dimensional Kinematic Analysis. Previous studies of stepping gaits, along with the majority of other equine kinematic research, has been limited to two-dimensional analysis in the sagittal plane, which ignores movements in the frontal and transverse planes. This is not an unreasonable simplification with regards to the normal motion patterns of the equine limbs. Over millions of years, the horse's limbs have evolved in such a way that the joints distal to the shoulder and the hip move primarily in the sagittal plane, which is energetically efficient. However, small out-of-plane movements also occur. Herring *et al.* (1992) described fetlock joint motion in sagittal and

frontal planes. By making comparisons between the walk, trot, and canter, it was determined that the amount of motion in the frontal plane was velocity-dependent.

Although motion outside of the sagittal plane is restricted anatomically, even simple visual observations can detect out of plane motion in the gaited horse. The termino of the Peruvian Paso is a good example of this motion. The forelimbs show an outward rotation during the swing phase that starts at the shoulders and moves down through the distal joints. Judges score the quality of the termino and during a horse show, the Peruvian Paso is evaluated from different angles to determine the degree of termino as the horse performs the paso gaits (Imus 1995).

Three-dimensional kinematic analysis has been applied to various aspects of human movement through the establishment of specialized laboratories in which patients are evaluated for clinical diagnosis and assessment of treatment using three-dimensional kinematic analysis. In this analysis technique, certain prerequisites need to be followed including the definition of a coordinate system in three-dimensional space. The purpose of a coordinate system is to define the relative position between two bodies. During kinematic analysis, a calibration frame is used to orient the movements in relation to the space in which they are occurring, which is described as a global coordinate system (GCS).

Grood and Suntay (1983) were the first to introduce an anatomically-based coordinate system for the description of three-dimensional rotational and translational motion of the knee joint. Based on it's anatomical definition, this is described as a joint coordinate system (JCS). Subsequently, Soutas-Little *et al.* (1987) developed a JCS to describe the motion of the ankle joint.

With regard to equine three-dimensional motion analysis, Fredricson and Drevemo (1971) described the three-dimensional movements of the hoof using markers attached to a glass-fiber-molded shoe. Their methodology applied aerospace technology to describe the hoof movements within a GCS, which was related to the local environment rather than the horse's anatomy. Three-dimensional analysis using a GCS has also been applied to describe quantitative variables associated with equine carpal lameness (Peloso *et al.* 1993).

The results of these studies were described in terms of three, mutually perpendicular, anatomical planes: the sagittal, transverse and frontal planes. A drawback to this type of multi-planar analysis is that it cannot measure internal/external rotational motion, and therefore, we can not determine the relationship between internal/external rotation and abduction/adduction or flexion/extension of the joint. Furthermore, since each plane is measured separately, the relationship between flexion/extension and adduction/abduction is speculative. The true relationship between these joint motions can be evaluated only if all of these motions are measured concurrently within the same anatomically-based coordinate system. A JCS is an anatomical coordinate system based upon the limb segments comprising the joint. The joint motions are tracked and calculated within a JCS, which allows for the measurement of internal/external rotation and the determination of the relationship between joint motions.

Heleski (1991) described a methodology for measuring three-dimensional carpal and fetlock joint motions using a JCS. The shortcoming to the methodology was associated with marker placement restrictions. Three-dimensional analysis requires the use of three, non-collinear markers on each limb segment. Two of these markers are

aligned with an anatomical axis of the segment and the third is perpendicular to that axis. This requirement limits the locations that can be used for placement of the markers and does not allow the selection of marker sites that fulfill other criteria, such as minimization of skin displacement relative to underlying bony landmarks. To date the primary limitation to equine three-dimensional motion analysis using a JCS has been the lack of a targeting scheme for three-dimensional analysis of equine joint motion that overcomes the limitations described above without disturbing the natural movement of the horse.

Equine Net Joint Moments and Joint Powers. Kinematic analysis describes the movements without considering the forces that cause the movement. Kinetic analysis measures these forces and the resulting mechanical energetics (Winter 1990). During locomotion, continuously changing internal and external forces during the gait are characterized by joint moments and energy patterns throughout the stride (Winter and Robertson 1978). Although the kinematics may be identical, the patterns of energy production across joints can be very different (Winter 1990). Understanding the synergistic patterns of these forces gives a more complete picture of the mechanics of the gait.

The net joint moment indicates the torque produced across a joint by the muscles, tendons, and ligaments, and is calculated by combining videographic and force data with morphometric measurements using a link-segment model and an inverse dynamic solution (Clayton *et al.* 1998). Certain assumptions are made concerning the link segment model: 1) the mass of each segment is located at its center of mass, 2) the center of mass remains fixed, 3) joints are considered to be hinges, 4) each segment's mass moment of inertia about the center of mass is constant, and 5) each segment's length

rem

exa

infe

mo

mo

ad

jou

pol

199

pow

m

are

The

pat

ou

hig

you

nee

dis

wa

pa

remains constant. The forces acting on a link segment model include gravitational forces, external forces, and muscle and ligament forces. This model requires the following information for the calculation of net joint moments: segment positions and joint angular movements, ground reaction forces and the center of pressure, and segment morphometric and inertial data (Winter 1990)

Joint power is a measure of the mechanical work done across the joint and is calculated as the product of the net joint moment and the joint angular velocity. Positive joint power occurs when the net joint moment and joint angular velocity have the same polarity, and negative power occurs when they have opposite polarities (Colborne *et al.* 1997). Positive joint power indicates that power is being generated and negative joint power indicates power absorption (Colborne *et al.* 1997). During power generation, the muscles are performing a concentric contraction, and in power absorption, the muscles are performing an eccentric contraction (Colborne *et al.* 1997).

Most of the studies on joint moments and powers have been in human subjects. The findings have helped to differentiate sub-samples of the population, to detect gait pathologies, to make recommendations for treatment of gait pathologies, and to assess the outcome of such treatments. For example, Chao *et al.* (1983) found older adults had a higher knee flexion moment and a higher planter flexion moment in the ankle than younger adults. The same age differences may be true for the horse, and if so, age would need to be a consideration when selecting test subjects. Davids *et al.* (1996) found differences in the net joint moments of the hip, knee and ankle between children with and without cerebral palsy. Contrary to the normal walking pattern, children with cerebral palsy use the hip rather than the ankle as the primary power generator and the ankle

rather than the knee for power absorption. This demonstrates how adaptable the biomechanics of the gait are to changes in the body. Analysis of gait adaptations due to disease should be evaluated for the horse.

Analysis of net joint moments and joint powers may give insight into how the gaited horse maintains a stepping gait at faster speeds when non-gaited horses are performing a leaping gait. In human subjects, the patterns of energy transfer have been compared for the slow and fast walk. Peak power at push-off in the plantar flexor muscles increased from 180 W (Watts) at a slow walk to 490 W at a fast walk. Energy absorption during the initial deceleration ranged from 30 W at the slow walk to 125 W at the fast walk (Winter and Robertson 1978).

In horses, net joint moments have been described during the stance phase at the walk (Colborne *et al.* 1997; Colborne *et al.* 1998; Clayton *et al.* 2000a), the stance phase at the trot (Clayton *et al.* 1998) and the swing phase at the trot (Lanovaz *et al.* 1999). Net joint moments and joint powers have been measured to assist in understanding the effects of musculoskeletal pathologies and therapeutic shoeing. The effects of superficial digital flexor tendinitis on forelimb net joint moments and joint powers during the stance phase at the trot have been described (Clayton *et al.* 2000b) and the response to treatment with a heel wedge has been assessed (Clayton *et al.* 2000c). In another study, it was shown that horses compensated for the weight of shoes by increased energy generation on the flexor aspect of the elbow during early stance to overcome the additional inertia due to the weight of the shoes, and increased energy generation on the extensor aspect of the elbow in late stance to overcome the extra momentum as the limb was swinging forward (Singleton *et al.* 2000).

shown t

speed in

sites of

further

nature v

disturb

further

steppin

Conclu

biome

signifi

date h

interr

to the

This

such

can

for

will

Differences in energetic patterns across the joints at different walking speeds have shown that the hip joint is the primary site of increased energy generation as walking speed increases, assisted by the tarsus (Khumsap *et al.* 2000). Investigation of how the sites of power generation differ between the walk and the faster stepping gaits would give further insight into the mechanics of the non-walking stepping gait. Comparisons of this nature will elucidate the mechanism for increasing the speed of the gait without disturbing the footfall patterns. The information presented in this dissertation can be further applied for analysis of net joint moments and joint powers of the non-walking stepping gaits.

Conclusions

Over the years, great advances have been made in the study of equine biomechanics. Kinematic and kinetic studies of the walk and trot are providing significant insights into the mechanics these gaits. However, most of the evaluation to date have been two-dimensional analysis, which ignores adduction/abduction and internal/external rotation. Furthermore, the application of kinematic and kinetic analysis to the gaits of the gaited horse have been limited to analysis of the temporal variables. This limited analysis may be due to the unique gait characteristics that they exhibited such as out-of-sagittal plane motion and the lack of kinematic analysis techniques that can accurately measure these characteristics. The following studies provide a technique for measuring these unique gait characteristics and preliminary analysis of these gaits that will serve as a foundation for further investigation.

EXPE

CO

Summa

of a ho

pathol

establ

syste

devel

carpa

Intr

CHAPTER III

EXPERIMENT I: THE APPLICATION OF VIRTUAL MARKERS TO A JOINT COORDINATE SYSTEM FOR EQUINE THREE-DIMENSIONAL JOINT MOTION

Summary

Joint motions that occur in planes other than the sagittal plane affect the esthetics of a horse's movement and may change in response to certain types of locomotor pathology. Measurement of these motions has been limited due to the complexity of establishing a targeting scheme that creates a meaningful and repeatable joint coordinate system. This study presents a targeting scheme that meets the requirements for developing a joint coordinate system. The targeting scheme was applied to the equine carpal and fetlock joints, and the results compare favorably with previous equine studies.

Introduction

Although human kinematic research has utilized three-dimensional analysis in many applications (Grood and Suntay 1983; Soutas-Little *et al.* 1987; Cappozzo 1991), equine kinematic research has primarily focused upon two-dimensional motion analysis (Back *et al.* 1996; Galisteo *et al.* 1996; Hodson *et al.* 2000). Since the anatomy of the horse and human are so different, adaptation of the methodology for measuring three-dimensional motion in humans for use in horses is necessary. The objective of this study is to develop a methodology for measuring equine three-dimensional joint motion accurately and consistently. This study includes the theoretical and practical

considerations involved in using virtual marker methodology and the establishment of a joint coordinate system for measuring three-dimensional motion at the equine carpal and fetlock joints.

The Theory of Three-Dimensional Motion Analysis

Joint Coordinate System. Three-dimensional joint motions can be described by six independent coordinates comprised of three translations and three rotations. The majority of joint motion studies have measured the relative rotational motion between the two segments using Euler angles (Grood and Suntay 1983). The Cardanic/Eulerian rotation sequences describe three-dimensional joint motion through an ordered sequence of rotations about the axes of a selected, Cartesian coordinate system. The limitation to the Cardanic/Eulerian rotational method is that the joint orientation is attained by a specific temporal sequence of rotations about the selected axes. The primary rotation about the selected Cartesian coordinate system is followed by a second rotation about another, displaced coordinate axis, and a third rotation about a doubly displaced coordinate axis. Any variation in the ordered sequence will result in different values of the three-dimensional joint angles. For example, if the temporal sequence designates the first rotation as flexion/extension and this sequence is changed so that flexion/extension becomes the third rotation, the flexion/extension angle would be different for the two sequences even though the actual angle was identical. This limitation has caused problems when repeating research trials, and in interpreting and comparing clinical data (Woltring 1994).

To overcome the restriction of the Cardanic/Eulerian rotation sequence, Grood and Suntay (1983) proposed a coordinate system that is independent of the order of the occurrences of the translations and rotations. The three rotational axes consist of two axes embedded into the limb segments that make up the joint of interest and a third that is the common perpendicular to the fixed axes of the two limb segments. The orientation of the third axis is determined by the cross product of the unit base vectors of the fixed axes. The third axis, which is not fixed to either segment, is described as the floating axis. Since the two fixed axes are within the segments, the rotations are dependent upon the choice of the embedded axes. Thus, the rotational sequence is classified as a geometrical sequence.

In the case of the human knee, the joint coordinate system designates that flexion/ extension occurs about the femoral fixed axis, internal/external rotation about the tibial fixed axis, and adduction/abduction about the floating axis (Grood and Suntay 1983). Therefore, the angles between the floating axis and the anterior axis of each bone determine joint flexion and tibial rotation. Joint adduction/abduction is measured from the angles between the tibial and femoral segmental fixed axes. These three calculated angles are termed Euler angles.

The first component in measuring equine three-dimensional motion is to adapt the joint coordinate system developed for human joints and to apply it to the equine joints. Heleski (1991) utilized the joint coordinate system described by Grood and Suntay (1983) to measure equine three-dimensional joint motion. The study encountered difficulties in identifying suitable locations for the markers used to track segmental

movements. In this study, we overcame these difficulties by developing a virtual marker targeting system.

Three-Dimensional Marker Methodology. The marker placement guidelines for three-dimensional kinematic analysis are that the markers should be located in areas that are subject to minimal skin displacement, visible to at least two cameras throughout the stride, and allow the construction of a meaningful and repeatable segmental coordinate system. In previous studies, the requirements for three-dimensional marker placement have been restrictive (Heleski 1991). Furthermore, Heleski (1991) attached the 3-D tracking markers to a strap that was placed around the horse's limbs. This strap was prone to motion error so that as the limb moved the strap would shift from it's original location. In order to overcome these limitations while achieving the requirements stated above, two sets of markers are used to fulfill the marker placement guidelines: virtual markers establish the segmental coordinate system while tracking markers are used to follow the segmental movements. The tracking markers are placed on sites that are readily visible throughout the stride and for which skin displacement is minimal. The spatial relationship between the two sets of markers is established with the horse in a standing position. During locomotion, the locations of the virtual markers are calculated from the tracking marker coordinates using transformations developed from the standing position.

The development of this type of targeting system assumes that the biological system being studied is composed of a series of rigid bodies. In other words, each limb segment is treated as rigid, and movements of the soft tissues are ignored. This is a reasonable simplification in the distal limbs of the horse. For each of these rigid rods (or

limb segments), a segmental coordinate system is created as a reference for movement measurement. The use of virtual markers is based on a knowledge of the distance and orientation between the origin of the segmental coordinate system and a defined point on the segment, together with a known transformation between the global coordinate system and the segmental coordinate system. When these conditions are fulfilled, then at any instant in time the same point on the segment can be located in the global coordinate system (Soutas-Little 1996).

The virtual marker locations are subject to the requirements listed earlier for three-dimensional targeting schemes in that two markers must lie along the anatomical axis of the segment and the third must be placed perpendicular to that axis. The virtual markers define the anatomical segmental coordinate system. Their location is recorded videographically on a standing file, but it is not necessary for the virtual markers to remain on the limb while the horse is in motion. In addition to the virtual markers, three tracking markers are attached to each segment at readily visible locations where skin displacement is minimal. The tracking markers are recorded on the standing file and while the horse is in motion. They define an arbitrary tracking segmental coordinate system. A transformation between the tracking segmental coordinate system and the global coordinate system is calculated from the tracking files. Transformations between the anatomical and tracking segmental coordinate systems are developed from the standing file. These transformations are used to calculate the coordinates of the virtual markers and to locate the virtual markers as if they had been present during locomotion. The virtual marker system allows compensation for skin displacement and facilitates tracking in areas of the limb that may be hidden from the camera during locomotion.

Transformations. Transformations are used to determine the location of the virtual markers during locomotion from a knowledge of the position of the tracking markers. The tracking segmental coordinate system (TSCS) is determined by three tracking markers fixed to each segment that move with the segment throughout the motion. The origin of the TSCS is determined (Figure 3.1).

The first axis is calculated from the cross product of the vectors from the origin to the two other markers (1):

(1) $\hat{i} = r_1 \times r_2 / | r_1 \times r_2 |$

The second axis is calculated by the cross product of the vector from the origin to the third marker and the first axis (2):

(2) $\hat{k} = r_2 \times \hat{i} / | r_2 \times \hat{i} |$

Lastly, the third axis is calculated by the cross product of the first and second axis (3):

(3) $\hat{j} = \hat{k} \times \hat{i}$

The coefficient of these unit vectors are the directional cosines, λ, between the TSCS and the global coordinate system (GCS):

(4) $\hat{i} = \lambda_{xX}\hat{I} + \lambda_{xY}\hat{J} + \lambda_{xZ}\hat{K}$

(5) $\hat{j} = \lambda_{yX}\hat{I} + \lambda_{yY}\hat{J} + \lambda_{yZ}\hat{K}$

(6) $\hat{k} = \lambda_{zX}\hat{I} + \lambda_{zY}\hat{J} + \lambda_{zZ}\hat{K}$

These directional cosines, λ, between the TSCS and GCS, expressed in terms of a 3 x 3 rotational transformation matrix, [T], allows for the reference from the TSCS to the GCS.

The translational vector, R_o, is drawn from the origin of the GCS to the TSCS. Vector R_v is drawn between the origin of the GCS to the virtual marker (Figure 3.2).

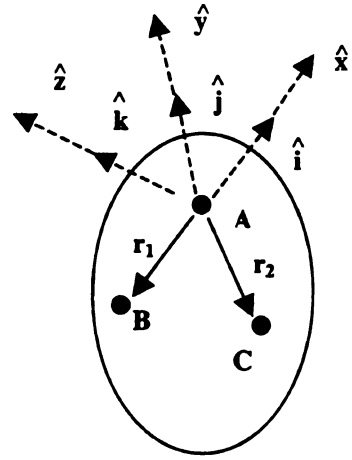

Figure 3.1. Three noncollinear markers, A, B, and C, fixed to a rigid body. The origin, marker A, of the tracking segmental coordinate system and the x, y, and z axes are indicated as well as the unit vectors $\hat{i}$, $\hat{j}$, $\hat{k}$ of the axes, respectively.

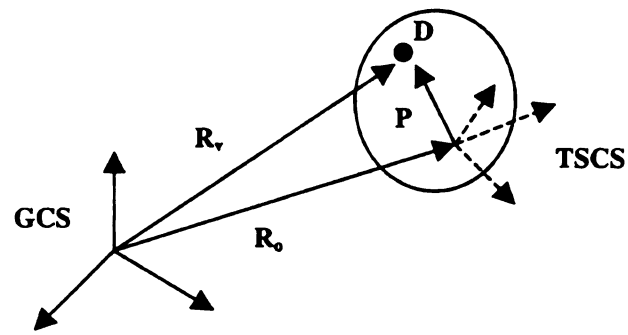

Figure 3.2. The virtual vector location is calculated from R_v, the vector from the global coordinate system (GCS) origin to the virtual marker D; R_o, the vector from the GCS origin to the tracking segmental coordinate system (TSCS) origin; and P, the vector from the TSCS origin to the virtual marker D.

Vectors from the TSCS origin to the virtual targets are calculated and expressed in terms of the GCS (7):

$$(7) \qquad P = R_v - R_o$$

The virtual vector P is further transformed from the GCS to the TSCS using the rotational transformation matrix [T] to form the virtual vector p (8):

$$(8) \qquad p = [T]\, P$$

Since the segment is assumed to be rigid, the virtual vector expressed in terms of TSCS will not change regardless of the orientation of the segment. For each frame, the orientation of the TSCS can be calculated from the tracking markers. The transformation matrix and the virtual vectors can then be used to transform each virtual vector for that segment from the TSCS back to the GCS (9):

$$(9) \qquad R_v = R_o + [T]^T p$$

Therefore, for each frame of motion data, the location of the virtual marker is expressed in terms of the GCS as if it had actually been tracked.

Euler Angles. After the transformations have been calculated and the segmental coordinate systems have been established, the joint coordinate system is determined for the measurement of three-dimensional joint motion. The joint angles can be measured from the embedded segmental coordinate system determined by the virtual vectors. The axes of the embedded segmental coordinate systems are denoted as the following: $\hat{x}_r$, $\hat{y}_r$, and $\hat{z}_r$ for the radius; $\hat{x}_m$, $\hat{y}_m$, and $\hat{z}_m$ for the metacarpus; and $\hat{x}_p$, $\hat{y}_p$, and $\hat{z}_p$ for the proximal phalanx. For each segment, the z-axis runs through the long axis of the segment, the x-axis runs medial/lateral, and the y-axis runs dorsal/palmar. At the carpal joint, for example, the $\hat{x}_r$ axis of the radius is designated as the flexion/extension axis, $\hat{e}_1$, and the

$\hat{z}_m$ axis of the third metacarpus is the internal/external rotation axis, $\hat{e}_3$. The floating axis, the adduction/abduction axis, is calculated by the cross product of the $\hat{e}_1$ and $\hat{e}_3$ axes, $\hat{e}_2$ (Figure 3.3):

(1) $\hat{e}_1 = \hat{x}_r$ Flexion and Extension

(2) $\hat{e}_3 = \hat{z}_m$ Internal and External Rotation

(3) $\hat{e}_2 = (\hat{e}_1 \times \hat{e}_3) / | \hat{e}_1 \times \hat{e}_3 |$ Adduction and Abduction

The joint Euler angles are (Figure 3.3):

(4) Flexion (-) / Extension (+) = $-a\sin (\hat{e}_2 \cdot \hat{z}_r)$

(5) Adduction (-) / Abduction (+) = $a\sin (\hat{e}_1 \cdot \hat{e}_3)$

(6) Internal (-) / External Rotation (+) = $a\sin (\hat{e}_2 \cdot \hat{x}_m)$

The joint angles are defined so that joint motion is described relative to their respective axes in that flexion/extension is relative to $\hat{e}_1$, internal/external rotation to $\hat{e}_3$, and adduction/abduction to $\hat{e}_2$.

At the fetlock joint, the $\hat{x}_m$ axis of the third metacarpus is designated as the flexion/extension axis, $\hat{e}_1$, and the $\hat{z}_p$ axis of the proximal phalanx is the internal/external rotational axis, $\hat{e}_3$. The floating axis, the adduction/abduction axis, is calculated by the cross product of the $\hat{e}_1$ and $\hat{e}_3$ axes, $\hat{e}_2$ (Figure 3.4). Joint motion is measured using the same calculations as the carpal joint with $\hat{z}_r$ replaced with $\hat{z}_m$ and $\hat{x}_m$ replaced with $\hat{x}_p$. The above calculations follows that of Soutas-Little *et al.* (1987) in which the coordinate system is rotated 90° from the coordinate system used in Grood and Suntay (1983) so that the relationship between the two approaches can be expressed as follows: $\sin \alpha = -\cos(\alpha+90)$. This approach is more applicable for clinical evaluation.

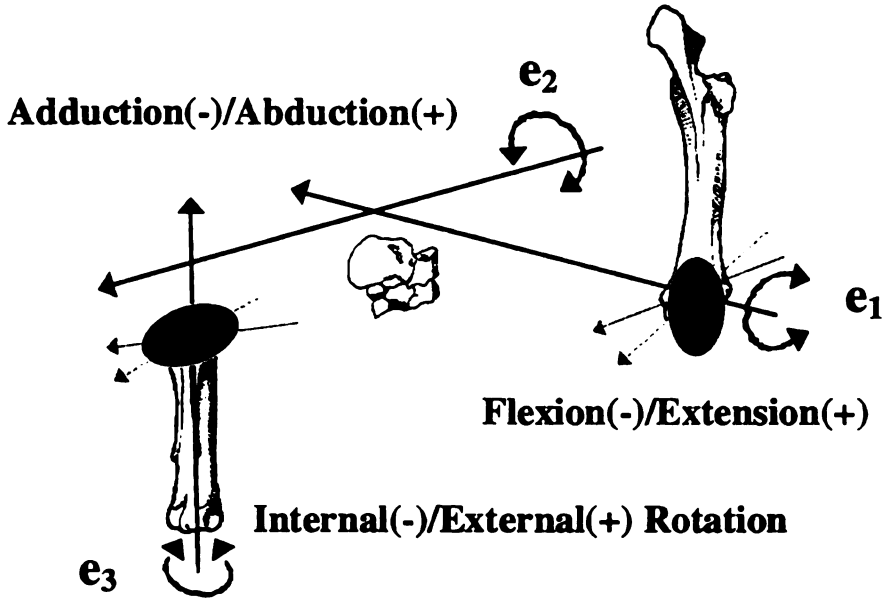

Figure 3.3. Caudolateral view of an exploded limb showing the radius, carpus, and metacarpal segements to illustrate the segmental axes used to develop the joint coordinate system. The orientations and locations of the flexion/extension (e_1), adduction/abduction (e_2), and internal/external rotation (e_3) axes are shown.

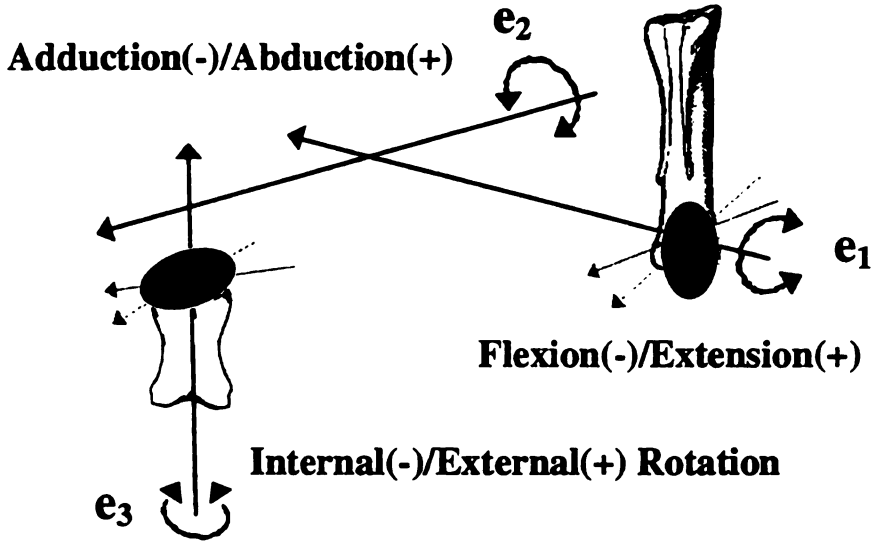

Figure 3.4. Caudolateral view of an exploded limb showing the metacarpal and proximal phalangeal segements to illustrate the segmental axes used to develop the joint coordinate system. The orientations and locations of the flexion/ extension (e_1), adduction/abduction (e_2), and internal/external rotation (e_3) axes are shown.

Appli

devel

sound

calcul

angle

joint

appl

forel

with

ma

dis

wi

Th

ph

Te

bo

a

se

Pl

Application of the Joint Coordinate System and Virtual Markers

Subject. The methodology for measuring three-dimensional joint motion was developed at the walk using a non-gaited horse that was determined to be clinically sound. The results were compared with previously published data of joint angles calculated using well-established techniques for two-dimensional analysis and with joint angles calculated from three-dimensional analysis.

Markers. To track the three-dimensional motion of the equine carpal joint using a joint coordinate system and virtual marker methodology, two sets of markers were applied to the antebrachial, metacarpal, and proximal phalangeal segments of the right forelimb. The virtual and tracking markers consisted of polystyrene hemispheres covered with retro-reflective tape.

Three virtual markers were attached to a rigid "L" structure (Figure 3.5). A virtual marker "L" structure was taped securely to the skin overlying the proximal radius, the distal third metacarpus, and along the length of the proximal phalanx of the right forelimb with the long axis of the "L" parallel to the anatomical axis of each segment (Figure 3.5). Three tracking markers were attached to the antebrachial, metacarpal, and proximal phalangeal segments of the right forelimb using super glue (Future Glue, Pacer Technology, Ranch Cucamonga, California).

The tracking markers were placed over palpable anatomical landmarks on the bones where skin displacement is minimal or for which correction algorithms are available. The antebrachial tracking markers were placed on the distal end of the segment in a triangular formation (Figure 3.5). The metacarpal tracking markers were placed in a similar arrangement on the proximal end of the segment (Figure 3.5). On the

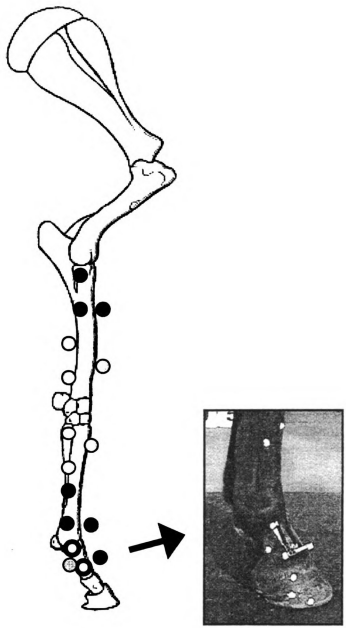

Figure 3.5. Location of the virtual markers (black spheres), tracking markers (gray spheres) and markers (clear spheres) used as both virtual and tracking markers during the standing file to establish virtual marker locations relative to tracking markers. Picture shows the virtual "L" structure on the proximal phalanx.

proximal phalanx, the locations of the two virtual markers aligned along the long axis of the segment were used for two of the tracking markers and the third tracking marker was placed on the dorsal aspect of the segment to form a triangular formation (Figure 3.5).

Video Recording and Analysis. Two 60 Hz CCD camcorders attached to two Super VHS tapedecks (Panasonic AG-450, Matsushita Electric Corp., Secausus, NJ) were oriented at 60° to the horse's plane of motion, separated from each other by a distance of 609 cm, and located at a distance of 500 cm from, and perpendicular to, the line of motion. A 500-watt lamp was placed behind each camcorder to illuminate the retro-reflective markers during recording. The rectangular calibration volume measuring 342 cm x 190 cm x 210 cm was defined by thirty points.

A three-second standing file was recorded with the horse in a normal standing position with both the tracking markers and the virtual marker structures in place. The virtual marker structures were then removed, except for the two markers on the proximal phalanx that were also used as tracking markers. The horse was recorded on videotape as it moved at a walk with only the tracking markers attached.

The videotapes were digitized with the aid of the Ariel Performance Analysis System (Ariel Dynamics, Trabuco Canyon, California) and analyzed using custom software. For the standing file, the positions of the tracking and virtual markers were digitized manually. For the walking sequence, the tracking markers were digitized automatically in both camcorder views. Using the calibration frame previously described and the direct linear transformation method (Abdel-Aziz and Karara 1971), the three-dimensional coordinate values of the digitized markers were calculated. The raw data were filtered using a fourth order Butterworth digital filter, with a cut off frequency of 6

Hz. T

the vir

tracke

coord

using

dumm

walki

joint

addi

type

Res

equ

Peak

(Fig

(-36

mov

flexe

appr

Hz. The GCS was determined by the calibration frame. Using the digitized locations of the virtual and tracking markers, the segmental coordinate system was determined and tracked through the stride using the previously described transformations. The joint coordinate system and the three-dimensional joint motion were calculated and measured using the previously described Euler angle methodology. The joint angles measured during the standing file were expressed as the zero value and the angles recorded during walking were measured relative to the standing angle.

Statistics. Four strides of the walk were used to measure the three-dimensional joint motion of the carpus and the fetlock. Graphs were plotted for flexion/extension, adduction/abduction, and internal/external rotation of each joint. Peak values for each type of motion were determined and means and standard deviations were calculated.

Results

Carpal Joint Motion. During the stance phase, the carpus maintained an angle equivalent to standing angles, then showed a single flexion cycle during the swing phase. Peak flexion angle was -65° $\pm$ 2.6° at 80% of the stride. The small standard deviation (Figure 3.6) indicates that there was little variability between strides.

The carpus was adducted during early and late stance and reached peak adduction (-36° $\pm$ 6.4°) at 85% of the stride (Figure 3.7). The carpus showed very little rotational motion, with peak value for internal rotation (-6° $\pm$ 3.2°) at midswing (Figure 3.8).

The three joint motions appeared to be coupled. During midswing, the carpus flexed, adducted, and internally rotated. Towards the end of the swing phase, the carpus approached the standing joint angles in preparation for the start of stance.

Figure 3.6. Mean (dark line) ± 1 S.D. (light line) walking carpal flexion (-)/extension (+) angle relative to the standing carpal flexion joint angle.

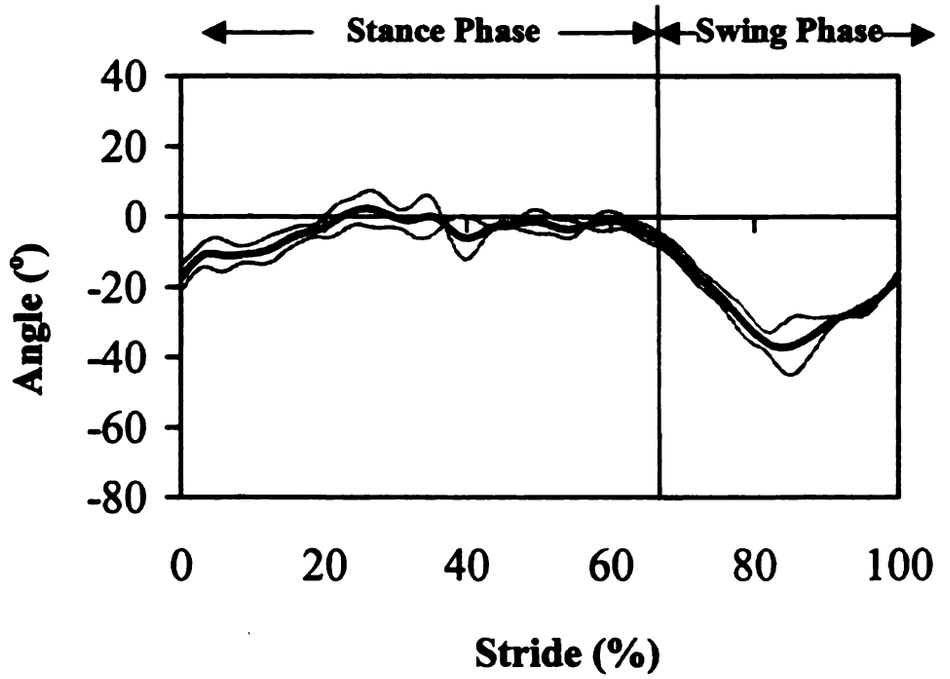

Figure 3.7. Mean (dark line) ± 1 S.D. (light line) walking carpal adduction (-)/abduction (+) angle relative to the standing carpal adduction/abduction joint angle.

Figure 3.8. Mean (dark line) ± 1 S.D. (light line) walking carpal internal (-)/external (+) rotation angle relative to the standing axial rotation joint angle.

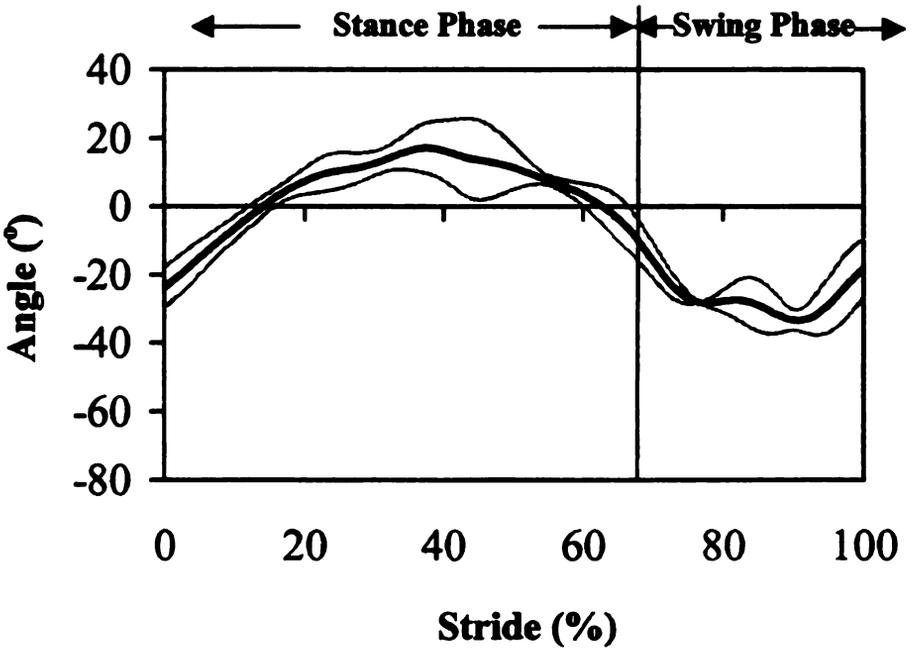

Figure 3.9. Mean (dark line) ± 1 S.D. (light line) walking fetlock flexion (-)/extension (+) angle relative to the standing carpal flexion joint angle.

Fetlock Joint Motion. During the stance phase, the fetlock extended, abducted, and internally rotated. Flexion/extension showed 50° range of motion at the fetlock joint (Figure 3.9). Peak extension (19° ± 4.1°) occurred in midstance. During breakover the fetlock flexed and showed two flexion peaks during the swing phase.

The fetlock showed a maximal abduction of 5° ± 8.4° around the time of midstance, and was then adducted during late stance and throughout the swing phase (Figure 3.10). The fetlock had 10° range of adduction/abduction joint motion.

The fetlock was internally rotated by about 15° during most of stance (Figure 3.11). During breakover, the fetlock showed a small peak of external rotation, then was internally rotated through the remainder of swing. The fetlock had 20° range of internal/external rotational motion.

Discussion

The joint coordinate system established in this study allowed a meaningful description of three-dimensional joint motion for the equine carpus and fetlock. Heleski (1991) first proposed the application of a joint coordinate system to the equine carpal and fetlock joints and performed some preliminary measurements at the walk and trot. Marker visibility and difficulty in tracking the markers throughout the stride were identified as problems in the methodology. This study addresses these problems by developing a virtual tracking system.

To date, Heleski's study of two young Arabian horses is the only comparable three-dimensional study using a JCS to measure carpal and fetlock joint motions of the walk and trot. In comparing the overall joint motion trends reported by Heleski with

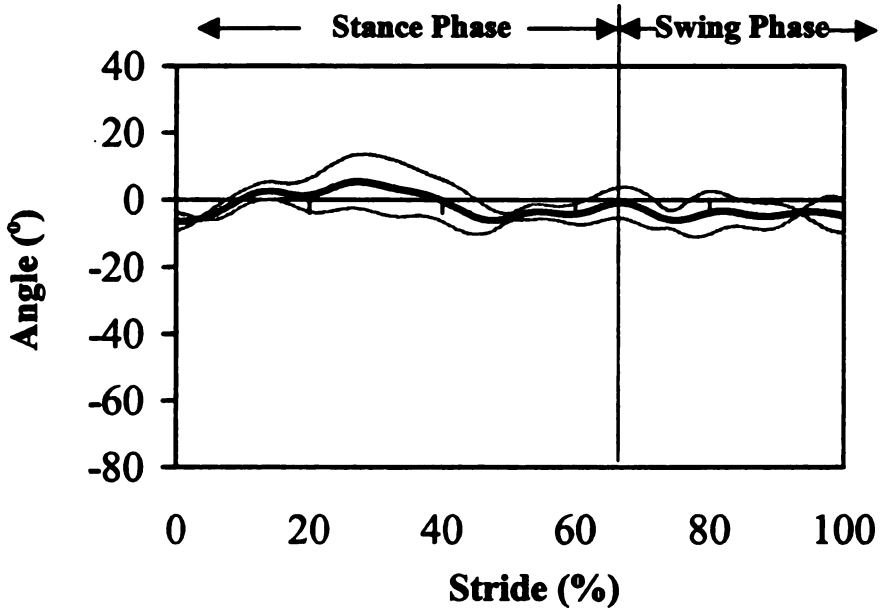

Figure 3.10. Mean (dark line) ± 1 S.D. (light line) walking fetlock adduction (-)/abduction (+) angle relative to the standing fetlock adduction/abduction joint angle.

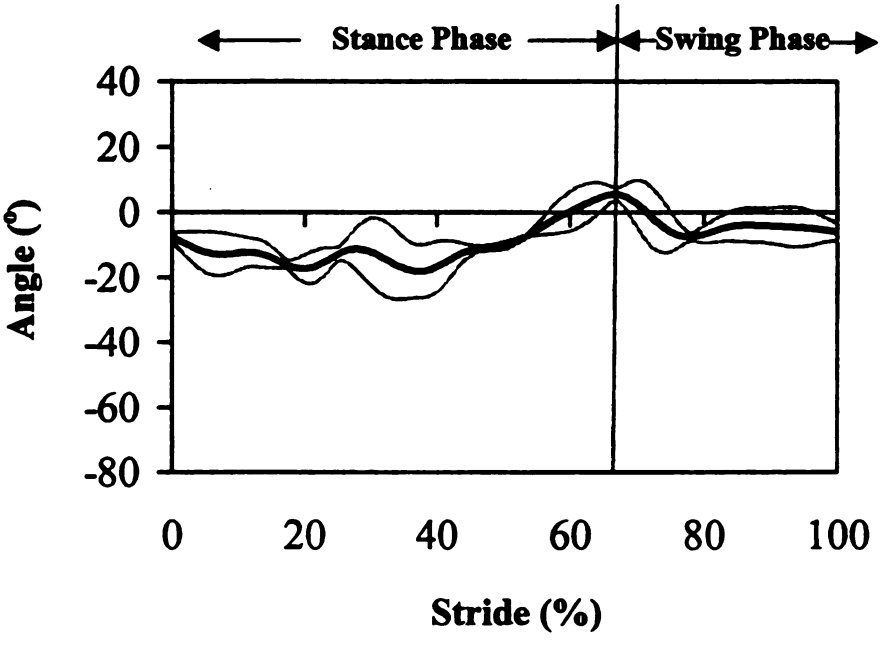

Figure 3.11. Mean (dark line) ± 1 S.D. (light line) walking fetlock internal (-)/external (+) rotation angle relative to the standing fetlock axial rotation joint angle.

those found in the present study, the motion patterns were quite similar and the peaks occurred at approximately the same times in the stride. Fetlock flexion/extension had a similar range of motion in both studies. Carpal flexion/extension range of motion was 17° greater in the two horses measured in Heleski's study, but there was 20° less carpal adduction than was measured in this study. The subject used in this study was also an Arabian, with the only obvious difference being that it was much older than Heleski's subjects. To date, no studies have measured the effect of age on equine three-dimensional joint motion. Fetlock adduction/abduction was very inconsistent from stride to stride in Heleski's study which was ascribed to problems with added motion of the straps to which the tracking markers were attached and difficulties in marker visibility. The smaller variability in the present study was a consequence of the improved accuracy resulting from the use of virtual markers. Both carpal and fetlock internal/external rotational ranges of motion and timing of the peaks were similar in the two studies.

In the following chapters, the virtual marker "L" structure was replaced with virtual markers attached directly onto the skin with some of the virtual markers also used as tracking markers. The changes in virtual marker methodology were described in greater detail within the respective chapters. The adjustments in methodology reduced the number of markers, which facilitated the clear distinction between markers, especially on the distal aspect of the limb, and reduced the time taken for marker placement. The new placement of the markers was used in chapter IV (Experiment II) to allow for simultaneous collection of two-dimensional data for comparison of the flexion/extension values. Although the virtual marker placement was slightly different, the established

axes of the joint coordinate system were the same so that joint motion was measured consistently throughout all three experiments.

A three-dimensional study of limb motions in the sagittal and frontal planes was performed using a multi-planar analysis (MPA) instead of a JCS (Herring *et al.* 1992). Since that study was performed at the trot and adduction/abduction angles were measured for the entire limb rather than the individual joints, it is not appropriate to make direct comparisons with this study. In the following chapter, the relationship between a JCS and MPA was further evaluated to facilitate the most appropriate methodology for analysis of equine locomotion, specifically the gaits of the gaited horse.

Two-dimensional studies have reported flexion/extension patterns and peak angles that are similar to this study. In Dutch warmblood horses, Back *et al.* (1996) found that the swing phase started at 60% of the stride with the peak carpal flexion angle of 60° occurring at mid-swing at 80% of the stride. Hodson *et al.* (2000) found that peak carpal flexion of 55° occurred at 75% of the stride in horses of mixed breeds.

Previous two-dimensional studies found similar fetlock flexion peaks during the swing phase (Back *et al.* 1995; Hodson *et al.* 2000). However, during the stance phase, Back *et al.* (1996) and Galisteo *et al.* (1996) found two extension peaks while this study along with Hodson *et al.* (2000) showed only one distinct peak. This difference is attributed to velocity. The studies by Back *et al.* (1996) and Galisteo *et al.* (1996) were performed at faster velocities (1.6 to 1.7 m/s) than Hodson *et al.* (2000) and this study (1.5 m/s). The slower velocity is associated with a reduced rate of limb loading which, in turn, decreases the rebound effect that is responsible for the slight flexion during mid-stance (Khumsap *et al.* in press). Thus, the two peaks of fetlock extension become more

distinct as velocity of the walk increases. The flexion/extension range of motion of the fetlock in this study was similar to Hodson *et al.* (2000). Both studies were conducted in the same laboratory and performed under similar experimental conditions, including velocity.

Since there have been so few studies of equine three-dimensional analysis using a JCS, comparisons with the present study are quite limited. The effects of variables such as age, velocity, and footing on walking kinematics have not even been studied using two-dimensional or multi-planar analysis. Now that the technique has been developed, these variables should be studied using a JCS to evaluate the effects in three dimensions. Just as human three-dimensional analysis has been applied to clinical settings, it is the recommendation of this researcher that further studies should also be conducted to test the usefulness of this methodology for clinical applications in horses.

In conclusion, a technique for measuring three-dimensional joint motion in a joint coordinate system using virtual markers was developed. A joint coordinate system measures joint motion within an anatomically-based coordinate system compared to multi-planar analysis, which measures joint angles using planar projections. Measuring three-dimensional joint motion using multi-planar analysis does not allow for the measurement of axial rotation and coupled joint motion, which was found in this study with the application of a joint coordinate system to a horse walking. A more detailed comparison of multi-planar analysis with a joint coordinate system is made in chapter four. The technique described in this study was applied to a horse walking to measure carpal and fetlock flexion/extension, adduction/abduction, and internal/external rotation. Comparison with an earlier three-dimensional study using a joint coordinate system

(Heleski 1991) indicated that the virtual marker methodology showed less variability from one stride to the next. Flexion/extension angles were similar to previous two-dimensional kinematic studies (Back *et al.* 1996; Hodson *et al.* 2000). The joint coordinate system using a virtual marker methodology described in this chapter was applied to the following chapters with slight alterations made, which are described in the respective chapters, to continue to improve upon the methodology.

E

Sum

motio

syste

JCS

joint

meas

dumn

move

phala

carpa

addu

axis o

plane

plane

were

adequ

horse

differ

CHAPTER IV

EXPERIMENT II: COMPARISON OF A JOINT COORDINATE SYSTEM VERSUS MULTI-PLANAR ANALYSIS

Summary

A kinematic multi-planar analysis (MPA) reduces a subject's three-dimensional motion to two-dimensional projections onto planes defined by a global fixed coordinate system (GCS). An alternative to this kinematic method is a joint coordinate system (JCS), which describes the three-dimensional orientation of the segments comprising the joint with respect to each other. This study compares carpal and fetlock joint kinematics measured using a MPA with those measured using a JCS. A Peruvian Paso was recorded during three walking trials using 60 Hz video camcorders. Skin markers tracked the movements and defined the anatomical axes of antebrachial, metacarpal, and proximal phalangeal segments. A JCS was established between the two segments comprising the carpal and fetlock joints to measure flexion/extension, internal/external rotation, and adduction/abduction at each joint. The MPA model used two markers aligned on the long axis of each segment and measured flexion/extension angles projected onto the sagittal plane of the coordinate system and adduction/abduction angles projected onto the frontal plane of the coordinate system. Carpal and fetlock flexion/extension angles for the walk were similar for the JCS and MPA indicating that sagittal plane analysis using a MPA is adequate when flexion and extension are the only measurements being made provided the horse's plane of motion is aligned with the plane of calibration. There were large differences in carpal and fetlock adduction/abduction angles measured using a MPA

comp

accur

inabil

comp

proje

meas

Introd

segme

in spa

define

betwe

coord

plane

been

of the

A lim

plane

estab

rotatio

as a

compared with a JCS. Analysis of the reasons for these differences indicated that the accuracy of frontal plane analysis to measure adduction/abduction is limited by it's inability to correct for out-of-plane rotations along the long axis of the segments comprising the joint. This finding clearly illustrates the inherent errors in using planar projections to measure multi-planar motions. It is recommended that a JCS be used to measure joint motions other than flexion/extension in the sagittal plane.

Introduction

Most of the studies of equine locomotion have measured movements of the limb segments and joints of the horse relative to a global coordinate system (GCS) that is fixed in space and oriented along the direction of travel of the subject. Often, segments are defined by two points placed along the long axis of the segment with the relative angles between two adjacent segments defining the joint angles. The three-dimensional coordinates of the points are projected onto the two-dimensional sagittal and frontal planes to give a multi-planar analysis (MPA) of segmental and joint motions. MPA has been used to describe vertical displacement, flexion/extension, and adduction/abduction of the fetlock joint (Herring *et al.* 1992) and the stifle and tarsal joints (Back *et al.* 2000). A limitation to MPA occurs when the segmental motion is not parallel to the projection plane causing the angular measurements in that plane to be distorted.

An alternative to MPA is to use an anatomically-based coordinate system established on each rigid segment. The joint angle can then be expressed as relative rotations between two adjacent segments. One method used to accomplish this is known as a joint coordinate system (JCS) (Grood and Suntay 1983). Heleski (1991) used a JCS

to describe three-dimensional carpal and fetlock joint angles of walking and trotting horses. The results were expressed in terms of flexion/extension, adduction/abduction, and internal/external rotation. It was concluded that the three-dimensional marker placement requirements were restrictive and prone to marker motion error. In order to overcome these limitations, a virtual marker methodology has been developed and used to establish a JCS for the carpus and fetlock (Chapter III, Experiment I).

The objectives are to compare carpal and fetlock joint kinematics measured simultaneously using a JCS with those from MPA in the sagittal and frontal planes.

Materials and Methods

Subject. The subject was a sound Peruvian Paso ridden at the walk. This breed was chosen because it is noted for a characteristic outward motion of the forelimbs during the swing phase of all it's gaits, which is known as a termino. Limb motion during termino offers an ideal opportunity to study exaggerated three-dimensional limb motion.

JCS Segmental Axes. Coordinate systems for the antebrachial, metacarpal, and proximal phalangeal segments were established as described in chapter three. The origin of the antebrachial coordinate system was located on the lateral styloid process on the distal radius. The antebrachial x-axis was directed laterally from the origin perpendicular to the antebrachial sagittal plane and on the same vector as a line from the medial to lateral styloid processes. The antebrachial z-axis, contained in the antebrachial frontal plane, ran from the origin proximally along the long axis of the segment at 90° to the x-axis. The antebrachial y-axis ran dorsally from the origin, perpendicular to the antebrachial frontal plane.

The origin of the metacarpal coordinate system was located on the lateral aspect of the distal end of the third metacarpus. The metacarpal x-axis was directed laterally from the origin perpendicular to the metacarpal sagittal plane and on the same vector as a line from the medial to lateral distal aspect of the third metacarpus. The metacarpal z-axis, contained in the metacarpal frontal plane, ran from the origin proximally along the long axis of the segment at 90° to the x-axis. The metacarpal y-axis ran dorsally from the origin, perpendicular to the metacarpal frontal plane.

The origin of the proximal phalangeal segment was located on the lateral aspect of the distal end of the proximal phalanx. The z-axis of the proximal phalangeal segment ran from the origin proximally along the long axis of the segment. Similar to the other segmental axes, the proximal phalangeal x and y-axes ran laterally and dorsally from the origin, respectively.

MPA Segmental Axes. The axes of the antebrachial, metacarpal, and proximal phalangeal segments used for the MPA corresponded to the z-axes of the segments as defined by the JCS. Therefore, the MPA segmental axes passed along the long axes of the antebrachial, metacarpal, and proximal phalangeal segments.

Data Collection. Kinematic data were collected at 60 Hz using four Super VHS camcorders (Panasonic AG-450, Matsushita Electric Corp., Secausus, NJ), arranged around the data collection area in increments of 60°. One camcorder was located towards the front of the horse, one towards the back of the horse and two towards the lateral aspect of the right side of the horse. A 500-watt lamp was placed behind each camcorder to illuminate the retroreflective markers during recording. The calibration volume (342 x 190 x 210 cm^3) was defined using 30 equally spaced points.

The horse was ridden along the runway at a walk. A trial was considered acceptable if the horse traveled at a consistent velocity (2.50-2.56 m/s) along a straight line that was parallel to the plane of calibration with all markers being clearly visible in the two lateral camcorder views (Figure 4.1).

Marker Placement. Reflective markers were attached to the skin overlying well-defined bony landmarks on the proximal and distal ends of the antebrachial, metacarpal, and proximal phalangeal segments on the lateral aspect of the limb (Figure 4.2). The tracking markers were located at sites that have been shown to have relatively little skin displacement during the walk (van Weeren *et al.* 1988). Corrections for skin displacement were not performed since 3-D correction algorithms and even 2-D corrections are not available for the Peruvian Paso breed or for Peruvian gaits. Current 2-D correction algorithms are based on Dutch Warmbloods and are very dependent on the gaits being measured (van Weeren *et al.* 1988). As for this study, the same markers were used for the two methodologies so any errors due to skin displacement were the same.

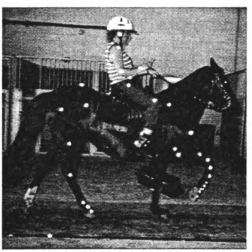

Figure 4.1. Data collection with tracking markers attached to the right forelimb during a walking trial.

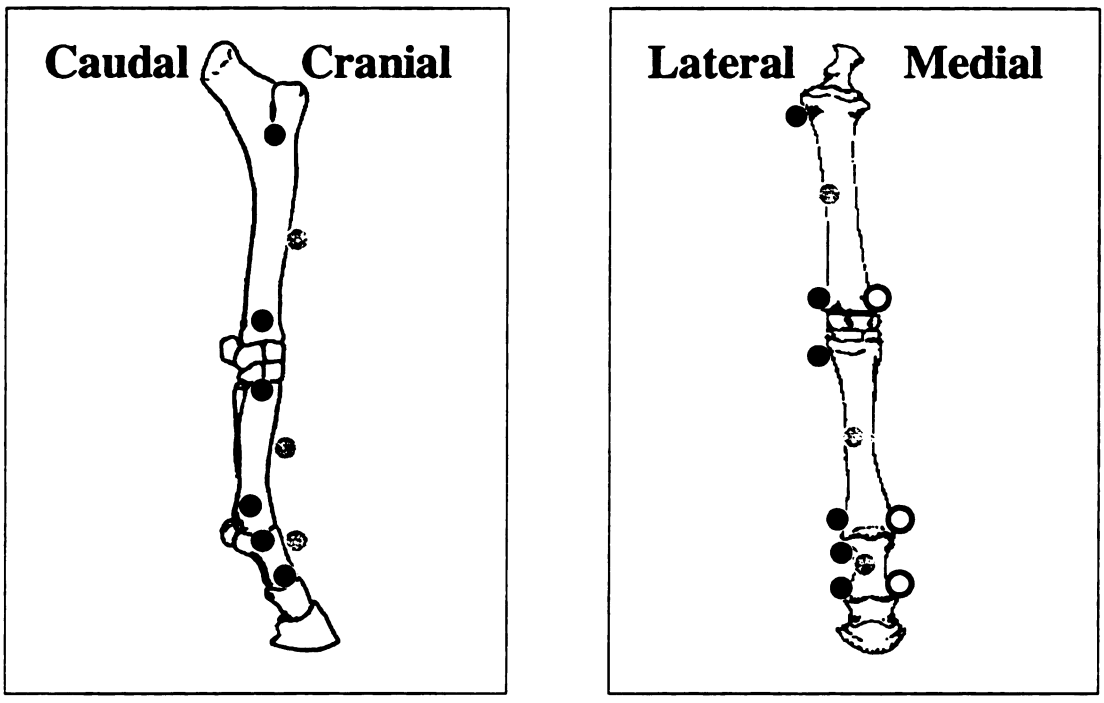

Figure 4.2. Marker placement during the standing file as seen in the lateral (left) and frontal (right) views. Virtual markers on the lateral aspect of the limb (black circles) for establishing the joint coordinate systems (JCS) were placed over bony landmarks on the proximal and distal ends of the antebrachial, metacarpal, and proximal phalangeal segments. A third virtual marker (open circles) was placed on the medial aspect of the distal extremity of each segment. Two of the JCS tracking markers (black circles) were the same as the lateral virtual markers. The third tracking marker (gray circles) was placed on the dorsal surface, midway between the other two tracking markers. The tracking markers (black circles) on the proximal and distal ends of each segment were used for multi-planar analysis (MPA). The virtual markers on the medial aspect were removed during the walking trials.

Segmental coordinate systems for the JCS were defined by the two lateral markers used for MPA together with a third marker attached on the medial styloid process of the radius, the metacarpal attachment of the medial collateral ligament of the fetlock, and the medial aspect of the distal end of the proximal phalanx. The medial markers were tracked using a virtual targeting system as described in Experiment I (Chapter III; Soutas-Little 1996) utilizing a fourth marker located on the cranial aspect of each segment, midway between the two lateral markers.

Two reflective markers were placed along the spine of the horse to determine the horse's angle of travel relative to the GCS during the trials. This information was used to align the horse's plane of motion with the GCS using a simple 2-D rotational transformation (Figure 4.3).

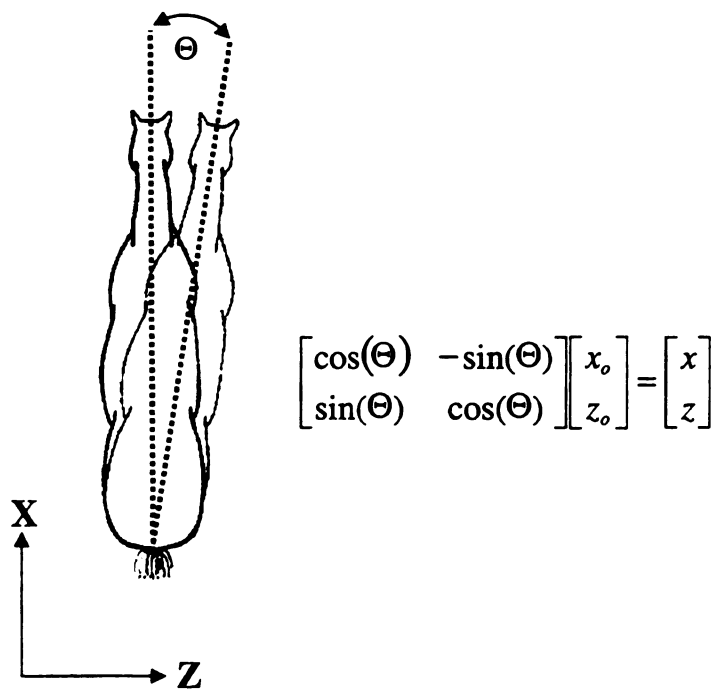

$$\begin{bmatrix} \cos(\Theta) & -\sin(\Theta) \\ \sin(\Theta) & \cos(\Theta) \end{bmatrix} \begin{bmatrix} x_o \\ z_o \end{bmatrix} = \begin{bmatrix} x \\ z \end{bmatrix}$$

Figure 4.3. Calculation used to correct sagittal plane measurements using MPA for the horse's angle of travel determined from the back markers (black spheres), where Θ is the angle that the horse is out-of-plane, x_o and z_o are the uncorrected marker coordinates, and x and z are the corrected marker coordinates.

Data Reduction. The skin markers were automatically tracked and digitized using a video analysis system (Ariel Performance Analysis System, Ariel Dynamics Inc, Trabuco Canyon, California). Three-dimensional locations of markers were obtained using direct linear transformation (Abdel-Aziz and Karara 1971). The three-dimensional coordinates were filtered using a fourth-order Butterworth digital filter at a cutoff frequency of 6 Hz. Joint motion in the MPA was described for the distal segment relative to the proximal segment (Winter 1990). The MPA was used to measure flexion/extension in the sagittal plane and adduction/abduction in the frontal plane. The JCS was established based on the system described by Grood and Suntay (1983). For the carpal joint, flexion/extension was measured around the antebrachial fixed x-axis, internal/external rotation was measured around the metacarpal fixed z-axis, and adduction/abduction was measured around a floating axis perpendicular to both the flexion/extension axis and the internal/external rotation axis. For the fetlock joint, flexion/extension was measured around the metacarpal fixed x-axis, internal/external rotation was measured around the proximal phalangeal fixed z-axis, and adduction/abduction was measured around a floating axis perpendicular to both the flexion/extension axis and the internal/external axis. For example, flexion occurred when the angle on the caudal/palmar aspect of the joint decreased, internal rotation occurred when the distal segment rotated medially relative to the proximal segment, and adduction occurred when the angle on the medial aspect of the floating axis decreased. Zero joint angle was defined as alignment of the proximal and distal segments. Flexion, adduction, and internal rotation were assigned negative values. Extension, abduction, and external rotation were assigned positive values. For carpal flexion/extension angles greater than

90°, an additional calculation was applied to overcome errors arising from taking the sine of an angle greater than 90° in the JCS calculations (Chapter III, Experiment I).

The mean curves for flexion/extension, abduction/adduction, and internal/external rotation of the carpal and fetlock joints at the walk measured by the JCS were graphed. The mean absolute difference between the adduction/abduction measured with the JCS and MPA were calculated. Segmental angles were determined in the sagittal view using the raw x coordinates for the proximal and distal markers that were aligned along the long axis. Segmental angles in the sagittal plane were measured from an axis perpendicular to the ground with the segment rotating around it's proximal end. An angle of 0° indicated the segment was vertical and an angle of 90° indicated the segment was horizontal. Protraction (cranial rotation of the distal end of the segment) was assigned a positive value and retraction (caudal rotation of the distal end of the segment) was assigned a negative value (Figure 4.4).

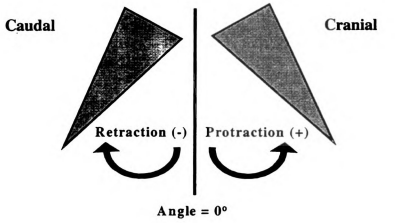

Figure 4.4. Measurement of the segmental angles in the sagittal plane. Negative values indicate retraction, positive values indicate protraction, and 0° indicates the segment is vertical.

The anatomical orientation and the location of the segmental axes relative to the GCS was explored in an attempt to understand the differences between the two methods. The mean difference between the raw z coordinates of the proximal and distal markers of the segmental long axis was calculated. A difference of zero indicates that the segment is aligned along the x-axis of the GCS (longitudinal axis of the horse). When z coordinates of the proximal and distal tracking markers were aligned with the corresponding axis of the GCS, only the sagittal view showed an angulation of the segment relative to the GCS. The mean angle between the JCS adduction/abduction axes and the x-axis of the GCS (longitudinal axis of the horse) and between the JCS flexion/extension axes and the z-axis of the GCS (mediolateral axis of the horse) were calculated.

Results

The following section describes the joint motion of the Peruvian Paso walk using the JCS and differences between the JCS and MPA measurements. The orientations of the joints and the proximal and distal segments comprising the joints are described at the times when there are marked differences between the two methods. Values for all individual trial measurements were graphed and included in Appendix A.

Carpal Joint. JCS standing angles showed that conformation of the right forelimb was such that the carpus was extended 2°, abducted 8°, and internally rotated -7°. JCS measurements showed that during the stance phase the carpus was extended, abducted, and internally rotated (Figure 4.5). Breakover began at 40% of the stride and lift off occurred at 55% of the stride. Throughout breakover and early swing, the carpus showed

flexion, abduction, and external rotation. At mid swing, the carpus reached peak flexion (-94°), abduction (23°), and external rotation (7°).

Flexion/extension patterns were similar when measured using the MPA and JCS, and the peak flexion angles, which occurred during mid-swing showed minimal differences between the two techniques (Figure 4.6). The adduction/abduction curves showed differences in the general pattern and timing of peaks (Figure 4.7) with the peak values demonstrating large differences between the MPA and JCS during the transition from stance to swing (Figure 4.8). Peak absolute difference (16°) between JCS and MPA adduction/abduction angles occurred around the time of lift off at 53% of the stride (Figure 4.8). At this point in the stride, the carpus was flexing and externally rotating (Figure 4.9). The radial segment was vertical in the GCS (sagittal plane angle 0°) at 53% of the stride (Figure 4.9). The difference in the z coordinates between the proximal and distal markers along the radial long axis was zero at 53% of the stride indicating the long axis was aligned along the x-axis of the GCS (Figure 4.9).

Fetlock Joint. JCS standing angles showed that the fetlock was extended 18°, adducted -11°, and internally rotated -13°. JCS measurements showed that during the stance phase the fetlock was extended and adducted (Figure 4.10). During breakover, which began at 40% of the stride, the fetlock flexed, abducted, and internally rotated. The direction of rotation changed just before lift off. Peak flexion (41°), abduction (2°), and external rotation (3°) occurred in early swing. During late swing, the fetlock extended, adducted, and internally rotated.

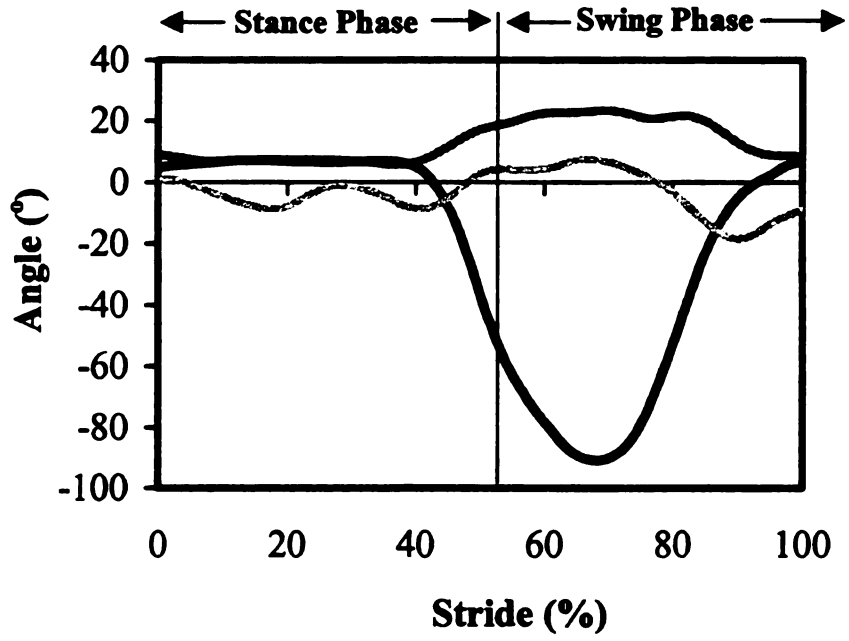

Figure 4.5. Mean carpal flexion (-)/extension (+) (black line), adduction (-)/abduction (+) (dark gray line), internal (-)/external (+) rotation (light gray line) using JCS.

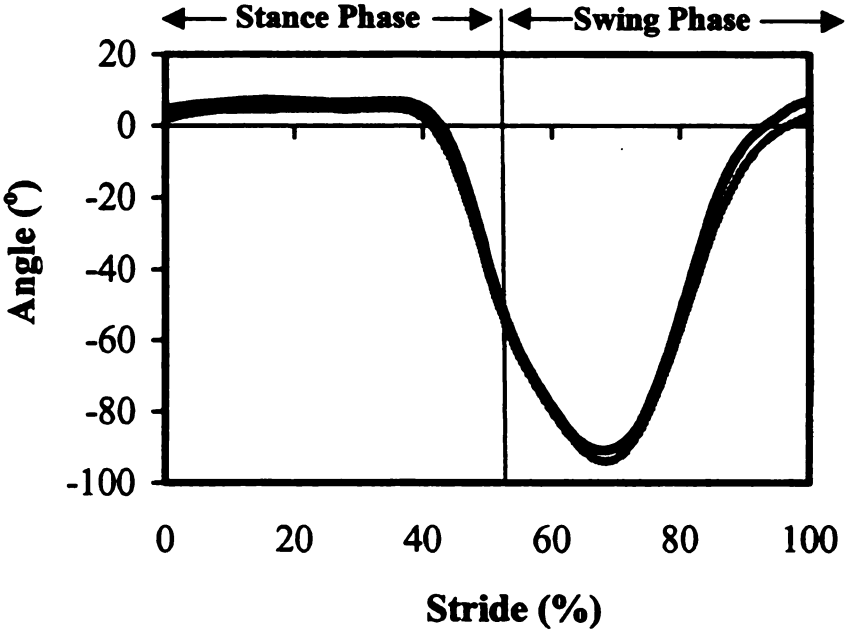

Figure 4.6. Mean carpal flexion (-)/extension (+) for JCS (black line) and MPA (gray line).

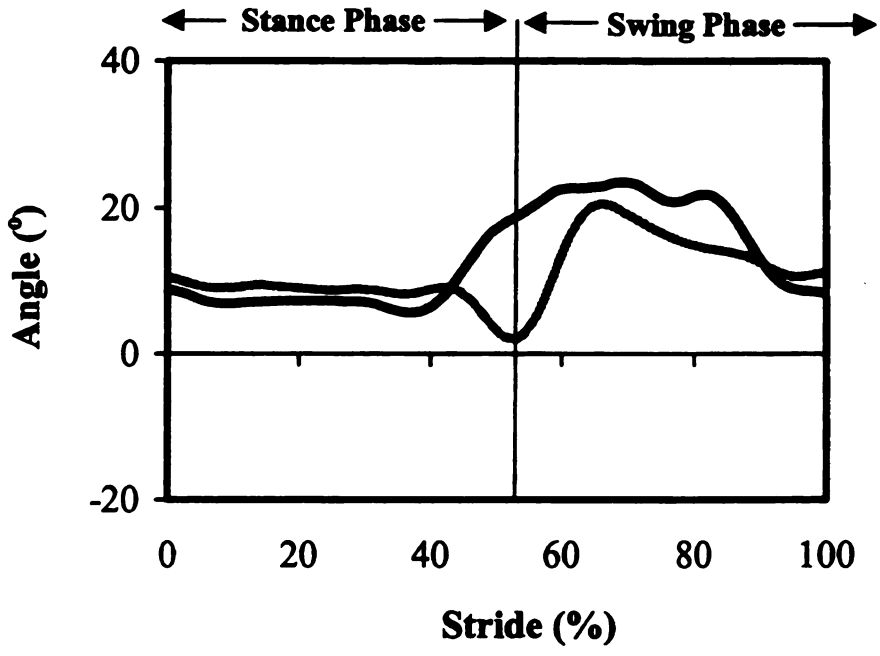

Figure 4.7. Mean carpal adduction (-)/abduction (+) for JCS (black line) and MPA (gray line).

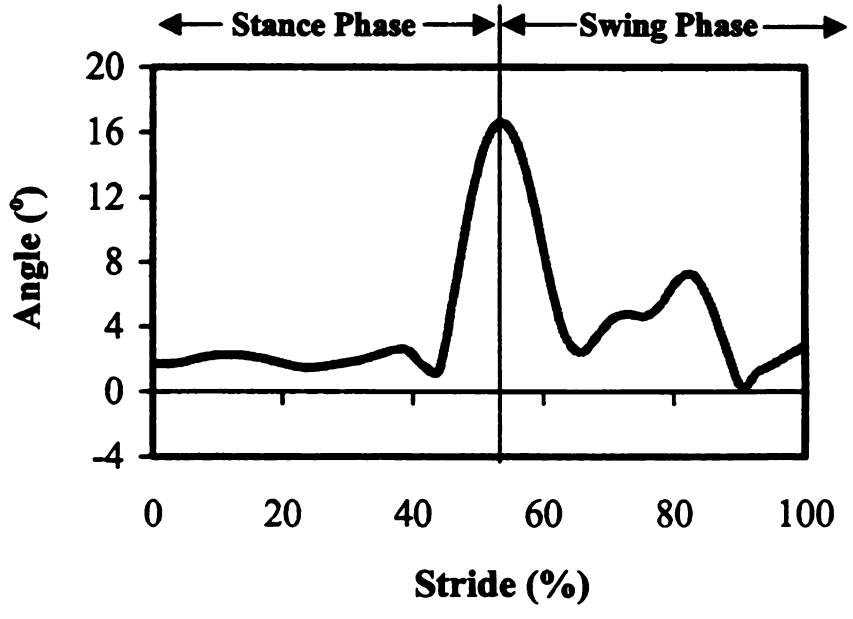

Figure 4.8. Absolute difference between carpal adduction (-)/abduction (+) measured using the JCS and MPA.

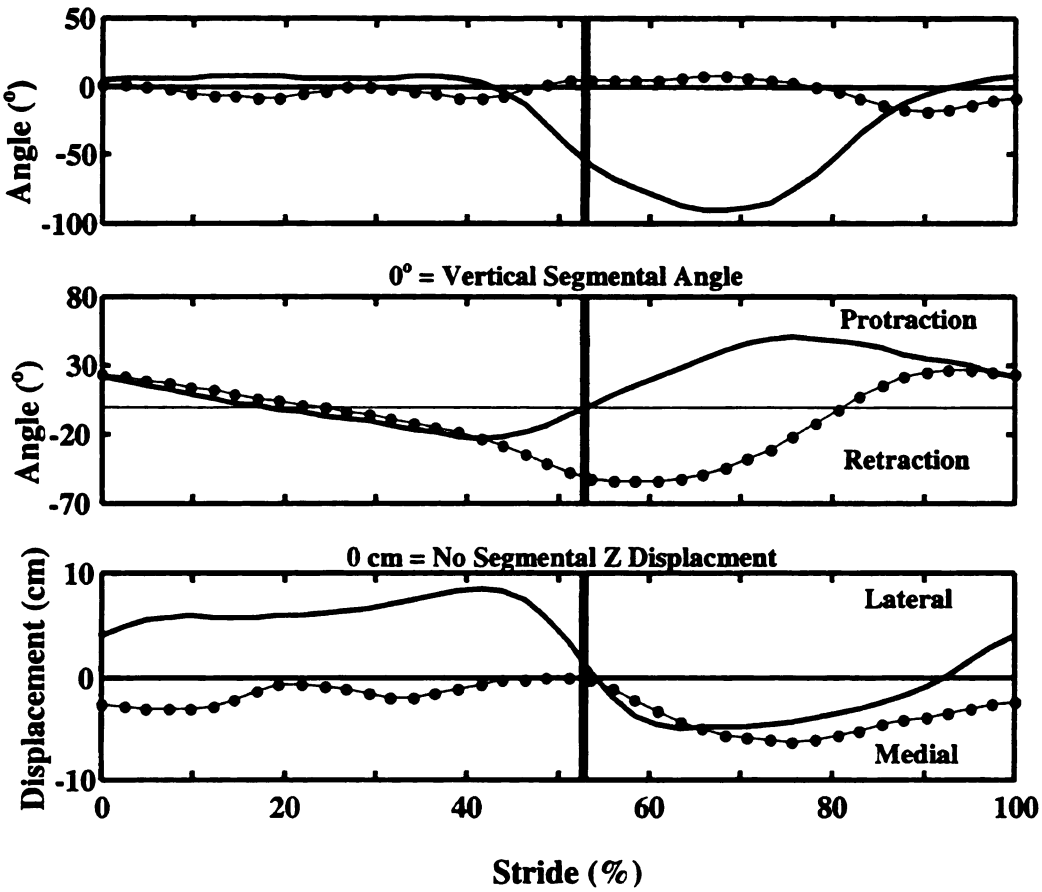

Figure 4.9. **Top graph**: Carpal flexion (-)/extension (+) (solid line) and internal (-) /external (+) rotation (dotted line) measured using the JCS. **Middle graph**: Segmental angles in GCS sagittal plane for antebrachium (solid line) and metacarpus (dotted line). **Bottom graph**: Z displacement between the proximal and distal tracking markers for the antebrachium (solid line) and metacarpus (dotted line). The thick vertical line at 53% of the stride is the time when carpal adduction/abduction angles measured with the JCS and MPA have the maximal difference.

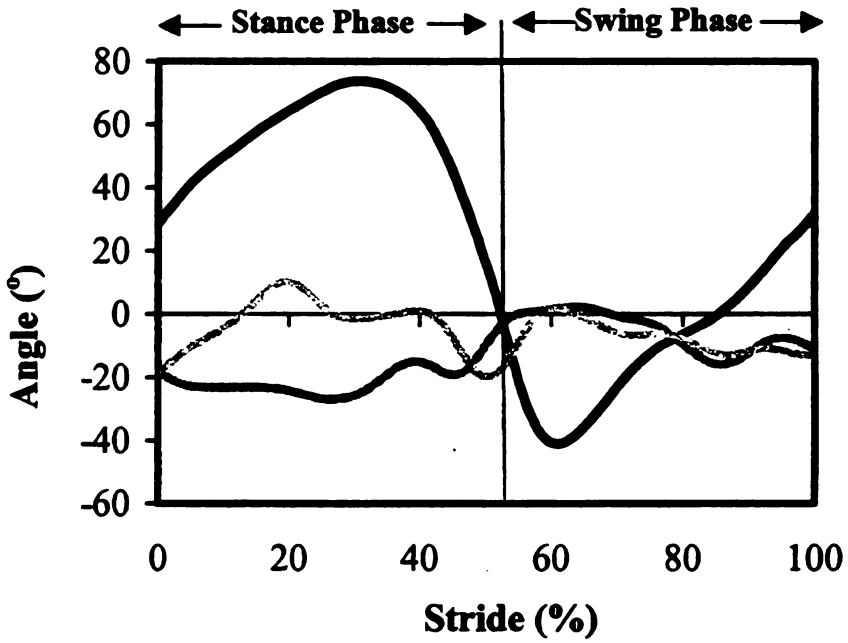

Figure 4.10. Mean fetlock flexion (-)/extension (+) (black line), adduction (-)/ abduction (+) (dark gray line), internal (-)/external (+) rotation (light gray line) using JCS.

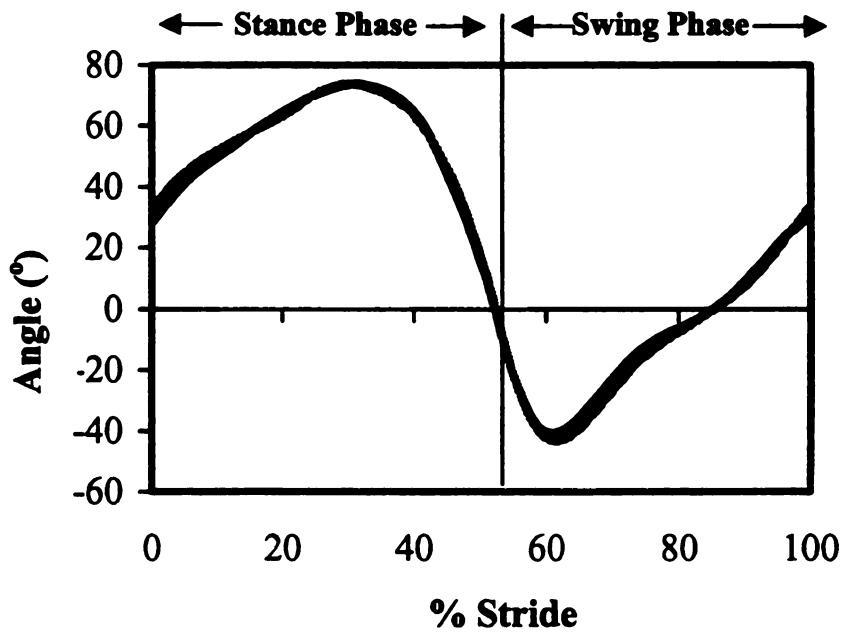

Figure 4.11. Mean fetlock flexion (-)/extension (+) for JCS (black line) and MPA (gray line).

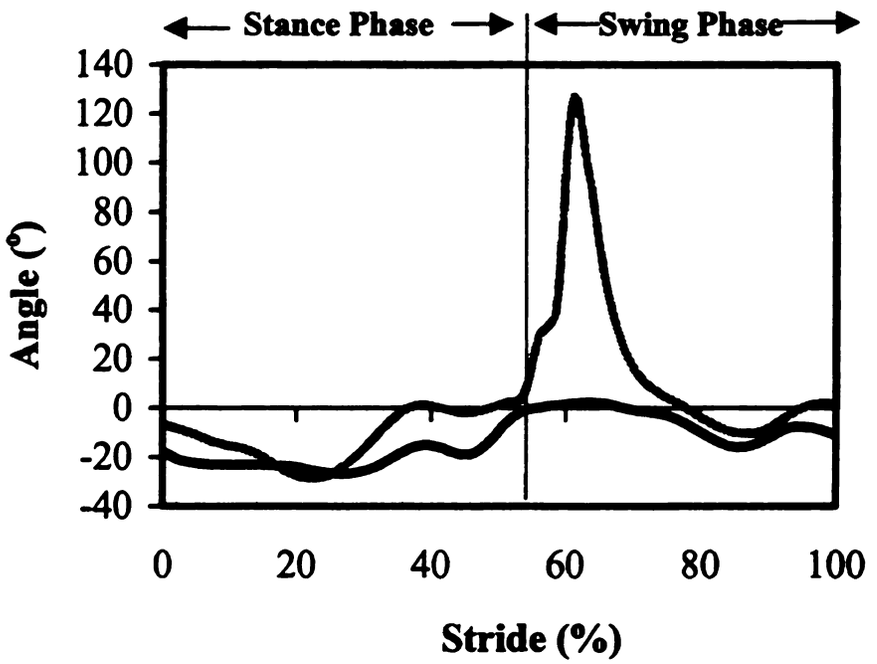

Figure 4.12. Mean fetlock adduction (-)/abduction (+) for JCS (black line) and MPA (gray line).

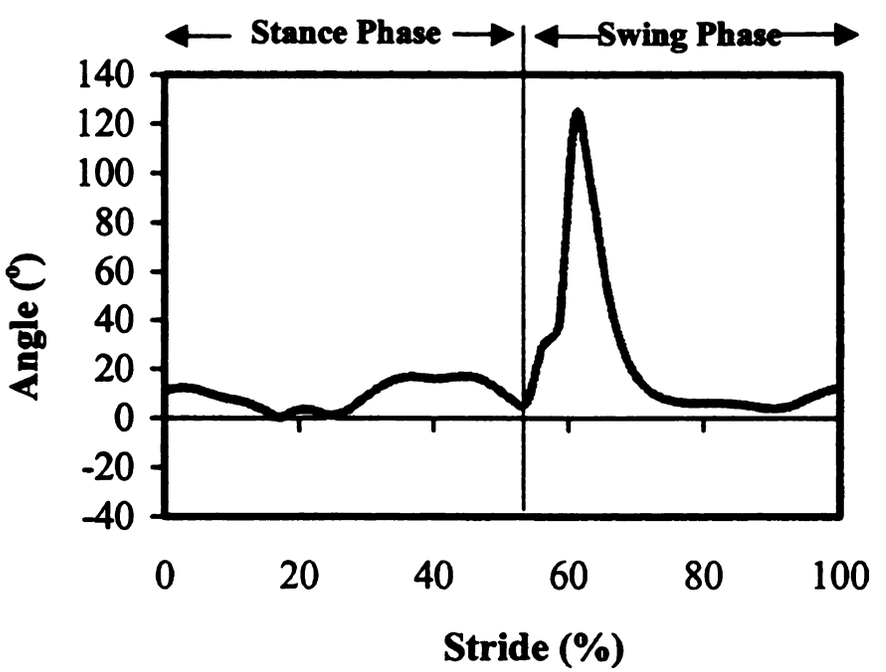

Figure 4.13. Absolute difference between fetlock adduction (-)/ abduction (+) measured using the JCS and MPA.

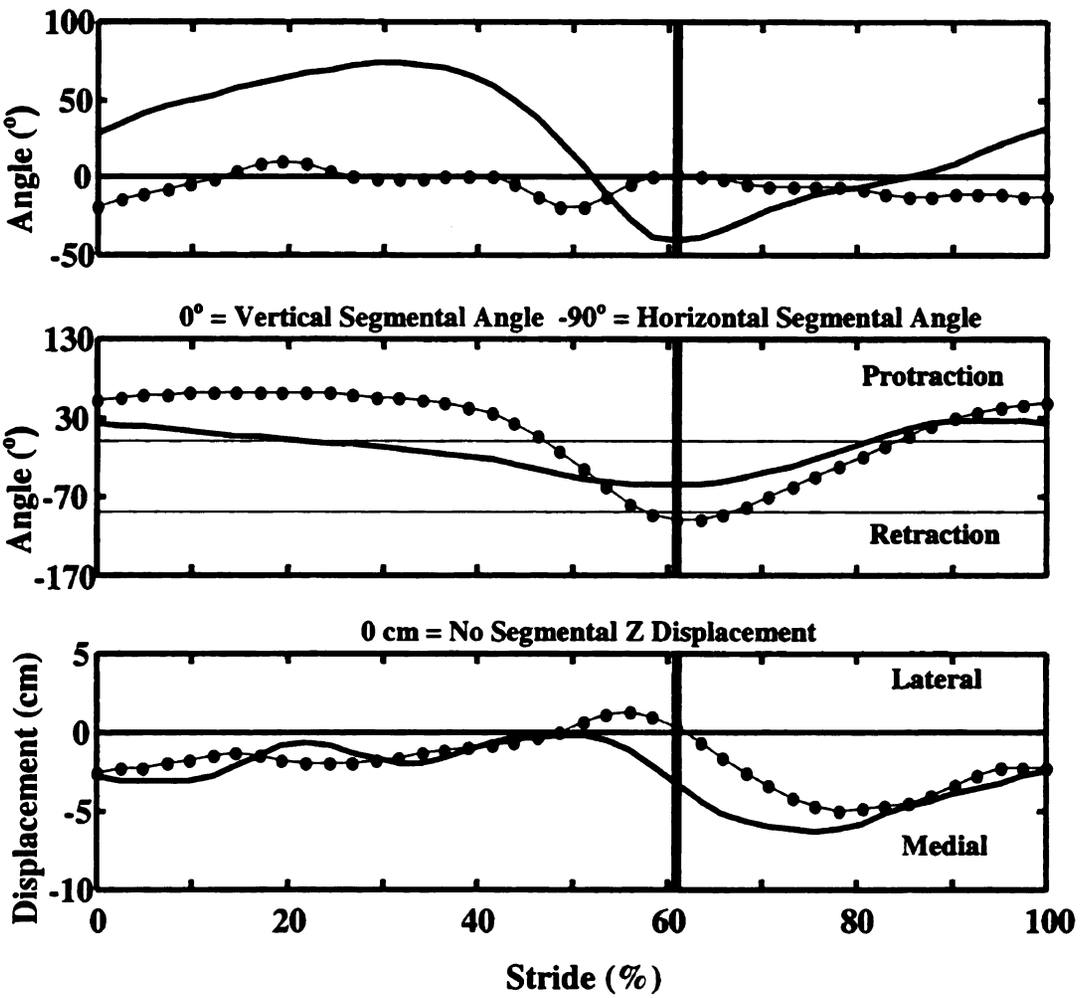

Figure 4.14. **Top graph**: Fetlock flexion (-)/extension (+) (solid line) and internal (-) /external (+) rotation (dotted line) measured using the JCS. **Middle graph**: Segmental angles in GCS sagittal plane for metacarpus (solid line) and pastern (dotted line). **Bottom graph**: Z displacement between the proximal and distal tracking markers for the metacarpus (solid line) and pastern (dotted line). The thick vertical line at 61% of the stride is the time when carpal adduction/abduction angles measured with the JCS and MPA have the maximal difference.

Fetlock flexion/extension patterns were similar when measured using the MPA and JCS (Figure 4.11) with extension during stance and flexion during swing. Both MPA and JCS showed adduction during stance with peak abduction during early swing, but the peak abduction angles were quite different between JCS and MPA (Figure 4.12). The peak absolute difference (136°) between the JCS and MPA adduction/abduction angles occurred at 61% of the stride (Figure 4.13), which coincided with peaks of flexion and a small amount of external rotation (Figure 4.14). As the absolute difference in adduction/abduction between the JCS and MPA increased, the pastern segment angle decreased reaching -90° around the time the adduction/abduction absolute difference peaked (Figure 4.14). The difference in z coordinates of the proximal and distal markers along the pastern long axis was zero at this point indicating that the pastern long axis was aligned with the x-axis of the MPA global coordinate system (Figure 4.14).

Discussion

Since the JCS is an anatomically-based coordinate system, it moves dynamically with the horse's anatomy so that the axes of the coordinate system make adjustments for the subject's angle of travel, conformation, and unique limb motion patterns, such as the termino. Since MPA is based upon a global coordinate system, the axes are not dynamic and do not adjust to the changes in anatomical orientation as the horse moves. This is the basis for the differences in adduction/abduction angles measured using JCS and MPA. Understanding the movement of the horse during locomotion will assist in locating where this limitation for MPA creates error in the measurements of adduction/abduction.

During the stance phase, the horse's body moved laterally over the supporting forelimb as shown by the z displacements in Figure 4.9, which shows the proximal end of the radius is lateral to it's distal end throughout stance. The antebrachium and metacarpus were retracted with approximately equal angular velocities until breakover when the antebrachium reversed its direction of rotation reaching a vertical position at lift off, while the metacarpus continued to be retracted. This combination of segmental motions resulted in carpal joint flexion. During breakover the horse's body moved medially until at lift off the proximal and distal ends of the antebrachium were aligned vertically when viewed in the frontal plane (Figure 4.9). Therefore, at lift off the antebrachium was vertical when viewed in either the sagittal or frontal plane. Under these conditions any axial rotation of the antebrachial segment would have a large effect on the adduction/abduction angle of the carpal joint as seen in the frontal plane using MPA (Figure 4.15). This orientation of the proximal segment and the error that is created under the conditions described above is illustrated in the 3-D surface graph (Figure 4.16). This shows the effects of different combinations of axial rotation of the proximal segment and flexion of the joint due to retraction of the distal segment on the adduction/abduction error in the MPA measurements. The derivations of this relationship is given in Appendix B. When axial rotation of the proximal segment occurs, it creates an adduction/abduction error in the frontal plane measurements.

At lift off (55% of the stride), the pastern segment had rotated beyond the horizontal (sagittal plane angle -92°). At this time, the difference between the z coordinates of the proximal and distal markers on the pastern long axis was zero so that the distal aspect of the segment was not visible in the frontal view during the time that the

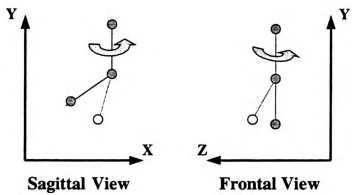

Figure 4.15. The true flexion/extension (sagittal view) and adduction/abduction (frontal view) angles (solid line) and the angular errors (dashed line) created in the apparent position of the distal segment by a rotation of the proximal segment when measured using MPA. The illustration shows the apparent rotation of the distal segment after rotation of the proximal segment although there is no real change in the flexion/extension (left) and adduction/abduction (right).

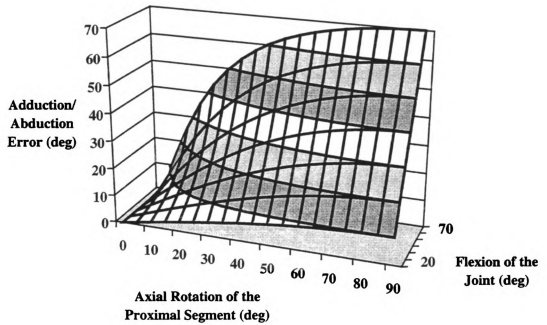

Figure 4.16. Contour surface showing adduction (-)/abduction (+) error measured by MPA in the frontal plane as a result of different combinations of created by axial rotation and flexion when the proximal segment is vertical in the sagittal plane. The shading along the contour indicates the error (deg), the vertical line along the contour indicates axial rotation of only the proximal segment (deg), and the horizontal line indicates the joint flexion angle (deg). The error is based on calculations shown in Appendix B.

pastern segment was rotated beyond –90°. Under these conditions, the angle of the pastern segment was difficult to measure in the frontal plane because the pastern segment was behind the metacarpal segment when the sagittal plane angle was –90° or the pastern segment was hidden behind the metacarpal segment when it rotated beyond –90°. Under these circumstances, any axial rotation of the metacarpal segment, even without flexion/ extension or adduction/abduction of the fetlock joint, allowed the pastern segment to become visible in the frontal view. Thus, axial rotation of the metacarpus was misinterpreted as adduction/abduction of the fetlock joint in MPA. The sudden large peak in MPA fetlock adduction/abduction just after lift off (Figure 4.12) occurred during a period of axial rotation of the metacarpus while the pastern segment angle was past the horizontal, but the adduction/abduction angle of the fetlock was not changing. Internal rotation of the metacarpus created an artificial abduction of the fetlock in the frontal view. External rotation would have created the impression of fetlock adduction. If there were no metacarpal axial rotation, the pastern segment could not be tracked using MPA until the amount of retraction angle decreased to less than –90°.

Using MPA, Back *et al.* (2000) studied the effect of heel wedges on frontal plane motion of the hind pastern relative to the metatarsus. The problems described above for frontal plane measurements of the fetlock joint were avoided by measuring the changes in adduction/abduction with and without heel wedges during the stance phase only. The findings presented here show that smaller differences were found between JCS and MPA adduction/abduction measurements during stance. The hind fetlock joint was found to show increased abduction with the heel wedges during stance. Limiting frontal plane

measurements to the stance phase reduced some of the problems in using MPA, but would not completely resolve errors due to differences in the JCS and MPA axes.

Based on in vitro studies of pastern joint loading, Degueurce *et al.* (2000) described the three movements of the joint as always being associated. The relationship between the different types of movement affects the axes of the JCS. For example, the JCS adduction/abduction axis is perpendicular to both the flexion/extension and internal/external rotational axes. Therefore, flexion/extension and/or internal/external rotation will cause a shift in the orientation of the adduction/abduction axis. This dynamic quality of the JCS axes allows for the depiction of the relationship or coupling between the three joint movements. On the other hand, the MPA axes do not move with the anatomy nor do they account for the relationship between the three joint movements. Therefore, comparing measurements made using the dynamic axes of the JCS with those made using the static axes of MPA will undoubtedly show differences, especially when the orientation of the segments and joints fulfil the conditions described above. The angle between the JCS adduction/abduction axis and the GCS x-axis is illustrated in Figure 4.17. The minima and maxima of the traces represent the minimal and maximal absolute differences between the adduction/abduction angles measured using the JCS and MPA indicating that the adduction/abduction axis of the JCS has a significant effect on the measured angle.

The dynamic quality of the JCS adduction/abduction axis is illustrated in Figure 4.18 for the carpus and Figure 4.19 for the fetlock. Each graph represents a single stride. The JCS adduction/abduction axis originating from the y displacement curve of the joint center was plotted for every 3% of the stride. It can be seen that the orientation of the

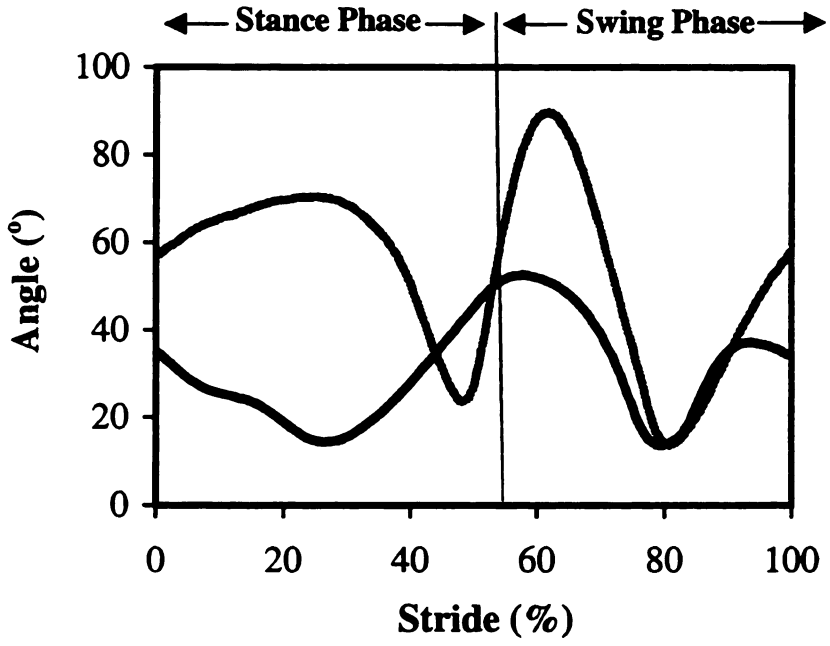

Figure 4.17. Angle between the JCS adduction/abduction axis and the x-axis of the GCS for the carpal joint (black line) and the fetlock joint (gray line).

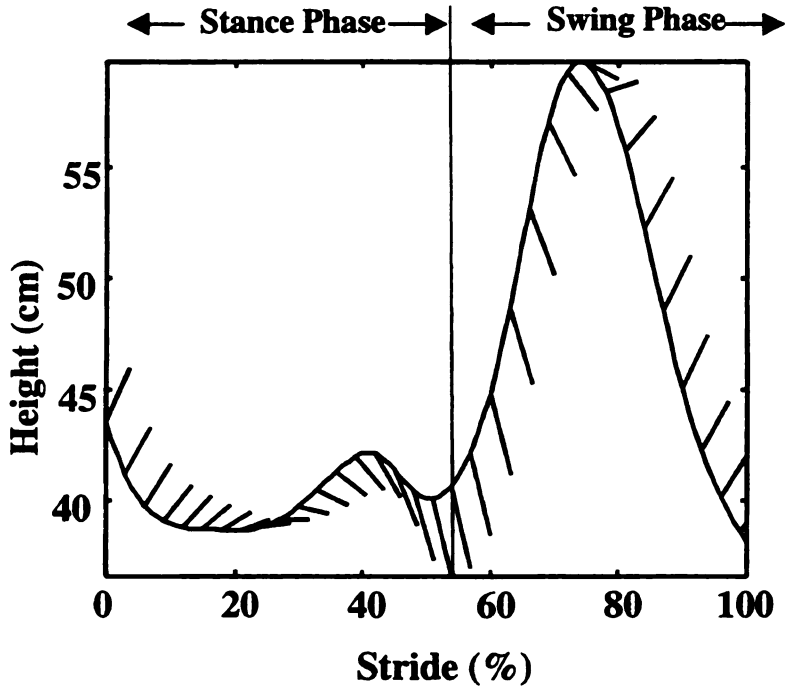

Figure 4.18. Y displacement of the carpal joint center throughout a single stride and the corresponding orientation of the JCS carpal adduction/abduction axis within the sagittal plane shown at intervals of 3% of the stride.

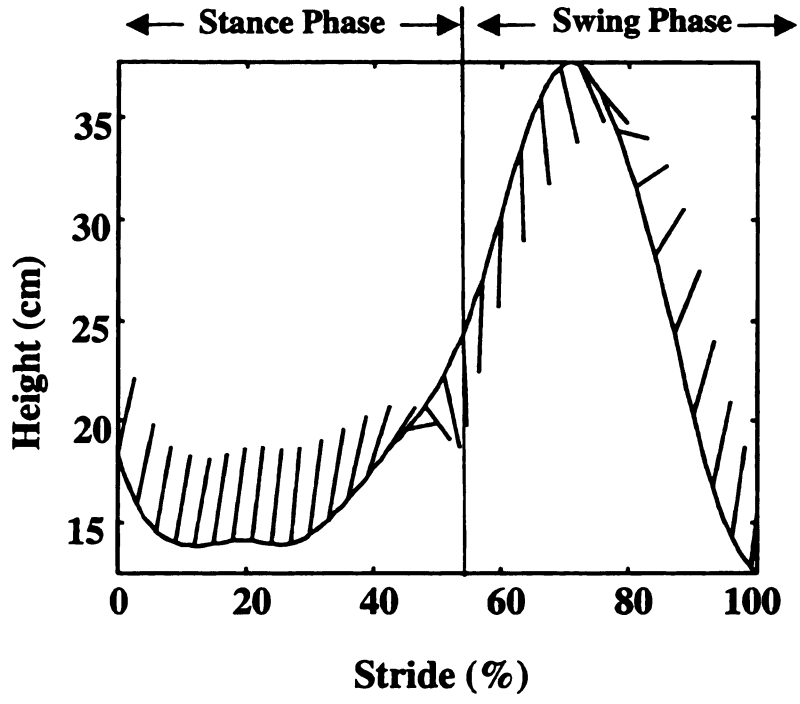

Figure 4.19. Y displacement of the fetlock joint center throughout a single stride and the corresponding orientation of the JCS carpal adduction/abduction axis within the sagittal plane shown at intervals of 3% of the stride.

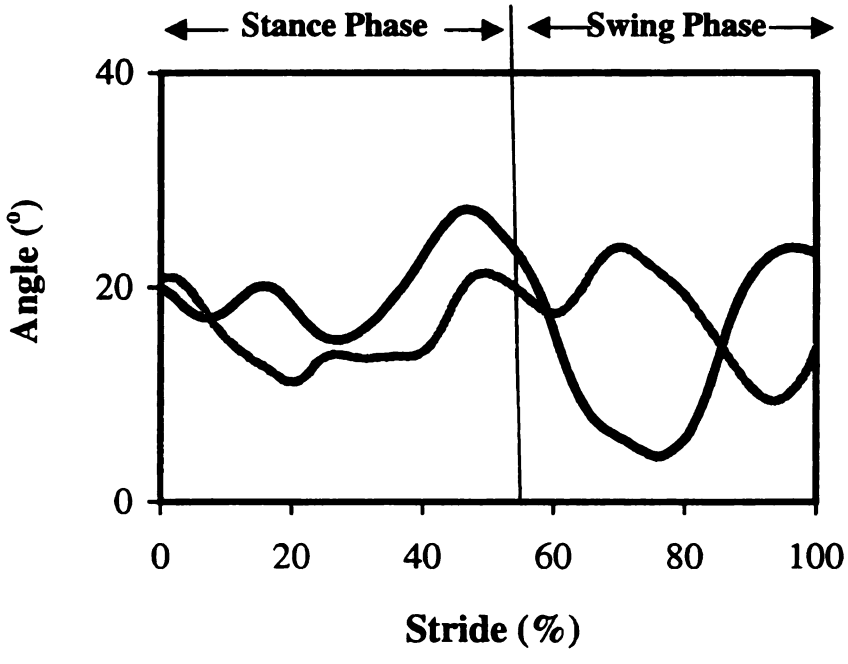

Figure 4.20. Angle between the JCS flexion/extension axes and the z-axis of the GCS for the carpal joint (black line) and the fetlock joint (gray line).

adduction/abduction axis as seen from the sagittal view changes as the joint center moves vertically throughout the stride. The y displacement of the joint center was chosen as the variable for the vertical axis to facilitate visualization of the motion of the joint in the sagittal plane throughout the stride. For the MPA measurements, the adduction/ abduction axis does not move with the limb motion. Therefore, when the orientation of the JCS adduction/abduction axis is not parallel with the corresponding GCS axis as seen during breakover (Figure 4.18) there are more differences measured between the JCS and MPA adduction/abduction angles. Around 20% of the stride (Figure 4.18), the JCS and MPA adduction/abduction axes are almost parallel resulting in less error (Figure 4.8).

The angle at which the horse traveled through the data collection area was transformed during post-processing of the data so that it was aligned with z-axis of the JCS. This resulted in a relatively small difference between the flexion/extension axis of the JCS and z-axis of the GCS (4° to 26°; Figure 4.20) compared with the relatively large difference between the adduction/abduction axis of the JCS and x-axis of the GCS (14° to 92°; Figure 4.17). Thus, differences between the flexion/extension measurements for the two techniques were minimized. However, even after correcting for the horse's angle of travel, there were small differences in the flexion/extension measurements due to the fact that axial rotation was not accounted for when using MPA. The angular difference between the JCS and MPA flexion/extension axes at the fetlock were fairly consistent throughout the stride with peak differences corresponding with peak adduction/abduction axes differences. The fact that the peak angular difference in the JCS and MPA carpal flexion/extension axes occurred during stance whereas the peak angular difference in adduction/abduction axes occurred during swing may be due to the lateral movement of

the body over the limb during stance and the accompanying change in radial orientation due to this rotation. Differences due to radial orientation may be minimized by choosing appropriate axes for establishing the radial segmental coordinate system.

A limitation to the JCS used in this study was the selection of the primary axis used for establishing the segmental coordinate system. In order to facilitate direct comparisons with earlier three-dimensional analyses using a JCS, the axis created by the two virtual markers along the segmental long axis was used as the base axis for establishing the segmental coordinate system. However, the radius is wider proximally than distally and the proximal marker is somewhat lateral to the distal marker. This affects the orientation of the coordinate system so that it may not truly represent the load bearing axis of the antebrachium. The greater the discrepancy, the greater will be the off-set of the base axis from the load bearing axis of the segment. This also explains why the peak absolute difference between the JCS and MPA carpal adduction/abduction is slightly offset from the point at which the radius is vertical as seen on the bottom graph in Figure 4.9. In future studies, it may be preferable to use the axis through the medial and lateral markers on the distal aspect of the segment as the base axis of the antebrachial coordinate system so that difference in size of the proximal and distal radial epiphyses has less effect on measuring the load bearing axis of the segment.

Conclusions

Human kinematic studies have applied three-dimensional analysis using a JCS to describe the relative rotations between segments (Grood and Suntay 1983; Soutas-Little *et al.* 1987). Since the JCS is oriented to the subject's anatomy, rather than to the

calibrated space through which the movement occurs, the subject does not have to move completely straight through the data collection area. The JCS method has the additional benefits of measuring axial rotations and having the ability to detect coupling between the three types of joint motion. However, the JCS setup for tracking an anatomical coordinate system is lengthy and in equine subjects it may not be practical for most clinical applications. The additional effort involved in using a JCS rather than MPA is justified if it offers improvement in the accuracy in the measurements of joint motion. The results of this study show that carpal and fetlock joint kinematics measured in the sagittal plane using MPA compared well with flexion/extension angles measured using a JCS. Therefore, MPA appears to be adequate for measurement of flexion and extension of the carpus and fetlock at the walk provided corrections are made to align the angle of travel with the GCS established by the calibration frame.

Previous studies have measured carpal and fetlock adduction/abduction angles between the forelimb and the ground (Herring *et al.* 1992; Peloso *et al.* 1993) rather than between the proximal and distal segments comprising the joint, which limits the accuracy of this measurement. Comparisons between the adduction/abduction angles of the carpal and fetlock joints using MPA and JCS showed quite different patterns and magnitudes with the two techniques. The fact that the JCS gave a more accurate interpretation of movements in the frontal plane indicates that it is more appropriate than MPA for describing adduction/abduction. The reasons for problems with frontal plane measurements cited in this chapter should be considered in measuring any type of equine locomotion using MPA.

It is concluded that the need to use a JCS versus MPA depends on the objectives of the study. If the only measurements required are flexion/extension in a sagittal plane, then planar analysis using a MPA appears to be adequate, provided care is taken to ensure that the subject moves straight and parallel with the plane of calibration. For measurements of other types of joint motion, it is recommended that more than two tracking markers are used per segment and a JCS or a similar anatomically-based system be used.

CHAPTER V

EXPERIMENT III: THREE-DIMENSIONAL MOTION OF THE CARPUS AND FETLOCK IN THE FORELIMB OF THE MISSOURI FOX TROTTER

Summary

The objective of this study was to measure carpal and fetlock joint kinematics of the flat walk and fox trot to provide a more comprehensive description of these gaits and to assist in distinguishing between them. During the flat walking stance phase, the carpus and the fetlock were extended and abducted. At breakover, the carpus was internally rotated as the fetlock was externally rotated. During early swing, the carpus and fetlock decreased the abduction angle as the joints flexed. At mid swing, the carpus reached peak internal rotation and the fetlock reached peak external rotation. At the fox trot, the carpus was abducted and extended during stance. There was a period of carpal external rotation that peaked before breakover followed by a cycle of flexion that peaked in mid-swing. The fetlock was extended throughout stance and showed a flexion cycle during swing. This joint showed a small amount of adduction and internal rotation during stance and switched to abduction and external rotation at breakover that continued throughout the swing phase. Although magnitudes between gaits were insignificant, except for carpal external rotation, the carpal and fetlock adduction/abduction patterns are different. Velocity, stride and stance durations, diagonal step duration, peak carpal external rotation, and carpal and fetlock adduction/abduction patterns distinguish the flat walk from the fox trot.

Introduction

The four-beat stepping gaits of the gaited horse are recognized by the sequence and timing of the limb placements, together with the characteristic limb movement styles. These are measured as the temporal, linear, and angular kinematics. The Missouri Fox Trotter gaits are the flat walk and the fox trot, both of which are described as four-beat, lateral sequence, stepping gaits that lack a period of suspension. The flat walk has a regular rhythm while the fox trot has an irregular rhythm with diagonal couplets. The flat walk is described as a faster version (5 mph) of the walk (Ziegler 2000). Hildebrand (1965) described the fox trot as a fast, lateral sequence, diagonal couplets walk. Clayton and Bradbury (1994) measured the temporal variables of the fox trot and found that lateral advanced placement was significantly longer than diagonal advancement placement, thus confirming that the rhythm of the gait is characterized by diagonal couplets. As a consequence of the irregular rhythm, the diagonal bipedal support periods were significantly longer than the lateral bipedal support periods. The angular kinematics of the fox trot have not been described. In chapters three (Experiment I) and four (Experiment II) the three-dimensional kinematics of the walk of the non-gaited horse and the Peruvian Paso were shown to have carpal and fetlock joint motion in the frontal and transverse planes. The objectives of this study are to describe the three-dimensional carpal and fetlock joint motions of the flat walk and fox trot of the Missouri Fox Trotter.

Materials and Methods

Subjects. The subjects were six Missouri Fox Trotters. The criteria for inclusion in the study were that the horses were sound, were registered as Missouri Fox Trotters,

and were naturally able to perform the flat walk and the fox trot gaits. The horses were ridden by an experienced gaited horse rider. Trials were excluded from the study if the horses were determined not to be performing the gait properly according to the following gait standards (Ziegler 2000):

Flat Walk: The flat walk is a regular, four-beat gait with a lateral sequence of footfalls: LH-LF-RH-RF. The support sequence alternates between periods of tripedal and bipedal support with approximately equal amounts of time being spent in diagonal bipedal and lateral bipedal support phases. The flat walk is performed at a faster velocity than the walk while maintaining a regular rhythm. If the rhythm becomes irregular, the horse is performing a fox walk.

Fox Trot: The fox trot is a four-beat stepping gait with a lateral sequence of limb placements similar to the walk. Unlike the flat walk, the fox trot is characterized by an irregular rhythm with diagonal couplets and longer periods of diagonal bipedal support than lateral bipedal support. A horse performing this gait gives the appearance of walking with the front limbs and trotting with the hind limbs. The fox trot is performed at a faster speed than the flat walk, otherwise the horse is performing a fox walk.

The fox walk is a transitional gait between the flat walk and the fox trot. It is characterized by a four-beat rhythm with lateral sequence of footfalls and diagonal

couplets, but does not demonstrate the visual characteristics of the fox trot and is described by the breed association as an undesirable gait (Ziegler 2000).

In this study, temporal variables were measured for the flat walk and fox trot. Forelimb protraction/retraction was determined from markers overlying the proximal aspect of the scapular spine and the lateral aspect of the distal hoof. Angles were measured relative to a line drawn perpendicular to the ground in the sagittal plane. Protraction angles were assigned positive values and retraction angles were assigned negative values.

Segmental Coordinate Systems. The axes of the coordinate systems for the antebrachial, metacarpal, and proximal phalangeal segments were established as described in chapter four. Briefly, the origin of the antebrachial coordinate system was located on the lateral styloid process of the distal radius. The x-axis was directed laterally from the origin perpendicular to the antebrachial sagittal plane and on the same vector as a line from the medial to lateral styloid process. The z-axis, contained in the antebrachial frontal plane, ran from the origin proximally along the antebrachial long axis at 90° to the x-axis. The y-axis ran dorsally from the origin, perpendicular to the antebrachial frontal plane.

The origin of the metacarpal coordinate system was located on the lateral aspect of the distal third metacarpus. The x-axis was directed laterally from the origin perpendicular to the metacarpal sagittal plane and on the same vector as a line from the medial to lateral aspect of the third metacarpus. The z-axis, contained in the metacarpal frontal plane, ran from the origin proximally along the metacarpal long axis at 90° to the

x-axis. The y-axis ran dorsally from the origin, perpendicular to the metacarpal frontal plane.

The origin of the proximal phalangeal segment was located on the lateral aspect of the distal end of the proximal phalanx. The z-axis ran from the origin proximally along the long axis of the segment. Similar to the other segmental axes, the x and y-axes ran laterally and dorsally from the origin, respectively.

Marker Placement. Both tracking and virtual markers were attached to the right forelimb to establish segmental coordinate systems for the antebrachial, metacarpal, and proximal phalangeal sements. In horses 1-3, the segmental coordinate systems were established and tracked using virtual marker "L" structures together with the tracking markers described in chapter three (Figure 5.1). In horses 4-6, the segmental coordinate systems were established with two virtual markers along the lateral side of the long axis and a third virtual marker on the medial side of each segment. The tracking markers

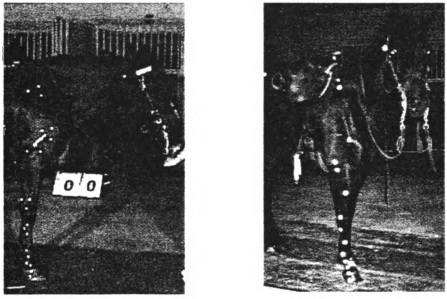

Figure 5.1. Tracking marker placement for horses 1-3 (left) and horses 4-6 (right).

were placed on the lateral and dorsolateral aspects of the segments as described in chapter four (Figure 5.1). Although the marker placements were different between horses 1-3 and horses 4-6, the segmental axes established by the markers were the same for all horses.

Two croup markers were placed along the sacral spine of horses 4-6 to determine vertical excursions calculated from the raw y coordinates. Markers were attached to the point of the elbow and the lateral aspect of the distal hoof for horses 1-3 to determine mediolateral shift of the body over the hoof calculated from the raw z coordinates.

Data Collection. The calibration volume (342 x 190 x 210 cm^3) was defined using 30 points. Kinematic data of the flat walk and fox trot were recorded using two 60 Hz camcorders (Panasonic AG-450, Matsushita Electric Corp., Secausus, NJ) placed on the lateral aspect of the right side of the horse and oriented at 60° to each other. Two additional camcorders placed in front of and behind the horse in increments of 60° to the lateral camcorders were used to locate the virtual markers on the medial aspect of the limb in the standing file. A 500-watt lamp was placed behind each camcorder to illuminate the retroreflective markers during recording.

The horses were ridden along the runway at a flat walk and fox trot. A trial was considered acceptable if the horse traveled at a consistent speed along a straight line that was aligned with the calibration volume with all markers being clearly visible in the two lateral camcorder views. Four trials were recorded for each horse at each gait.

Data Reduction. The frames of hoof contact, heel off and toe off were recorded for each limb and used to calculate stride duration, stance and swing durations of the right forelimb and right hind limb, and the time of onset and duration of breakover. The markers were automatically tracked and digitized using a video analysis system (Ariel

Performance Analysis System, Ariel Dynamics Inc, Trabuco Canyon, California). Three-dimensional coordinates of markers were obtained using direct linear transformation (Abdel-Aziz and Karara 1971). The raw data were filtered using a fourth-order Butterworth digital filter at a cutoff frequency of 6 Hz. The joint coordinate system (JCS), which was based on Grood and Suntay (1983), measured flexion/extension relative to the x-axis of the proximal segment, internal/external rotation around the z-axis of the distal segment, and adduction/abduction around a floating axis perpendicular to the proximal segmental x-axis and the distal segmental z-axis. Joint angles were expressed relative to the position of alignment of the proximal and distal segments. Flexion, adduction, and internal rotation were designated negative. Extension, abduction, and external rotation were designated positive.

Data Analysis. The angular measurements were time normalized to stride duration. Ensemble averages were calculated and plotted for the flexion/extension, adduction/abduction, and internal/external rotation of the carpal and fetlock joints at the flat walk and fox trot. Mean values $\pm$ SD were determined for the temporal variables, protraction/retraction angles, and maximal carpal and fetlock joint angles for both gaits. Mean values $\pm$ SD for each horse were graphed and included in Appendix C. Paired t-tests were used to determine differences for temporal variables and peak joint angular measurements between the flat walk and fox trot ($P < 0.05$).

Table 5.1. Gait characteristics (mean and ± SD) measured for the flat walk and fox trot strides used in this study. Significant differences (*) between gaits are given ($P < 0.05$). Measurements taken from horses 1-6 (n=6) unless indicated on table.

	Flat Walk	Fox Trot
Velocity (m/s)	1.75 ± 0.06*	3.17 ± 0.03*
Stride Duration (s)	1.17 ± 0.06*	0.63 ± 0.03*
Forelimb Stride Length (m)	1.95 ± 0.05	2.0 ± 0.03
Forelimb Stance Duration (s)	0.77 ± 0.06*	0.32 ± 0.02*
Forelimb Swing Duration (s)	0.40 ±0.05	0.31 ± 0.03
Forelimb Breakover Duration (s)	0.04 ± 0.01	0.03 ± 0.01
Hindlimb Stance Duration (s)	0.78 ± 0.06*	0.33 ± 0.03*
Hindlimb Swing Duration (s)	0.35 ± 0.04	0.31 ± 0.01
Hindlimb Breakover Duration (s)	0.04 ± 0.01	0.03 ± 0.01
Lateral Step Duration (s)	0.30 ± 0.01	0.23 ± 0.02
Diagonal Step Duration (s)	0.32 ± 0.03*	0.10 ± 0.01*
Protraction/Retraction Range of Motion (°)	57 ± 3	64 ± 2
Protraction (°)	22 ± 4	28 ± 3
Retraction (°)	-35 ± 4	-36 ± 2
Croup Vertical Excursions (cm) (Horses 4-6)	7 ± 1	9 ± 2
Mediolateral Shift over Hoof (cm) (Horses 1-3)	6 ± 3	4 ± 1

Table 5.2. Standing angles for carpal and fetlock flexion/extension (F/E), adduction/abduction (Ad/Ab), and internal/external (I/E) rotation of the six Fox Trotters and the mean and ± SD for all horses. Angles are measured relative to the position of alignment of the proximal and distal segment. Flexion, adduction, and internal rotation are assigned negative values.

	Horse #						
	#1	#2	#3	#4	#5	#6	Mean (± SD)
Carpal F/E (°)	3	5	5	6	3	-3	3 (3)
Carpal Ad/Ab (°)	3	7	10	4	3	2	4 (3)
Carpal I/E Rotation (°)	2	-2	-4	5	-2	-3	-1 (4)
Fetlock F/E (°)	30	19	31	24	20	33	26 (7)
Fetlock Ad/Ab (°)	6	8	4	6	8	2	6 (2)
Fetlock I/E Rotation (°)	3	7	5	2	2	4	4 (2)

Table 5.3. Mean (SD) for peak values of three-dimensional joint motions of the carpus and fetlock for the flat walk and fox trot (n=6). Significant differences (*) between gaits are given ($P < 0.05$). Joint motions occurring at different phases of stride were not statistically compared (†). The percent of stride at which the peaks occurred is in square brackets under the peak value.

	Flexion/extension (deg)		Internal/external rotation (deg)		Adduction/abduction (deg)	
	Flexion	Extension	Internal (minimal external rotation)	External	Adduction (minimal abduction)	Abduction
Flat Walk Carpus	-64 (3) [72%]	8 (4) [11%]	-17 (6) [69%]	12 (8)* [39%]	-4 (6) † [83%]	10 (6)* [94%]
Fox Trot Carpus	-67 (6) [74%]	10 (4) [17%]	-11 (6) [86%]	3 (4)* [28%]	4 (2) † [8%]	20 (3)* [78%]
Flat Walk Fetlock	-30 (1) [67%]	56 (3) [23%]	2 (9) [48%]	27 (6)† [73%]	3 (3) † [82%]	27 (6) † [40%]
Fox Trot Fetlock	-26 (7) [65%]	58 (4) [37%]	-2 (8) [23%]	30 (9)† [68%]	-6 (7) † [16%]	18 (7) † [54%]

Results

Flat Walk. The velocity of 1.75 ± 0.06 m/s was achieved using a stride length of 1.95 ± 0.05 m and a stride duration of 1.170 ± 0.06 s (Table 5.1). The forelimb stance phase occupied the period from 0 to 48% of the stride with breakover starting at 40% of the stride and lasting 0.04 ± 0.01 s. The forelimbs demonstrated a maximum protraction angle of 22° ± 4 and maximum retraction angle of -35° ± 4.

The three-dimensional standing angles of the carpus and fetlock for each horse are shown in Table 5.2. During stance, the carpus was slightly extended and abducted (Figure 5.2). Maximal extension of 8° was recorded at 11% of the stride, but maximal abduction of 10° did not occur until the swing phase around 94% of the stride (Table 5.3). The carpus rotated externally throughout most of stance, with peak value occurring around the start of breakover. A peak in internal rotation occurred around lift off and a larger peak (-17°) in mid swing around the time of peak flexion (Figure 5.2, Table 5.3).

The fetlock was extended, abducted, and externally rotated throughout the stance phase with a distinct extension peak (56°) in mid stance. During breakover, there were decreases in abduction and external rotation. In the swing phase the fetlock joint had two flexion peaks. The larger flexion peak (-30°) at 67% of stride was followed by a smaller peak (-16°) at 85% of the stride (Figure 5.3). Peak abduction of the fetlock (27°) occurred at the start of breakover. The fetlock was externally rotated throughout the stride with peak external rotation (27°) occurring at 73% of the stride between the two flexion peaks (Figure 5.3).

Fox Trot. The velocity of 3.17 ± 0.03 m/s was significantly faster and was achieved using a significantly shorter stride duration of 0.63 ± 0.03 s and fore

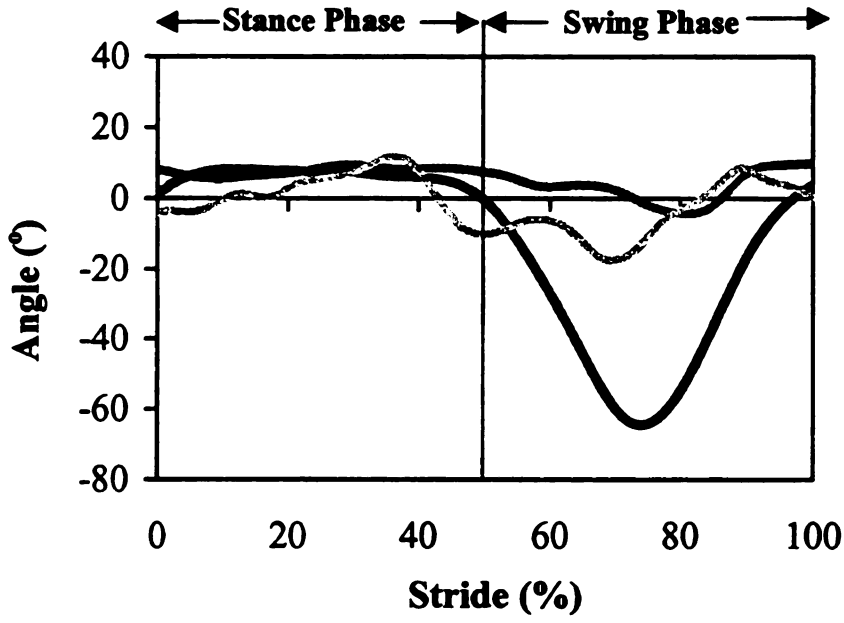

Figure 5.2. Mean carpal flexion (-)/extension (+) (black line), adduction (-) /abduction (+) (dark gray line), internal (-)/external (+) rotation (light gray line) of the flat walk (n=6).

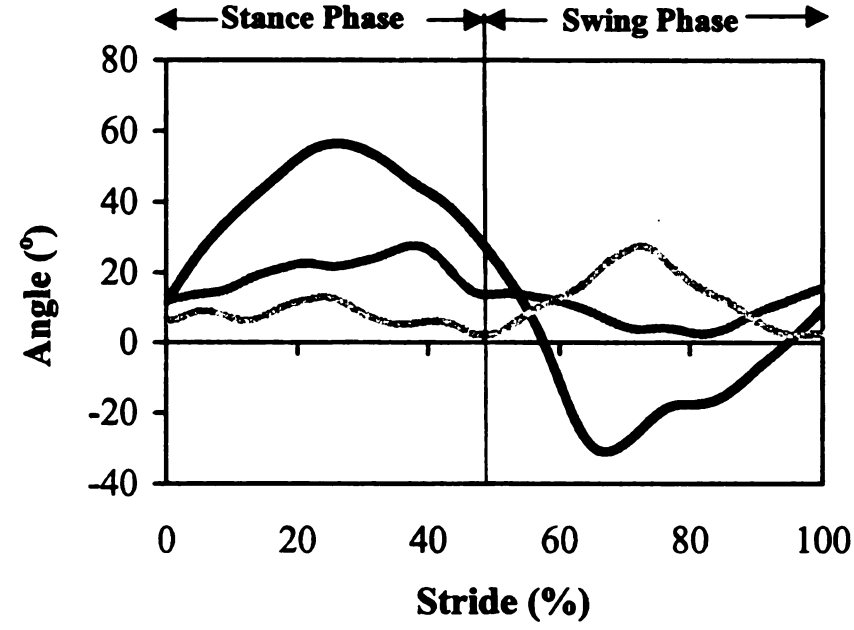

Figure 5.3. Mean fetlock flexion (-)/extension (+) (black line), adduction (-) /abduction (+) (dark gray line), internal (-)/external (+) rotation (light gray line) of the flat walk (n=6).

(0.32 ± 0.02 s) and hind limb (0.33 ± 0.03 s) stance durations (Table 5.1). Stride length did not differ between the flat walk and the fox trot. The forelimb stance phase occupied the period from 0 to 44% of the stride with breakover starting at 37% of the stride. There was a trend toward a reduction in breakover time in the fox trot, compared with the flat walk, especially in the forelimbs. An irregularity of rhythm with diagonal couplets was achieved using a shorter diagonal step duration of 0.10 ± 0.01 s and a longer lateral step duration of 0.23 ± 0.02 s compared to the flat walk. The forelimbs demonstrated a maximum protraction angle of 28° ± 3 and maximum retraction angle of -36° ± 2. Although these angles did not differ significantly between gaits, there was a trend toward greater forelimb protraction at the fox trot. In switching from the flat walk to fox trot, the range of croup vertical excursions increased by 2 cm (horses 4-6) and mediolateral shift over the hoof decreased by 2 cm (horses 1-3; Table 5.1).

The carpus was extended through stance with peak extension (10°) at 17% of the stride, after which the carpus flexed slowly at first, then more rapidly during breakover. The carpus reached peak flexion (-67°) around 74% of stride (Figure 5.4, Table 5.3). Throughout the entire stride, the carpus was abducted with maximum abduction (20°) at mid swing. Maximum carpal abduction angles were significantly different between gaits (Table 5.2). The carpus showed minimal axial rotation during stance, but was internally rotated from the start of breakover through the swing phase with a peak value of -11° (Figure 5.4). Peak external rotation was significantly less in the fox trot than the flat walk (Table 5.3).

The fetlock joint was extended throughout stance with peak extension (58°) during late stance around the start of breakover. The fetlock extension angle gradually

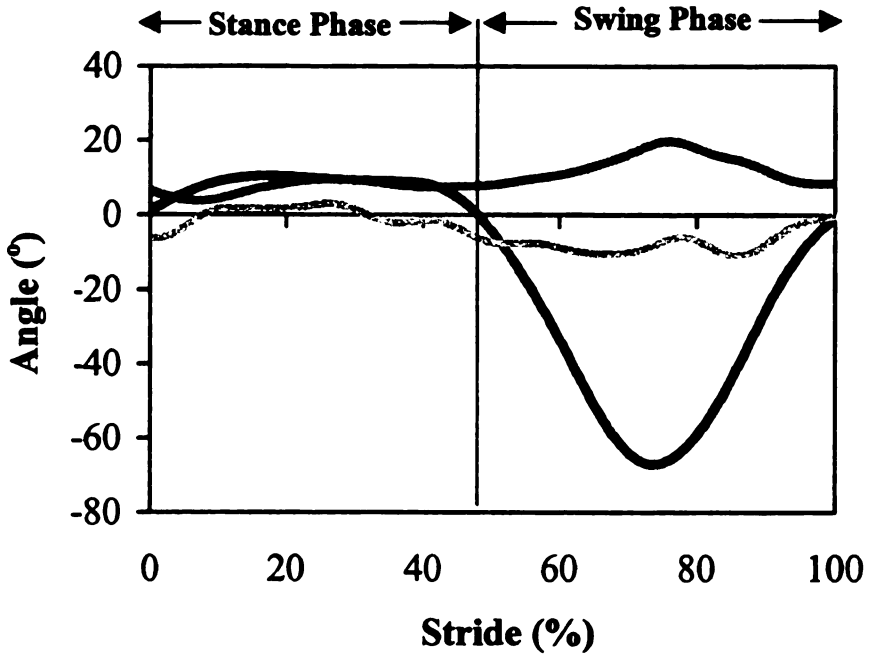

Figure 5.4. Mean carpal flexion (-)/extension (+) (black line), adduction (-)/ abduction (+) (dark gray line), internal (-) /external (+) rotation (light gray line) of the fox trot (n=6).

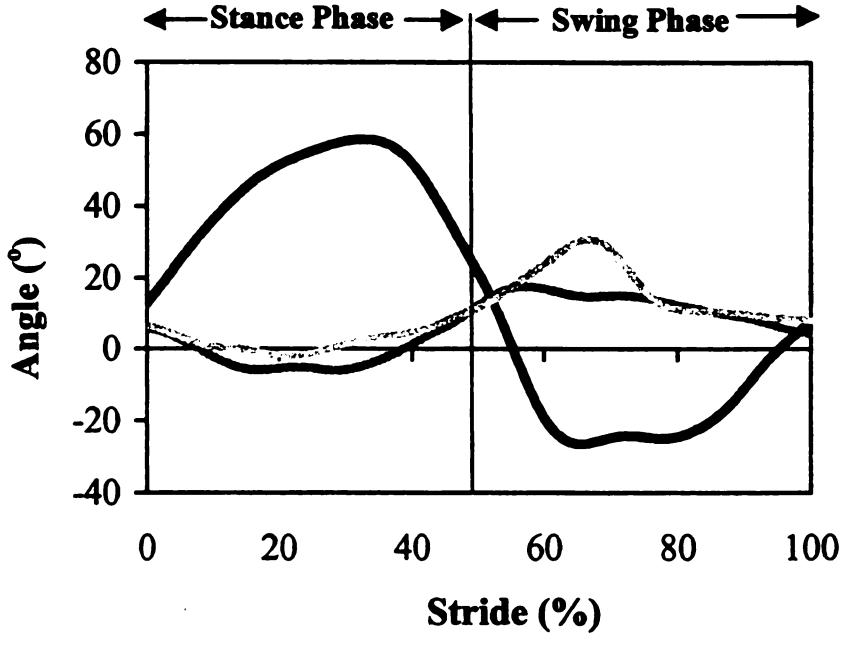

Figure 5.5. Mean fetlock flexion (-)/extension (+) (black line), adduction (-)/ abduction (+) (dark gray line), internal (-)/external (+) rotation (light gray line) of the fox trot (n=6).

decreased throughout breakover and into early swing. There was a flexion peak (-26°) in early swing, followed by a slightly smaller flexion peak (-25°) in mid swing (Figure 5.5). The fetlock showed a small amount of adduction in the middle of the stance phase, but was abducted during breakover and throughout swing, reaching peak abduction (18°) in early swing. There was little axial rotation during stance, but the fetlock showed external rotation during breakover and throughout swing with a distinct peak in early swing (30°), coinciding with the first flexion peak.

Discussion

In the equine limbs, motions of the joints distal to the hip and shoulder are largely restricted to the sagittal plane as a result of anatomical constraints that have evolved to minimize energy expenditure during limb protraction and retraction (Budiansky 1997). Therefore, motions in the frontal and transverse planes are relatively small in most horses. However, in chapter three and four, the carpus and fetlock were found to demonstrate measurable amounts of adduction/abduction and internal/external rotation during walking. This chapter shows that adduction/abduction and internal/external rotation of the carpal and fetlock joints occur at both gaits.

Measurement of joint motions outside of the sagittal plane may assist in the distinction between the gaits of the gaited horse. For example, when comparing the flat walk and fox trot, the differences in flexion/extension are quite small, but there are larger differences in adduction/abduction and internal/external rotation. At the carpus, although there are slight differences in the peak flexion and extension, the motion outside of the sagittal plane shows greater differences between gaits, particularly between the peak

abduction and external rotation. At the fetlock, flexion/extension profiles are similar for the two gaits, except peak extension occurs later in the fox trot, but the motions outside of the sagittal plane show larger differences, particularly in the timing of the peak values. The similarities between the forelimb sagittal plane joint motions in the two gaits may explain why the fox trot is described as walking in the forelimbs (Imus 1995).

The measurement of temporal variables further assists in differentiating between gaits in that velocity, stride duration, diagonal step duration, and fore and hind limb stance durations show significant differences between gaits. The stride length was similar for both gaits, which indicates that the Fox Trotter increases stride rate rather than stride length to increase speed. This is in contrast to dressage horses moving from a collected to extended walk in which stride length makes a much larger contribution to changes in speed than stride rate (Clayton 1994), but is similar to recreational horses that increase walking speed primarily by increasing stride rate (Nicodemus *et al.* 2000c).

Hind limb kinematics were not measured in detail in this study, but visual observations along with croup vertical excursions measurements indicate an increase in hindquarters vertical excursions in the fox trot, which is a common characteristic noted in the fox trot (Imus 1995). Croup markers on horses 4-6 showed that vertical excursions increased by 2 cm at the fox trot compared with the flat walk (Table 5.1).

Earlier studies have described the temporal characteristics of the fox trot (Clayton and Bradbury 1994; Hildebrand 1965), but the angular kinematics of the limbs have not been reported. The Missouri Fox Trotter was chosen for this study to further describe the gaits of this breed, the flat walk and fox trot, using three-dimensional kinematic analysis. The results have shown that the ranges of abduction/adduction and internal/external

rotation of the carpal and fetlock joints of the Missouri Fox Trotter were larger than the ranges of motion of the non-gaited horses analyzed in chapter three and in earlier equine three-dimensional joint motion studies (Heleski 1991).

Carpal Joint. Although significant differences were found between the peak magnitudes of external rotation and abduction, the patterns of motion in all three planes were similar for the flat walk and fox trot. The carpus was abducted through the majority of the stride for both gaits, but the abduction was greater at the fox trot during swing.

Fetlock Joint. The flexion/extension patterns were similar for the two gaits except that peak extension occurred later in the stance phase for the fox trot than the flat walk. The extension pattern of the flat walk was more similar to a trotting profile than a walking profile (Heleski 1991). During breakover, the decrease in extension and beginning of flexion were more gradual in the flat walk due to a longer period of breakover. The flat walk showed more abduction during stance than the fox trot in which there was a slight adduction in mid stance. The internal/external rotation patterns were quite similar for the two gaits.

The most distinct kinematic difference between gaits was the reversal of the adduction/abduction curve during the stance phase of the fetlock (abducted in the flat walk, adducted in the fox trot). The following observations assist in explaining this reversal. At the flat walk, the horse's body spends most of the stride in tripedal support, and it is during a tripedal support phase with two fore and one hind limbs that peak fetlock abduction occurs. In measuring the raw z coordinates of elbow and hoof markers placed on horses 1-3, it was found that during this tripedal support phase the body shifted laterally over the stationary hoof in preparation for the following lateral bipedal support.

After the tripedal support phase with two hind limbs and one forelimb, the body moved medially in preparation for the following diagonal bipedal support phase. During the flat walk, the three horses demonstrated a mediolateral shift over the hoof of 6 cm compared to 4 cm in the fox trot in which diagonal bipedal support phases predominate with the body more centered to maintain balance (Table 5.1). Further analysis of the body motion relative to the limb segments using more appropriate marker placement on the horse's trunk would assist in substantiating these findings.

Differences between gaits for the carpal and fetlock adduction/abduction patterns are also apparent during the swing phase with peak carpal and fetlock adduction occurring during the flat walk swing phase and peak carpal and fetlock abduction during the fox trot swing phase. As described earlier, mediolateral movements of the body relative to the forelimb during stance cause adduction/abduction joint angular patterns that are specific to the gait. As a consequence of these body movements, the flat walk shows a decrease in abduction during breakover whereas the body motion of the fox trot shows increased abduction during breakover. Due to the twisting of the joint at lift off and the inactivity of the tendons and ligaments around the joints during early swing, the flat walk continues the pattern of decreasing abduction that started during breakover and the fox trot continues the pattern of increasing abduction. During late swing, when the tendon and ligaments around the joint become active to prepare the distal limb for ground contact, the direction of movement changes the abduction trends and in both gaits the abduction angles revert back toward the standing angles. Measurements of muscular activity and calculation of net joint moments and joint powers of the Missouri Fox Trotter

would assist in supporting these explanations of the differences in swing phase adduction/abduction patterns between the two gaits.

Gait Comparisons. Previous two-dimensional kinematic studies of the forelimb at the walk (Hodson *et al.* 2000) measured a slower velocity (1.4 m/s) with a similar stride duration (1.27 s) to the flat walk (1.170 $\pm$ 0.06 s) and a longer stride duration than the fox trot (0.631 $\pm$ 0.027 s). Hodson *et al.* (2000) reported a somewhat shorter walking forelimb stance duration at the walk (0.662 s) than the flat walk (0.77 $\pm$ 0.06 s) and a protraction/retraction range of motion (43.9°), which was less than either the flat walk (57° $\pm$ 3) or the fox trot (64° $\pm$ 2). At the trot, Back *et al.* (1994) reported a higher velocity (4.0 m/s) than the fox trot (3.17 $\pm$ 0.03 s), which was achieved using a slightly longer stride duration (0.67 s) with a shorter forelimb stance duration (0.27 s), and a smaller range of protraction/retraction (44.3°). The likely explanation for this is that the trotting horse utilizes the suspension phase, rather than the protraction/retraction range of motion to increase velocity. As for hind limb temporal variables, the flat walk hind stance duration (0.78 $\pm$ 0.06 s) fell within the range measured for a slow (1.033 s) to fast (0.383 s) walk (Nicodemus *et al.* 2000c), but the fox trot (0.33 $\pm$ 0.03 s) had a shorter hind stance duration. However, Holmstrom *et al.* (1994) measured a shorter hind stance duration at the trot (0.22 s) than the 0.352 s measured for the fox trot.

The flat walk and fox trot were found to have different flexion/extension characteristics than either the walk or trot. The fetlock flexion/extension range of motion measured by Hodson *et al.* (2000) in the walk (54°) was considerably smaller than the flat walk (86°) and the fox trot (84°), but Holmstrom *et al.* (1994) measured a larger range in the trot (92°). Back *et al.* (1994) found a larger range of flexion/extension at the carpus

(91°) of trotting Dutch Warmbloods compared with the flat walk (72°) and fox trot (77°). All of these gaits showed two distinct flexion peaks in the swing phase of the trotting fetlock that were also detected in the flat walk and fox trot.

Compared with the walk the flat walk has faster velocity with shorter stride and swing durations, but compared with the trot the flat walk has a slower speed with longer stride and stance durations. The fox trot has a faster velocity than the walk with shorter fore and hind stance and swing durations, but has a slower velocity than the trot with longer fore and hind limb stance durations. The stride duration of the fox trot is shorter than either the walk or trot giving a quicker stride rate. Compared with the walk and trot, both the flat walk and the fox trot have greater protraction/retraction, fetlock flexion/extension, carpal and fetlock adduction/abduction, and carpal and fetlock internal/external rotation ranges of motion. In the kinematic study of Back *et al.* (1994), trotting Dutch Warmbloods have a larger carpal flexion/extension range of motion than either the flat walk or fox trot. However, Heleski (1991) found a smaller range of carpal flexion/extension (76°) in trotting Arabians, which was similar to the ranges recorded in this study for the flat walk and fox trot. Differences in carpal flexion/extension between studies may be related to breed or gait. Galisteo *et al.* (1996) studied Andalusians, which are known to perform their gaits with much animation, and reported that the range of carpal flexion/extension was 92°, which was greater than either the flat walk or fox trot, while the fetlock range of motion in the Andalusians (84°) was similar to the flat walk and fox trot. Overall, the gait differences found in comparing two-dimensional studies of the walk and trot with this study demonstrate that the flat walk and fox trot are not only distinct from each other, but also distinct from the walk and trot.

Furthermore, comparisons between Heleski's three-dimensional data of the walk and trot with the flat walk and fox trot also show differences between the gaits outside of the sagittal plane. At the carpus, the adduction/abduction ranges of motion of the walk (14°) and trot (18°) were similar to the flat walk (14°) and fox trot (16°), respectively. As for the internal/external rotation, the trot (13°) was comparable to the fox trot (13°), but the walk (9°) was quite different from the flat walk (29°). At the fetlock, the adduction/abduction range of motion was smaller at the walk (7°) and trot (20°) than the flat walk (24°) and fox trot (24°). Internal/external rotation at the walk (9°) and trot (13°) were also smaller than for the fox walk (25°) and fox trot (32°). Comparing all the joint motions measured by Heleski (1991) with those measured in this study, the greatest differences were found not in sagittal plane motion, but in the measurements outside of sagittal plane. Therefore, it is concluded that further studies on the gaits of gaited horses need to apply three-dimensional analysis using a JCS to distinguish between their gaits.

In conclusion, in comparison to walk and trot, the flat walk and fox trot have distinct gait characteristics, particularly in the range of joint motion. The flat walk and fox trot show distinct similarities in the temporal variables and joint angular patterns and magnitudes. The main differences found between the two gaits were seen in the motion outside of the sagittal plane with significant differences in peak values of carpal external rotation and differences in the timing of the carpal abduction peak and the fetlock adduction/abduction peaks. Therefore, the Missouri Fox Trotter demonstrates similar ranges of joint motion between it's two gaits, especially in the terms of flexion/extension range of motion. Differences between the gaits affected the timing rather than the magnitude of the peaks.

CHAPTER VI

CONCLUSIONS

"And God took a handful of the West Wind and created the horse..."

-The Koran

From a "handful of wind" to the superb athlete seen today, the anatomy of the horse has evolved in order to survive in a changing environment and through these changes the horse, at the same time, has become more suitable to man's needs. The fox-sized eohippus dating back 55 million years has adapted over time into the modern-day's athletically efficient horse (Harris 1993). Some of the evolutionary changes in the equine anatomy were directed toward locomotor efficiency, a characteristic that was necessary to outrun predators. One such adaptation involved restricting the range of motion of the joints distal to the shoulder and hip so the movements of the distal limb are primarily those of flexion and extension in the sagittal plane. Planar motion of the limb is energetically efficient (Budiansky 1997).

The scientific study of equine locomotion has exploded during the past 20 years as a result of the availability of more powerful computers, which are needed to process the vast amounts of numerical data. The initial studies were two-dimensional analyses in the sagittal plane, which described flexion and extension of the joints, but neglected the relatively small amounts of adduction/abduction and internal/external rotation. More recently, interest in three-dimensional analysis has increased and the availability of more powerful computers has facilitated these complex analyses. Human kinematic analyses paved the way with the establishment of joint coordinate systems for the human knee and

ankle (Grood and Suntay 1983; Soutas-Little *et al.* 1987). In 1991, Heleski applied this technique to the horse, and her results showed that even in the athletically efficient limbs of the horse there were detectable amounts of adduction/abduction and internal/external rotation. The presence of joint motion outside of the sagittal plane raised the question of its importance in relation to the performance of different gaits and athletic activities.

The limitation of Heleski's (1991) equine three-dimensional study was that it encountered noise due to displacement between the strap used to anchor the tracking markers to the skin and visual loss of tracking markers in one of the camera views. In vitro studies have corrected for these problems by using bone pins (Degueurce *et al.* 2000; Chateau *et al.* 2000), but none of these studies has offered an opportunity to measure three-dimensional equine motion without disturbing the horse's natural gait.

Chapter Summaries

Experiment I. In this research program, the development of a virtual marker technique overcame the problems that Heleski (1991) encountered. The benefits of this new technique were particularly obvious in the repeatability of measurements from stride to stride, which resulted in consistent patterns and amplitudes from stride to stride in the flexion/extension and adduction/abduction angles for both the carpal and fetlock joints. The fact internal/external rotation showed relatively large variability even when using the virtual marker technique may be related to the fact that this joint motion is the last in the series of calculations so it is more sensitive to any noise due to factors such as skin displacement. Human studies have found that internal/external rotation is highly effected by skin displacement showing oscillations of $\pm$ 1° (Cappozzo 1991). Skin displacement

algorithms were not applied in this dissertation since only 2-D algorithms are available and application of these algorithms to a 3-D model may create unforeseen error. Furthermore, human three-dimensional analysis has described variations in the magnitude of the internal/external rotation due to imbalances in or instability of the step (Mann 1980). The same may be true in horses. Indeed hoof imbalances induced by adding lateral or medial wedges were associated with increases in fetlock adduction/abduction and axial rotation in an in vitro model under vertical loading (Chateau *et al.* 2000). Further studies of hoof imbalances in live horses, which induce abnormal shear forces, may show even greater three-dimensional joint motion, and perhaps more variability from one stride to the next. Greater three-dimensional equine joint motion is also likely to be evident with imbalances due to surface irregularities. However, the earlier equine three-dimensional studies (Heleski 1991) and the results presented in the third chapter of this dissertation, have shown that internal/external rotation is small for the walk in comparison to the range of flexion/extension and adduction/abduction.

The walk of the non-gaited horse measured in this study had smaller ranges of joint motion than the other gaits measured in this dissertation and similar ranges to those reported in earlier three-dimensional studies (Heleski 1991) except for carpal adduction/abduction. The horse measured in this study was an older pleasure horse. Analysis of other non-gaited horses trained to move with more animation, such as Park horses, may show larger ranges of motion. Another consideration is that horses may show an age-related increase in adduction as noted in human subjects (Chao *et al.* 1983), or adduction/abduction may be affected by hoof/shoe angle. Back *et al.* (2000) found that increasing the lateral angle of the hoof was associated with increased adduction of the

stifle joint and increased abduction of the tarsal and hind fetlock joints during the stance phase. Further research using a larger sample population would give insight into the effect of these variables on adduction/abduction.

Experiment II. Multi-planar analysis (MPA) measures flexion/extension and adduction/abduction. This technique is less time consuming and the joint calculations are less complex than using a joint coordinate system (JCS) to measure joint motions out-of-the sagittal plane making MPA more applicable to a clinical environment. Earlier studies (Herring *et al.* 1992; Back *et al.* 2000) have applied MPA to measure sagittal and frontal plane kinematics during the stance phase. An obvious limitation to MPA is that axial rotation can not be measured. For years, equine gait analysis has neglected measurement of axial rotation because the anatomy of the horse has evolved to primarily move in the sagittal plane. However, even in a visual evaluation of normal equine locomotion some axial rotation can be detected, but this motion can not be measured with MPA. One of the questions to consider is whether it is important to measure small amounts of axial rotation, especially in the Peruvian Paso, which is noted for "termino," an outward paddling motion of the forelimb originating from the shoulder. Furthermore, how does neglecting axial rotation effect the flexion/extension and adduction/abduction measurements using MPA? In studies of running humans, Soutas-Little *et al.* (1987) compared ankle joint kinematics measured using a JCS and MPA. The results showed large differences between the adduction/abduction angles measured by the two techniques. In this study, not only were the JCS and MPA measurements of a walking Peruvian Paso compared, but the reasons for the differences were explored in terms of joint, segmental, and axes orientations. It was concluded that when the horse moved

along the plane of calibration or corrections were made for the angle of travel, flexion/extension angles were similar between MPA and JCS. In comparing adduction/abduction angles for JCS and MPA, differences were found between the two techniques for both the carpus and fetlock with the largest differences occurring during the swing phase when the joints are actively externally rotating. Visually, the relationship between axial rotation and the MPA adduction/abduction error can be seen on Figure 6.1 when axial rotation is not accounted for it is interpreted as adduction/ abduction in the frontal plane. Therefore, we may simply conclude that in horses known to demonstrate large amounts of rotation, such as the Peruvian Paso, MPA measurements are skewed. However, the extent of MPA adduction/abduction error is not limited to the Peruvian Paso or other horses with large amounts of axial rotation of the limbs. In fact, MPA adduction/abduction error is created by a combination of factors that includes axial rotation, though peak error does not coincide with peak axial rotation. For the carpal joint, peak difference between JCS and MPA adduction/abduction measurements occurred when the radius was vertical with the ground and the proximal and distal aspects of the bone were aligned. At this point, the carpus was flexed and the joint was slightly externally rotated. When the proximal segment of a joint is oriented as described for the radius, then adduction/abduction error is a function of flexion and axial rotation. When either flexion or axial rotation increases, the MPA adduction/abduction error increases and this relationship is calculated using the steps described in Appendix B. As for the fetlock, during the period of peak difference between the adduction/abduction measured by the JCS and MPA, the pastern segment was either flexed to the horizontal so that the bone was viewed in the frontal plane along it's long axis or the pastern segment was

rotated beyond the horizontal so that it was hidden behind the metacarpus. At the same time, the proximal and distal ends of the pastern segment were aligned horizontally. With this combination of segmental orientations, any axial rotation causes adduction/ abduction error in that MPA misinterprets the rotation as adduction/ abduction.

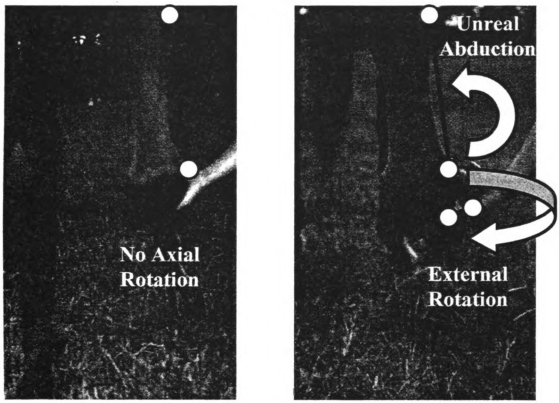

Figure 6.1. Frontal view measurements of the horse's forelimb are skewed due to external rotation of the antebrachium creating an abduction angle that is not real.

Another flaw in MPA is that it's axes do not move dynamically with the joint motion so that if the horse does not move parallel with the plane of calibration or if it has conformational or tracking abnormalities, such as knock-knees or paddling, the axes will not adjust for these changes creating errors in all three joint motion measurements. In this study, the horse's angle of travel was transformed so that it was aligned with the calibration frame. Consequently, only slight differences between the JCS and MPA flexion/extension measurements were found. When using the JCS, the adduction/ abduction axis moves dynamically with the other axes demonstrating the coupling of joint motions. MPA adduction/abduction is measured around a stationary axis so that coupling of joint motions and particularly internal/external rotation is neglected. Therefore, MPA does not address the effect of axial rotation on adduction/abduction, nor can it assess the coupling of joint motions. It is concluded that when using MPA the horse's angle of travel must be aligned with the plane of calibration to measure flexion/extension and that measurements outside of the sagittal plane should be done using a JCS.

The description of the joint motion of the Peruvian Paso was based on a single horse in order to limit variability due to individual styles of movement and conformational differences. Further studies utilizing larger sample populations should be conducted to better describe the joint motion of the termino. However, the Peruvian Paso joint motion measured in this study is briefly described in chapter four (Experiment II) because it is the first scientific description of the kinematics of the Peruvian Paso. The stance kinematics reflected the horse's standing conformation. The carpus was extended, abducted, and internally rotated during stance until breakover where it started to flex,

increase abduction, and externally rotate. These movements continued until late swing when the carpus extended, decreased abduction, and rotated internally. The fetlock was extended and adducted during stance with a small peak of external rotation in mid stance. The fetlock reaches peak extension just before breakover, then began to flex, abduct, and internally rotate during breakover. In early swing, the fetlock reached peak flexion, abduction, and external rotation, then began to extend, adduct, and internally rotate throughout the rest of the stride. For both joints, the majority of joint motion outside of the sagittal plane occurred during the swing phase, which is when the horse exhibits termino.

Limited generalization of the motion of the termino can be made from this single subject. Preliminary analysis of other Peruvian Pasos not used in this dissertation showed that intra-horse variability is small whereas inter-horse variability is larger, particularly with regard to axial rotation, which represents different degrees of animation of the termino. In the human comparison study of JCS and MPA measurements of the ankle (Soutas-Little *et al.* 1987), two runners were measured, but the subjects' measurements were not combined since their style of running created differences in the patterns of joint motion, especially during breakover and early swing. The horse measured in chapter four was an older pleasure Peruvian Paso. Other Peruvian Pasos measured, but not reported in this dissertation, included a nationally competitive show horse and a young, pleasure horse. The younger horse demonstrated less axial rotation, smaller protraction/retraction angles, and shorter stride, stance and swing durations than the show horse. All of these horses were barefoot and similarly trimmed so that in this preliminary analysis shoeing and trimming were not confounding variables. In addition to the collection of more data

describing normal Peruvian Paso joint motion, further research into the effects of training and shoeing are needed. Back *et al.* (1995) found significant differences in the temporal characteristics of the trot stride in young, Dutch Warmbloods after 70 days in training. Similar results may be seen in the Peruvian Paso. Motion outside of the sagittal plane may increase with training, especially in regards to the termino. The effect of medial and lateral wedges on stance phase frontal plane motion of the stifle, tarsus, and hind fetlock of Shetland ponies found that increased adduction/abduction coincided with the application of the wedges (Back *et al.* 2000). Research on the relationship of shoeing and the three-dimensional joint motion of the termino may find similar results.

Experiment III. In chapter five, the technique of three-dimensional analysis using a JCS was applied to the forelimb of Missouri Fox Trotters to measure the carpal and fetlock joint motion of the flat walk and the fox trot. The fox trot has been described as a gait in which the horse appears to walk with the forelimbs and trot with the hind limbs (Imus 1995). By changing the coordination patterns of the fore and hind limbs, the Missouri Fox Trotter can produce characteristics of the walk in the forelimbs and the trot in the hind limbs. However, the hind limbs during the fox trot do not have a suspension phase like the trot, but instead, have a period of overlap between the hind limb stance phases (Clayton and Bradbury 1995). Clayton and Bradbury (1995) defined the fox trot according to measured temporal characteristics as a fast, lateral sequence, diagonal couplets walk.

In chapter five (Experiment III) temporal comparisons between the flat walk and fox trot showed that the fox trot has a faster velocity, which is the result of a shorter stride duration due to reduced stance and swing durations, while stride length does not

change. By changing the footfall timing of the flat walk, the Missouri Fox Trotter was able to create another four-beat stepping gait with its own unique characteristics, the fox trot. In the sport of dressage, horses are required to maintain the tempo and rhythm of the walk during manipulations between collected and extended walk. However, it has been shown that dressage horses often demonstrate an irregular rhythm with lateral couplets at the extended walk (Clayton 1995). Lateral couplets are also a characteristic of the running walk, a gait performed by some gaited horse breeds. Perhaps this shared gait adaptation between the dressage extended walk and the four-beat non-walking stepping gaits allow horses to perform the walk at a faster velocity without changing to a leaping gait. Gait adaptations will be discussed later in more detail.

The walk of the Missouri Fox Trotter demonstrates a relatively long stance duration and breakover during which the carpus shows a greater range of internal/external rotation and the same fetlock adduction/abduction range. In comparison, the fox trot demonstrated greater or similar ranges of joint motion except for carpal internal/external rotation, while the horse was rapidly picking up and placing down its hooves at a more rapid rate, but with a similar stride length. These gait characteristics of the fox trot were associated with higher vertical forces, which result in more extension of the fetlock as the joints absorb the forces during stance. Preliminary analysis of ground reaction forces collected during the Missouri Fox Trotter trials show a slightly higher vertical ground reaction force at the fox trot than the flat walk, which may be the reason for the slightly larger fetlock extension found in the fox trot. With a shorter period of breakover during the fox trot, fetlock flexion is more rapid than in the flat walk. Interestingly, the fetlock extension profile during stance of the flat walk resembles a normal fetlock trotting

profile, which may explain why the differences between the vertical ground reaction forces are not as large as seen between the walk and trot. Larger differences were found between the mediolateral ground reaction forces of the flat walk and fox trot, which may be associated with the differences in patterns and amplitudes of adduction/abduction and axial rotation. Further kinetic analysis of the Missouri Fox Trotter will assist in explaining the similarities and differences of the flat walk and fox trot.

For both the carpal and fetlock joints, the flat walk and fox trot show similar ranges of motion, but there are differences in the adduction/abduction patterns. As described in chapter five, these differences may be explained by the shifting of the horse's body over the supporting limb and adjustments in the weight shifts between gaits. In the fox trot, the horse spends most of stance in a diagonal bipedal support phase, similar to the trot, and spends less time in a tripedal support phase unlike the flat walk.

Therefore, the body has less time to rotate over the limb so the horse lifts up and over the body instead of a mediolateral shift increasing vertical excursions of the croup that reaches peak y displacement during swing and decreasing mediolateral range of motion of the elbow relative to the hoof during stance. This may be an adaptation for shortening the time taken to rotate over the limb. During breakover, when the body is shifting from a tripedal to diagonal bipedal support and preparing for lift off of the forelimb, is when the largest shift in carpal internal rotation and fetlock abduction are measured. During a diagonal bipedal support phase the weight of the body is more centralized where as the weight of the body in a tripedal support phase is offset toward the side that has two limbs on the ground. The longer period of tripedal support during the flat walk means the weight of the body is more offset throughout the stride.

Therefore, the differences in limb support and how the body moves over the limb, such as the longer period of rotation of the body over the limb during the flat walk compared to the increased vertical excursions and decreased mediolateral limb motion during the fox trot, may explain differences in adduction/abduction patterns. This adaptation to rapidly move the body over the limb during the fox trot is also apparent in the rapid flexing of the fetlock during the breakover as seen in a trotting flexion/extension profile.

In comparing the flat walk to the fox trot, while exhibiting some similarities, both have unique gait characteristics, particularly in the three-dimensional joint angular motion. Therefore, using the ranges measured in earlier two-dimensional kinematics of the walk of non-gaited horses for determining abnormalities in the Missouri Fox Trotter would be limiting even with the flat walk. In fact, the flat walk demonstrated a larger range of motion, except for carpal adduction/abduction, than what was measured for the walk of the non-gaited horse in chapter three. On the other hand, differences between the walk of the Missouri Fox Trotter compared to the fox trot were small apart from the few exceptions discussed earlier, which may be useful in the detection and treatment of lameness. These conclusions emphasize the importance of knowing the normal ranges of motion for the gaits of the gaited horses in order to distinguish normal and pathological motion patterns.

Gait Adaptations

Measuring only sagittal plane kinematics is not the whole story of the gait. In some gaits such as the walk, the internal/external rotation may be small, but neglecting the influence of internal/external rotation can distort the other measurements. In the gaits

performed by gaited horse breeds, out-of-sagittal plane joint motion is a significant characteristic of the gait that may help to explain how these horses are able to use stepping gaits at faster velocities while non-gaited horses switch to the trot. Although this dissertation only studied a few gaits for a few breeds, each gait demonstrated unique characteristics that may be described as adaptations. The following section describes some theories regarding the origins of these adaptations.

Limb interference has been identified as a cue to the horse to make a transition to another gait (Hildebrand 1978). The larger ranges of flexion/extension, adduction/ abduction, and internal/external rotational motion in the Missouri Fox Trotter may allow these horses to avoid interference between limbs and to continue using stepping gaits at faster velocities. Since only forelimb kinematics were measured, the relationship between hoof placements and interference could not be determined. Future studies measuring the over-tracking distances and arcs of the distal (hoof) limb movement in the different planes relative to the position of the hoof that is in stance will assist in determining the presence of interference. This would be particularly important for the Tennessee Walking Horse, which is known for having a large amount of over-tracking with the hind limbs (Imus 1995).

Gaited horses may be able to perform their gaits with this greater range of motion due to anatomy, training, and/or shoeing. Shoeing studies have shown that the application of medial/lateral hoof wedges increase the out-of-sagittal plane motion in the stifle, tarsus, and fore and hind fetlocks (Back *et al.* 2000; Chateau *et al.* 2000). The subjects used in this study had no special training or shoeing, but were described to have selective breeding. This breeding may have resulted in the inheritance of certain

conformational traits needed to perform these gaits. Slade (1993) found particular conformation correlated well with the quality of the performance of the running walk in several gaited breeds. Similar studies on conformation of the Peruvian Paso and Missouri Fox Trotter may lead to similar results.

At faster velocities the horse's limbs are subjected to increased vertical ground reaction forces (Khumsap *et al.* in press), and increased forces have also been shown to act as a cue for the horse to switch gaits (Rubin and Lanyon 1982). Horses increase the flexion/extension of the joints to absorb increased ground reaction forces (Leach 1990). Preliminary analysis of the Missouri Fox Trotter ground reaction forces found higher mediolateral ground reaction forces in the fox trot than the flat walk, which suggests that the increased out-of-sagittal plane motion helps to absorb the out-of-sagittal plane ground reaction forces. Therefore, the larger range of joint motion outside of the sagittal plane, may allow the gaited horse to absorb the additional out-of-sagittal plane ground reaction forces producing stepping gaits at faster speeds without being cued to switch to a leaping gait. Understanding of the relationship of the mediolateral ground reaction forces and joint motion outside of the sagittal plane will need to entail further analysis of the kinetics and net joint moments and joint powers.

Impulse is the amount of force applied over a period of time, such as a stance phase. If stance duration decreases, the force must increase to maintain the impulse. Studies of non-gaited horses (Khumsap *et al.* in press) have shown that as walking velocity increases, the hind limbs are subjected to significantly higher vertical ground reaction forces distributed over a shorter stance duration. Conversely, lame horses often use an increased stance duration as a means of reducing the peak forces by distributing

the force on the lame limb over a longer period of time (Keegan *et al.* 2000). Therefore, the longer stance duration of the fox trot compared to that reported in the trot (Back *et al.* 1994) may decrease the peak vertical ground reaction forces, thus delaying the cue to switch gaits.

The gaits of the gaited horse are described as being efficient (Imus 1995), and this is important because energy expenditure has been described as another cue to the horse to switch gaits (Hoyt and Taylor 1981). In competitive human race walkers, as speed approaches the upper limit for the walk, efficiency decreases until the walker breaks into a run by adding a suspension phase. This results in an increase in gait efficiency (Cavagna and Franzetti 1981). Therefore, it must be questioned whether the faster stepping gaits of the gaited horse are truly energetically efficient. Although gait efficiency was not measured in this study, some speculations can be made as to how the locomotor adaptations of the gaited horse adjust for gait efficiency. As the human competitive race walker increases speed, the flexion/extension of the joints increases to take advantage of the elastic properties of the muscles, ligaments, and tendons. This increased flexion/extension allows for greater storage and release of elastic energy (Cavagna *et al.* 1976). By increasing the fetlock extension of the fox trot during the stance phase, the Missouri Fox Trotter may also be utilizing this elastic property to help conserve energy. By preserving gait efficiency, the gaited horse can continue stepping through the gait at faster speeds without adding a suspension phase.

The amount of out-of-sagittal plane motion during stance may also be important to energy conservation through utilization of the elastic properties of the muscles, ligaments, and tendons responsible for movement. However, the amount of energy

conservation is limited due to the small amounts of muscles, ligaments, and tendons stretching as a consequence of adduction/abduction and internal/external rotation. Generally, elastic energy storage and release is thought to be more effective in leaping gaits. Wickler (2000) has studied the gait efficiency of the walk and trot and has made some observations on the gaits of gaited horses. From preliminary data, the non-walking stepping gaits were concluded to be inefficient, which suggests other factors such as training and environment have a greater influence on performance of these gaits than energy expenditure.

The large amount of out-of-sagittal plane motion in the gaited horse may be disadvantageous to structural soundness. This additional movement of the joints may be considered to contribute to instability of the joint, which may make the production of leaping gaits more difficult and uncomfortable for the horse. Due to the historically small numbers of gaited breeds, clinical histories are limited. Gaited horse owners have described suspensory ligament problems with the Peruvian Paso and hip dysplasia with the Tennessee Walking Horse. It is not known how much heredity and environment contribute to these problems. Evaluation of the anatomical structures of the limb joints and histories of joint problems specific to the breeds may give further insight into anatomical problems associated with these breeds and disadvantages of these gaits.

If gait efficiency is not a driving factor for production of the non-walking stepping gaits, external conditions may also be influential in gait production. A study of the effects of incline (Wickler *et al.* 1999) and added back weight (Wickler *et al.* 2000) on gait speed selection showed that a 10% incline was associated with a decrease in preferred speed of 0.31 m/s, whereas carrying extra weight equivalent to increasing body

weight by 18.5% was associated with a decrease in preferred speed of 0.16 m/s. A 10% increase in body weight and a 3.5% increase in treadmill incline increased stride frequency (Barrey *et al.* 1993). Along with being described as a mechanism for decreasing muscle stress (Wickler *et al.* 1999), these gait adaptations have been attributed to a fear of loss of balance (Zatisiorky 1994). Pat Parelli, a nationally recognized horse trainer, finds training a horse to lie down on cue is the most difficult maneuver to teach because of their instinctive fear of losing balance (Parelli 2000). This fear motivates the horse to make adaptations in their body stance so that they will always be balanced enough to flee from predators. By adding weight to their backs or inclining the terrain, the horse's balance is shifted and they must make adaptations to their stance and their gait to maintain balance. Dressage horses performing the half pirouette at the walk adapted for the loss of balance due to dynamic instability by adjusting the footfalls and support sequences creating an irregular walking rhythm with a longer hind stance and tripedal support (Hodson *et al.* 1999). The prolongation of hind stance led to increased overlap with the increased number of hooves on the ground giving a larger base of support. At slower walking velocities (0.96 m/s) horses increase their overlap and base of support by having a longer fore (1050 ms) and hind (1033 ms) stance durations and tripedal support (83% of stride duration). With increased velocity (2.89 m/s), the fore (367 ms) and hind (383 ms) stance durations and tripedal support (17% of stride duration) decreased (Nicodemus *et al.* 2000c). The North American Single-Footing Horse performing the road gait, a non-walking stepping gait with a regular rhythm, replaced the tripedal support phase of the walk with a single support phase that made up 41% of the stride (Nicodemus *et al.* 2000b). The horse relied more on the dynamic stability of the gait than

the overlap and the number of hooves on the ground to maintain balance. When looking back at the history of the breeds studied in this dissertation, the Missouri Fox Trotter and Peruvian Paso, these breeds were established to move over rugged terrain usually carrying heavy loads (Imus 1995). These horses were selected and bred to be able to adapt to these conditions without losing their balance, and so through time, the gaits that were suited for these conditions were established into the breeds.

This balance is maintained through the longer stance duration, comparative to the trot as discussed earlier, and the presence of tripedal support phases during the gait. The longer period of diagonal bipedal support of the fox trot (Clayton and Bradbury 1995) also maintains balance during locomotion because the line of support runs close to the horse's center of gravity (Hodson *et al.* 1998). These gait adaptations are necessary to maintain balance over uneven terrain.

Most of the studies on animal adaptations for balance have utilized deccerebrate cats in which the stepping patterns are adapted in accordance with changes in the nature of ground support (Yanagihara *et al.* 1993). Adjustment of limb patterns in an attempt to achieve dynamic stability is a learning process, especially in more complex adaptations. It involves several structures of the body including the head, vertebrae, and limbs. Studies of postural adjustment of cats with forelimb movement determined two patterns. A diagonal bipedal limb support initially was detected as a forelimb of the cat was moved. This limb support phase represented the least displacement of the center of gravity. After several trials, cats made a postural adjustment by shifting the head to the opposite forelimb and leaving three instead of two limbs on the ground (Bush and Clarac 1985). Although a learned process, it was more stable because the vertebral column

flexed laterally, which shifted the center of gravity to the center of the triangle formed by the three supporting limbs. Similar adaptations may be used by the gaited horses in the non-walking stepping gaits with complex postural adjustments being learned through adjusting the head, vertebrae, and limbs to find the most stable position.

This adaptation for increased stability may have been learned for survival in rugged terrain in breeds including the Missouri Fox Trotter and Peruvian Paso that originated from such an environment. This postural adaptation is seen in the Missouri Fox Trotter as each hind limb hits the ground the head shifts toward the single forelimb already on the ground (Nicodemus *et al.* 2000a). This action shifts to the center of the horse into the triangular base of support comprised of one fore and two hind hooves. This adjustment of the head and vertebrae is also an adaptation seen in equine forelimb lameness (Peloso *et al.* 1993), which further demonstrates the highly adaptive ability of the horse. Although terrain may not be a factor for gait adaptation for the modern Missouri Fox Trotter or Peruvian Paso, human interaction through training may remain as the driving force in encouraging these horses to make these adaptations, as seen in the temporal variables and three-dimensional joint motion, to produce the non-walking stepping gaits.

Recommendation for Future Studies

The application of three-dimensional analysis is necessary for quantifying such gait adaptations as out-of-sagittal plane joint motion. Furthermore, since multi-planar analysis was found inaccurate for measuring adduction/abduction and did not measure internal/external rotation, a joint coordinate system using the virtual marker methodology

is more suitable for the comprehensive and accurate measurement of joint motion. In all three experiments described in this dissertation, out-of-sagittal plane joint motion was detected and for each gait the pattern of joint motion was quite unique. For example, even in the walk of each of the three breeds in this dissertation showed different joint patterns and amplitudes of motion. The ability to measure movements outside of the sagittal plane is important in the complete understanding of the locomotion of the gaited horse. Furthermore, as seen in chapter three (Experiment I), even in the non-gaited horse joint motion outside of the sagittal plane is evident so that the non-gaited horse would benefit from three-dimensional analysis. Interestingly, the non-gaited horse demonstrated the largest range of carpal adduction/abduction measured in this dissertation and showed more adduction/abduction than earlier measurements of the non-gaited horse's walk (Heleski 1991). The differences in carpal adduction/abduction may be related to such factors as age and should be further investigated. Although adduction/ abduction differences between horses could be measured using MPA, in chapter four (Experiment II) this technique was found to create error that is a function of flexion and axial rotation in frontal plane measurements. The axial rotation measured for the walk of the non-gaited horse is small, but as determined in chapter four any amount of this rotation will create adduction/abduction error using MPA. Therefore, further three-dimensional analysis studies of both gaited and non-gaited horses should include the use of a JCS.

In the Missouri Fox Trotter, the flat walk and fox trot demonstrated similar patterns of joint motion, especially in the sagittal plane, which may explain why the fox trot is described as the horse walking on the forelimbs. Both gaits demonstrated similar

stride length and similar motion characteristics in that during stance the carpus extended, abducted, and externally rotated and the fetlock extended, and during swing the carpus flexed and internally rotated and the fetlock flexed and externally rotated. At the fox trot, an increase in velocity was associated with decreases in stride duration, fore and hind limb stance durations and tripedal limb support, while diagonal bipedal support increased. These changes in temporal characteristics from the flat walk to the fox trot coincide with kinematic differences in that the fetlock adduction/abduction pattern is flipped so that peak values of adduction/abduction occur at different phases of the stride and the carpus demonstrates a peak of abduction during swing. The fetlock extension peak occurred later in the stance phase for the fox trot than the flat walk, after which the fetlock began to flex rapidly during breakover and early swing. At the same time there was a change from tripedal support to diagonal bipedal support. These kinematic changes in joint motion patterns gave the appearance that the horse was walking on the forelimbs. Further analysis of the fox trotting hind limbs may find joint motion similar to a trot as indicated by the increase in vertical excursions of the croup during the fox trot. Differences such as the adduction/abduction patterns between gaits give insight into the joint mechanics for performing the two gaits, but further research on the muscle contribution and the effects of external conditions would give greater insight into the gaits of the Missouri Fox Trotter. Kinematics of other non-walking stepping gaits should be measured including further research on the Peruvian Paso. Research concerning the gaits of the gaited horse are important as the gaited horse population in the United States is growing rapidly. The number of veterinarians that are knowledgeable of these gaits is limited so that this research can assist in objectively describing the gaits and be a tool for

lameness and treatment evaluations. As seen in the flat walk and fox trot, the differences between gaits may be small, but these differences may prove to be important in assessing the quality of the gait or in the detection of lameness.

In all gaits, particularly those of the gaited horse in which gait adaptations are made so that the horse can continue the stepping gait at faster speeds, the application of three-dimensional analysis using a JCS is necessary for a complete picture of the gaits and these adaptations. With these special gait characteristics may come unique problems concerning both the health and the performance of the gaited horse that can only be fully addressed through analysis of motion outside of the sagittal plane. However, after finding measurable amounts of out-of-sagittal plane motion in the non-gaited walk and determining that differences in adduction/abduction measurements may be related to such factors as age, training and shoeing, it is the recommendation of this researcher that three-dimensional analysis should not exclude the non-gaited horse. Three-dimensional analysis using a JCS is recommended since MPA is restrictive due to corrections for the horse's angle of travel for flexion/extension measurements is needed, frontal plane measurements are skewed, and axial rotation can not be measured. Nevertheless, through these experiments it has come to the attention of this researcher that the following aspects of the JCS technique need to be further improved including the development of 3-D correction algorithms for skin displacement that encompass many different gaits and breeds and development of computer programs to facilitate tracking and processing three-dimensional data. As for the clinical application of a JCS, along with determining the ranges of normal joint motion of various gaits, it is necessary to develop graphing programs to assist in the visualization of three-dimensional motion. The JCS

methodology presented in this dissertation offers an opportunity to gain a more complete understanding of joint motion, which is important in differentiating between the non-walking stepping gaits of gaited horses for both clinical and performance applications.

Final Conclusions

The aim of this dissertation was to contribute to the discipline of equine biomechanics by developing a methodology for quantifying the locomotion of the gaited horse. A virtual marker methodology to facilitate three-dimensional analysis using a JCS was developed for the carpal and fetlock joints. The virtual marker methodology was found to be feasible and practical for three-dimensional analysis and the carpal and fetlock joint angles were repeatable over several strides. Comparisons were made between flexion/extension and adduction/abduction measurements using a JCS and MPA. The results showed that MPA was acceptable for flexion/extension measurements if the horse was moving parallel to the plane of calibration. Adduction/abduction error was found with MPA that contributed to axial rotations and segmental orientations along with differences in the JCS and MPA adduction/abduction axes. Three-dimensional analysis using a JCS was applied to the carpus and fetlock of the Missouri Fox Trotter during the flat walk and fox trot. Although stride length and carpal and fetlock ranges of motion were similar, velocity, stride and stance durations, diagonal step duration, carpal external rotation peaks, and carpal and fetlock adduction/abduction patterns were different between the gaits. Further application of a JCS using the virtual marker methodology as described in this dissertation is recommended for the continued development of the understanding of the gaits of the gaited horse.

APPENDICES

APPENDIX A: EXPERIMENT II

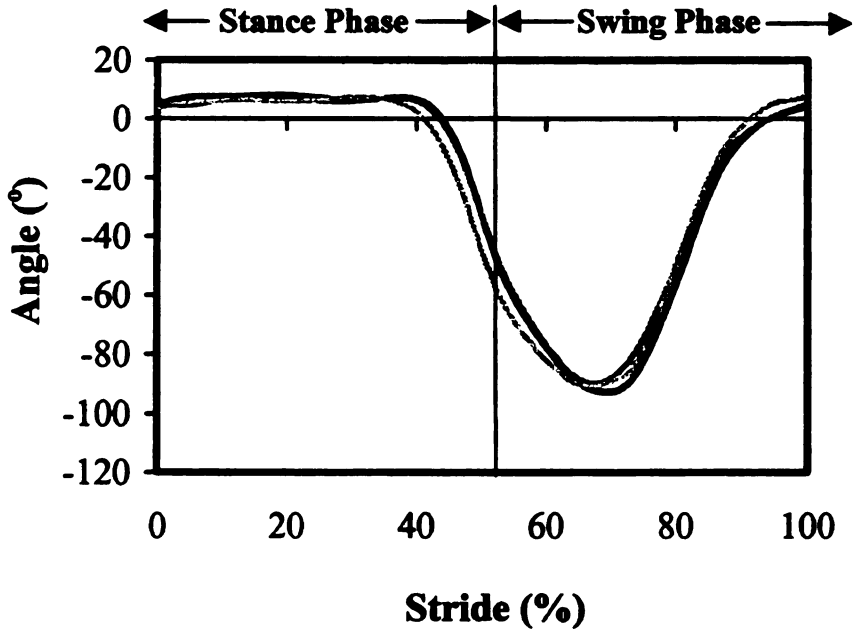

Figure A.1. JCS carpal flexion (-)/ extension (+) angles (°) measured for Peruvian walking trial 1 (black line), 2 (dark gray line), and 3 (light gray line).

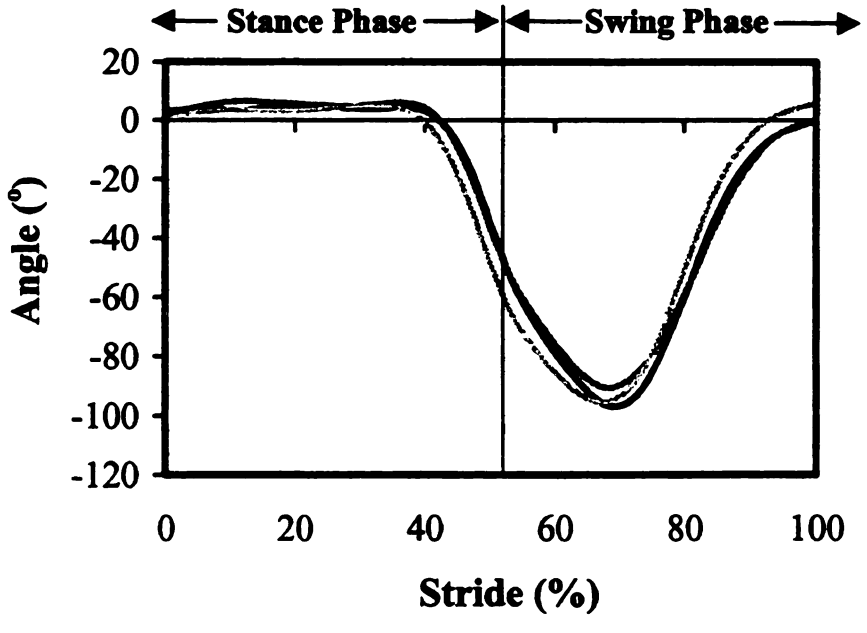

Figure A.2. MPA carpal flexion (-)/ extension (+) angles (°) measured for Peruvian walking trial 1 (black line), 2 (dark gray line), and 3 (light gray line).

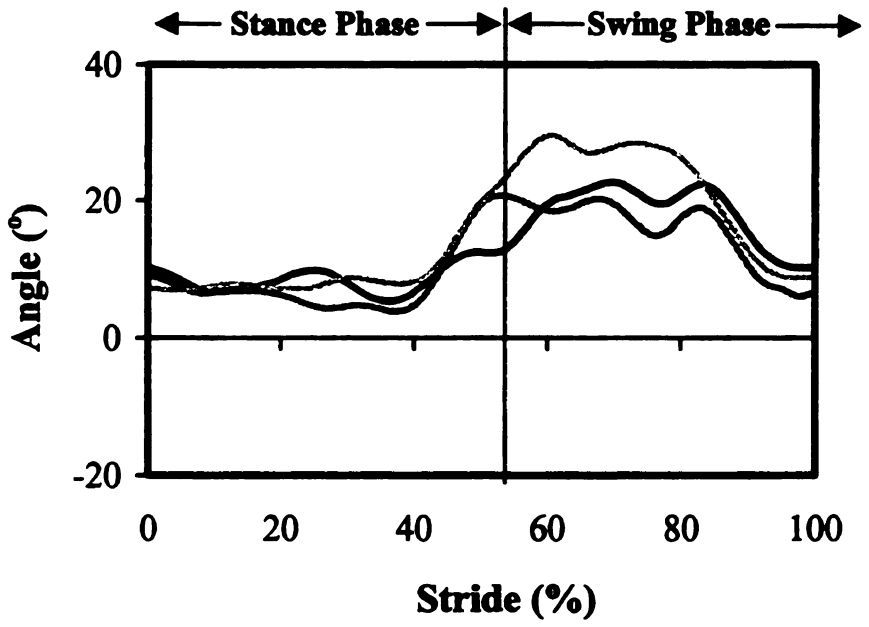

Figure A.3. JCS carpal adduction (-)/ abduction (+) angles (°) measured for Peruvian walking trial 1 (black line), 2 (dark gray line), and 3 (light gray line).

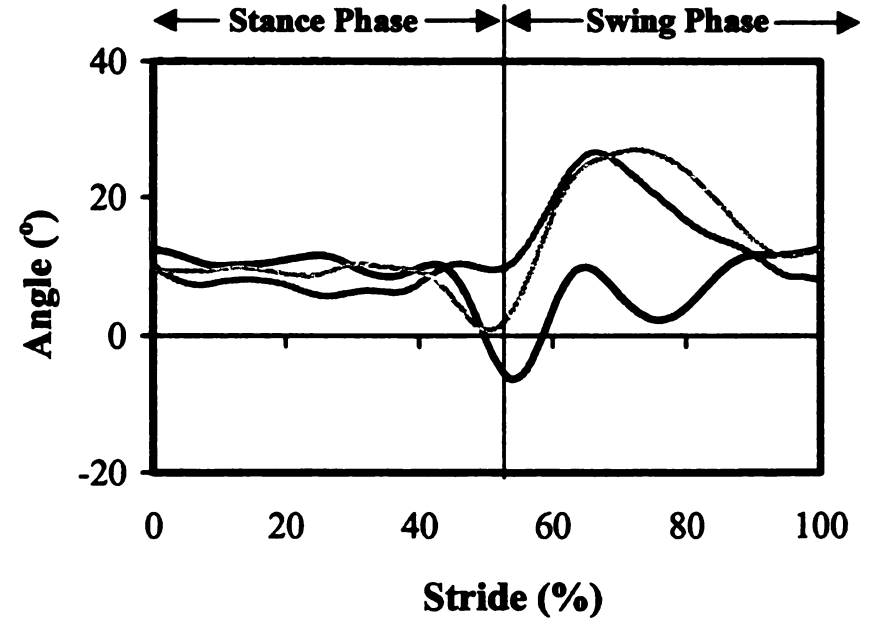

Figure A.4. MPA carpal adduction (-)/ abduction (+) angles (°) measured for Peruvian walking trial 1 (black line), 2 (dark gray line), and 3 (light gray line).

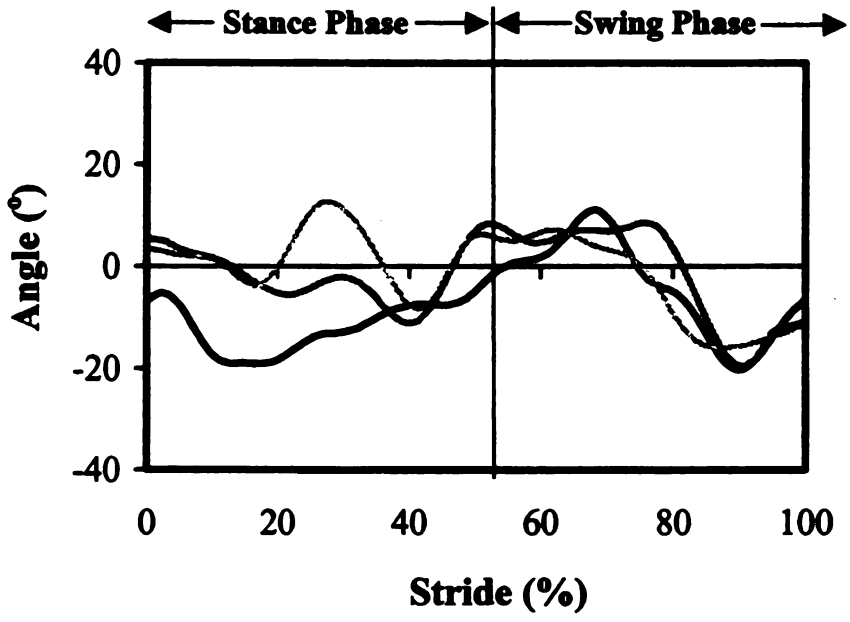

Figure A.5. JCS carpal internal (-)/ external (+) rotation angles (°) measured for Peruvian walking trial 1 (black line), 2 (dark gray line), and 3 (light gray line).

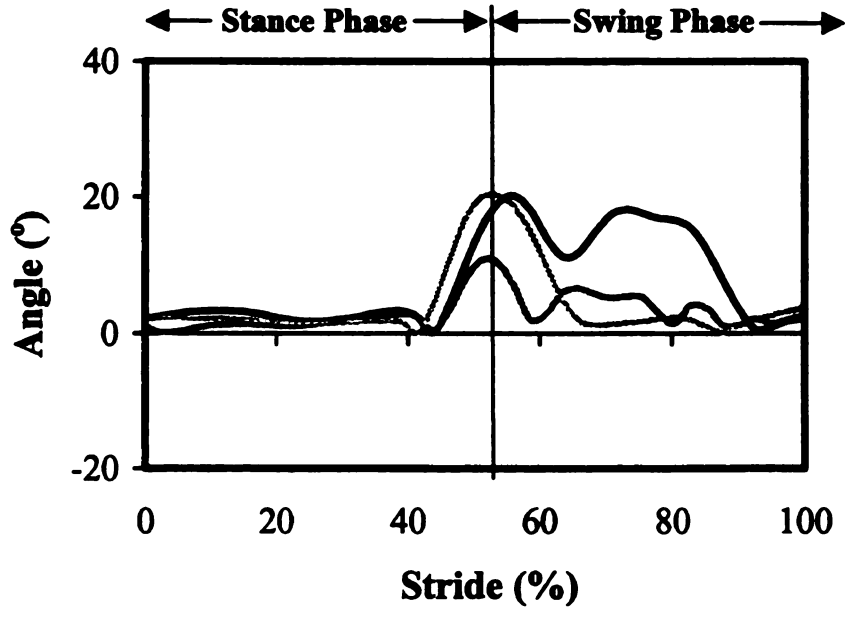

Figure A.6. Carpal absolute difference between JCS and MPA adduction (-)/ abduction (+) angles (°) measured for Peruvian walking trial 1 (black line), 2 (dark gray line), and 3 (light gray line).

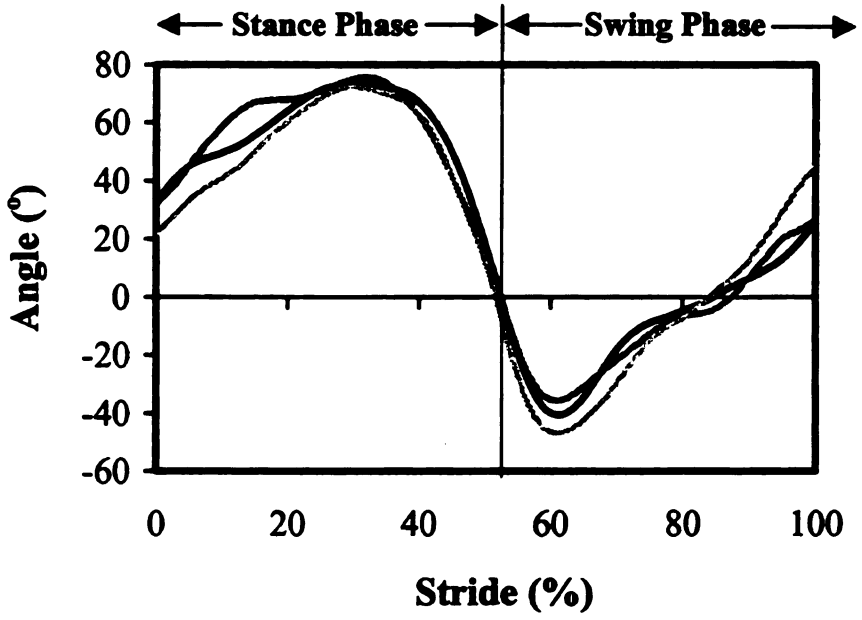

Figure A.7. JCS fetlock flexion (-)/ extension (+) angles (°) measured for Peruvian walking trial 1 (black line), 2 (dark gray line), and 3 (light gray line).

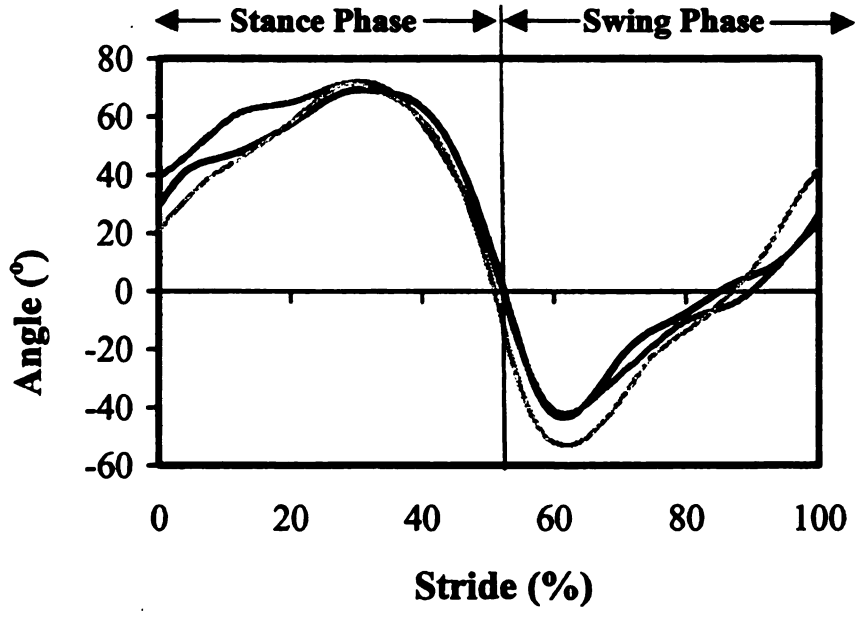

Figure A.8. MPA fetlock flexion (-)/ extension (+) angles (°) measured for Peruvian walking trial 1 (black line), 2 (dark gray line), and 3 (light gray line).

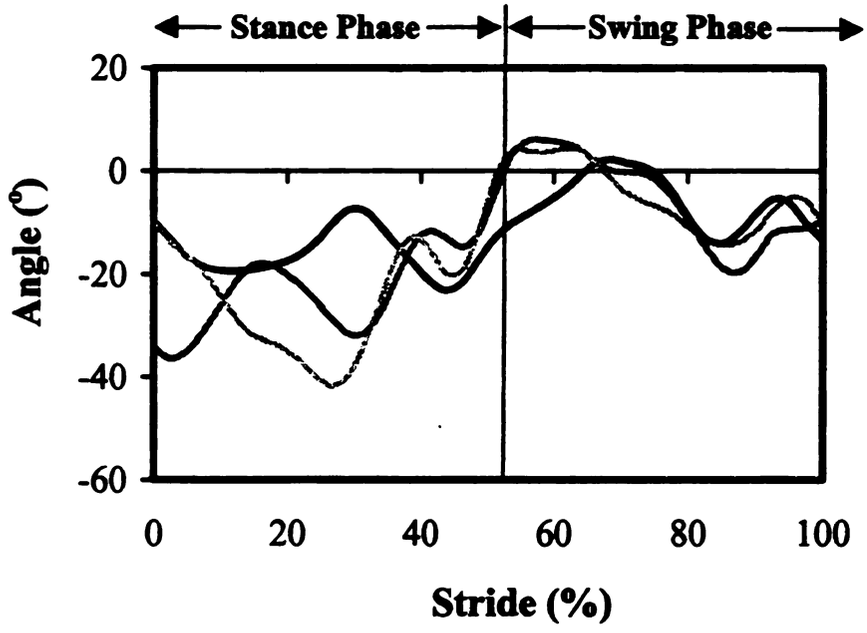

Figure A.9. JCS fetlock adduction (-)/ abduction (+) angles (°) measured for Peruvian walking trial 1 (black line), 2 (dark gray line), and 3 (light gray line).

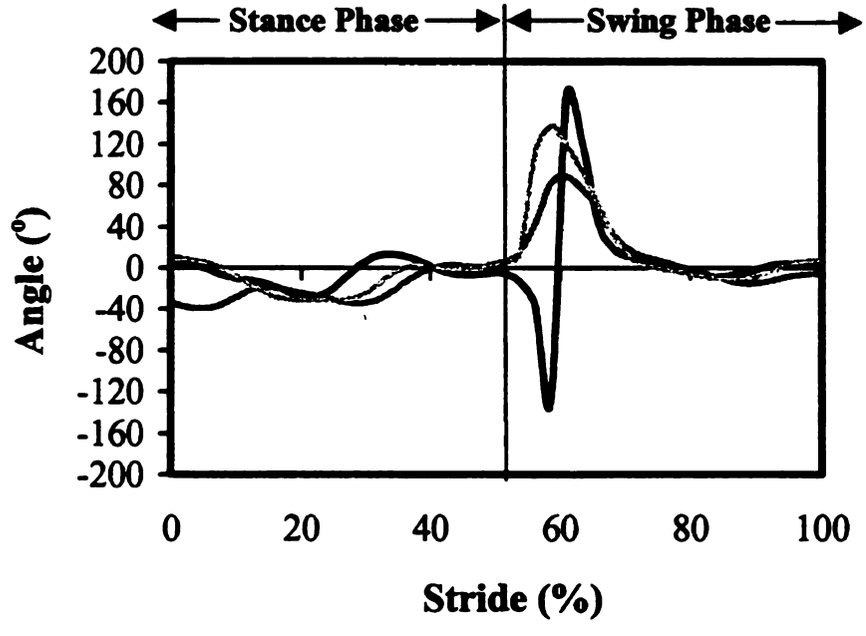

Figure A.10. MPA fetlock adduction (-)/ abduction (+) angles (°) measured for Peruvian walking trial 1 (black line), 2 (dark gray line), and 3 (light gray line).

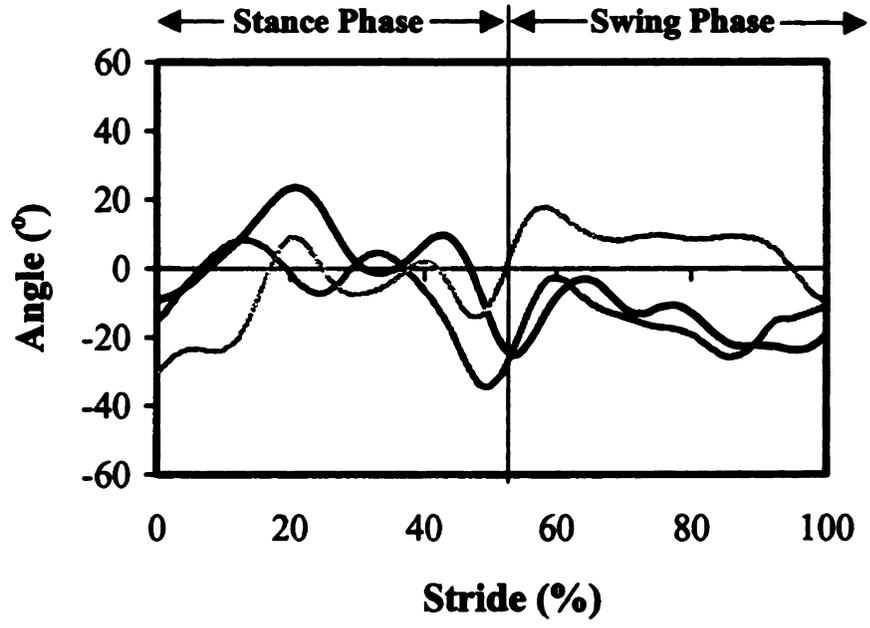

Figure A.11. JCS fetlock internal (-)/ external (+) rotation angles (°) measured for Peruvian walking trial 1 (black line), 2 (dark gray line), and 3 (light gray line).

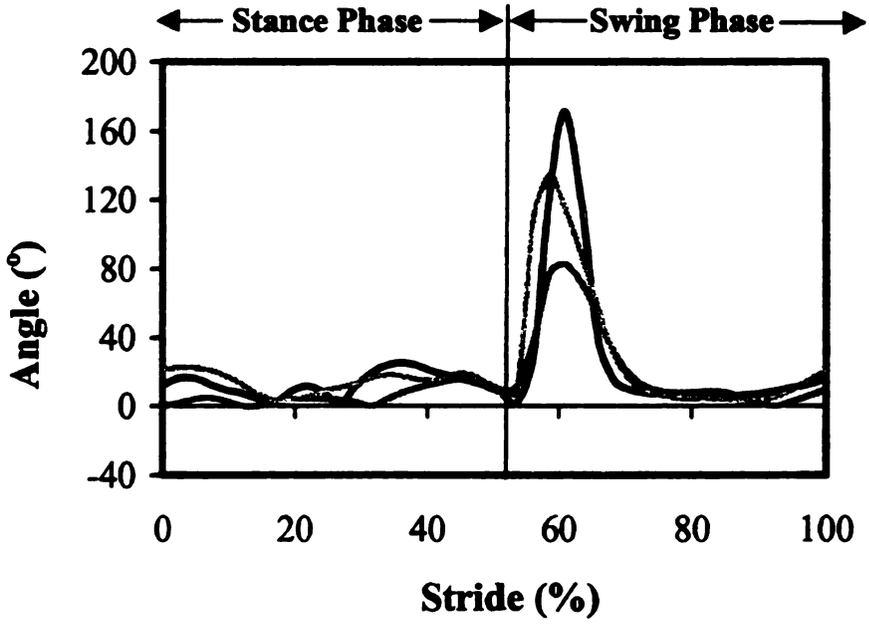

Figure A.12. Fetlock absolute difference between JCS and MPA adduction (-)/ abduction (+) angles (°) measured for Peruvian walking trial 1 (black line), 2 (dark gray line), and 3 (light gray line).

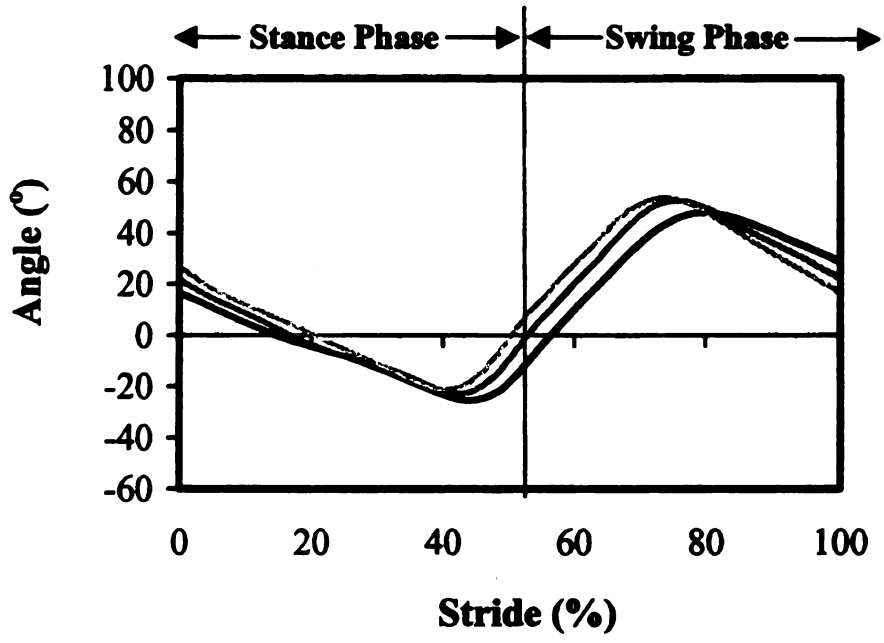

Figure A.13. Radius segmental flexion (-)/ extension (+) angles (°) measured for Peruvian walking trial 1 (black line), 2 (dark gray line), and 3 (light gray line).

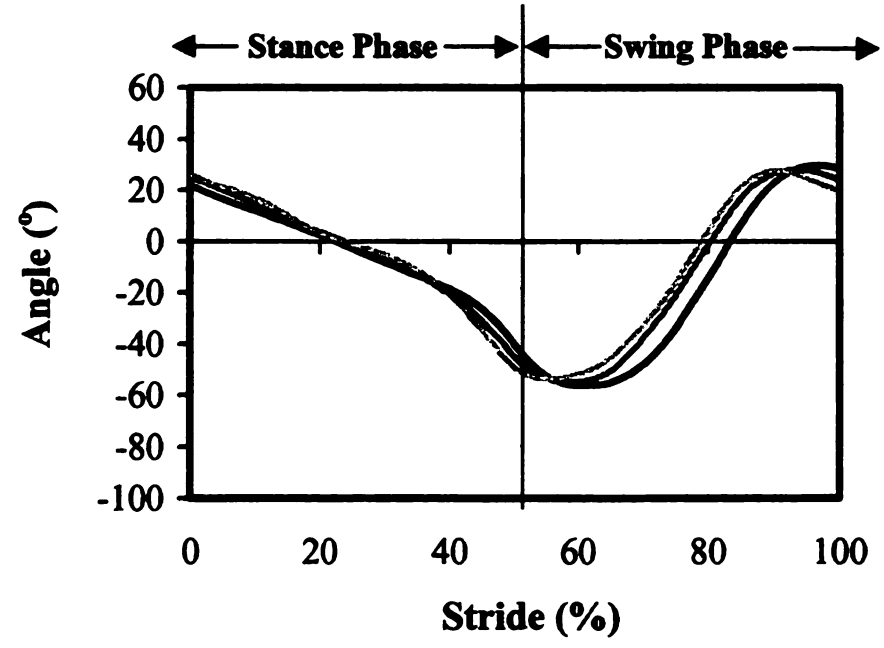

Figure A.14. Metacarpal segmental flexion (-)/ extension (+) angles (°) measured for Peruvian walking trial 1 (black line), 2 (dark gray line), and 3 (light gray line).

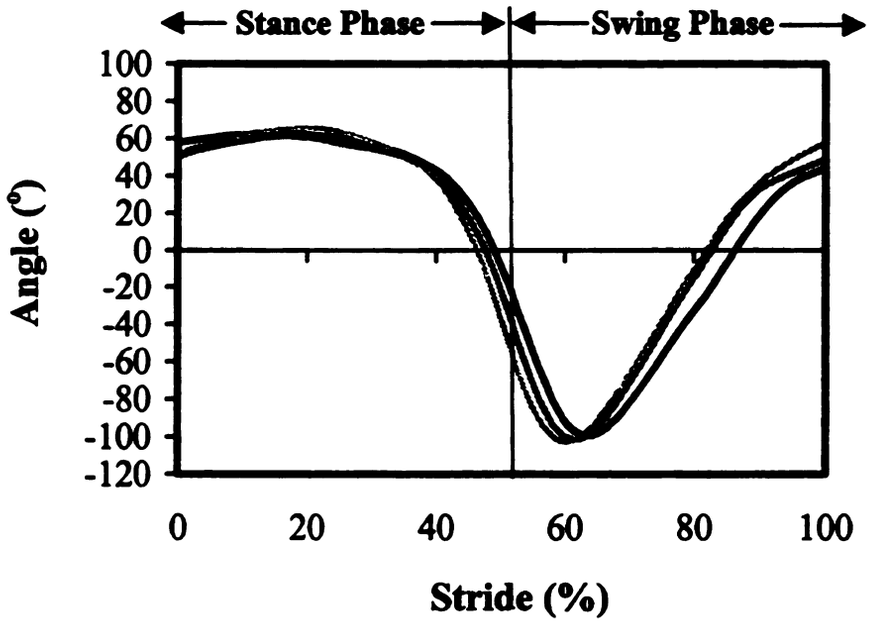

Figure A.15. Pastern segmental flexion (-)/ extension (+) angles (°) measured for Peruvian walking trial 1 (black line), 2 (dark gray line), and 3 (light gray line).

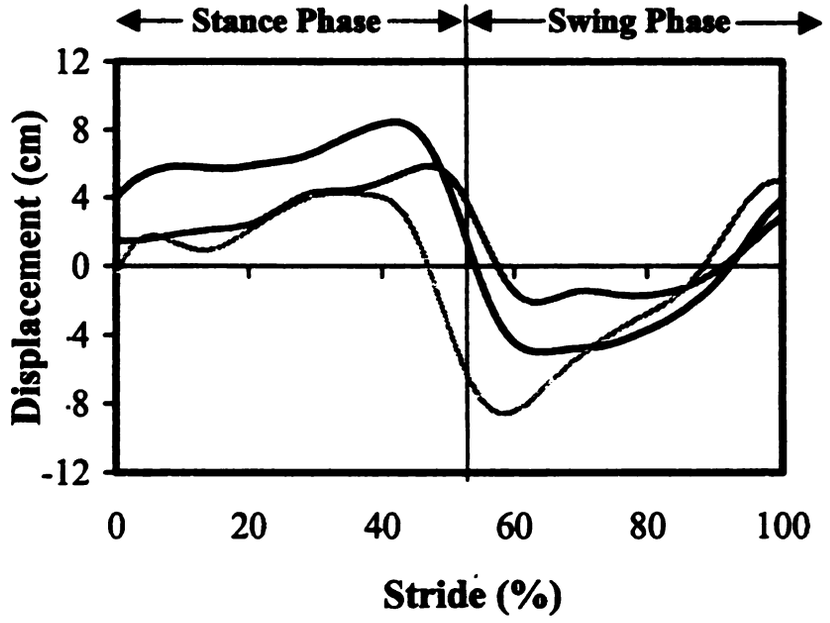

Figure A.16. Differences (cm) between the z-coordinates of the proximal and distal markers of the radius segment during Peruvian walking trial 1 (black line), 2 (dark gray line), and 3 (light gray line).

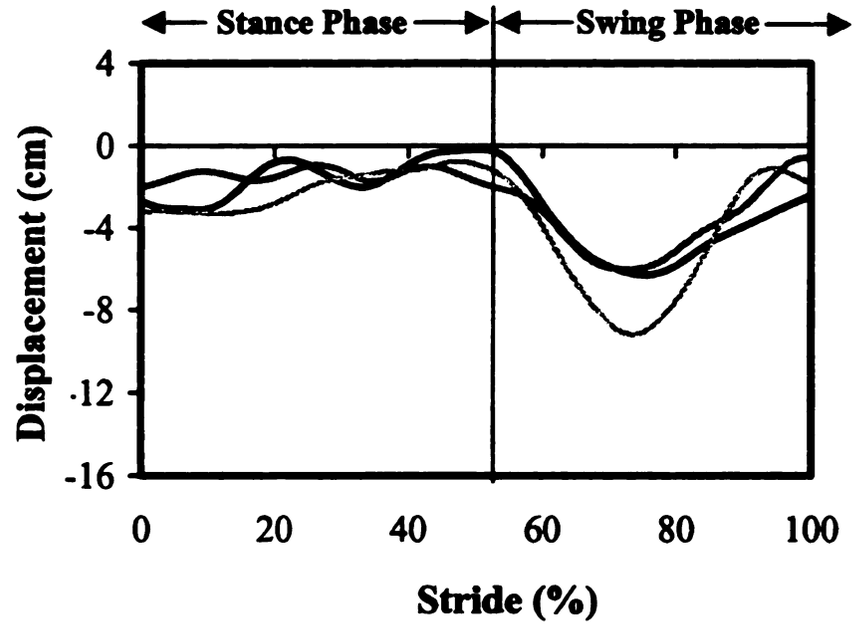

Figure A.17. Differences (cm) between the z-coordinates of the proximal and distal markers of the metacarpal segment during Peruvian walking trial 1 (black line), 2 (dark gray line), and 3 (light gray line).

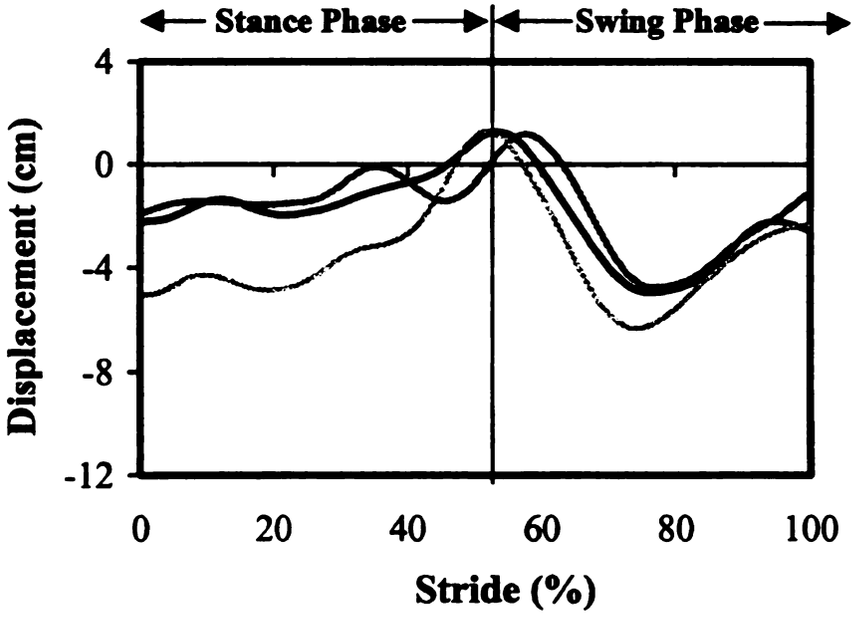

Figure A.18. Differences (cm) between the z-coordinates of the proximal and distal markers of the pastern segment during Peruvian walking trial 1 (black line), 2 (dark gray line), and 3 (light gray line).

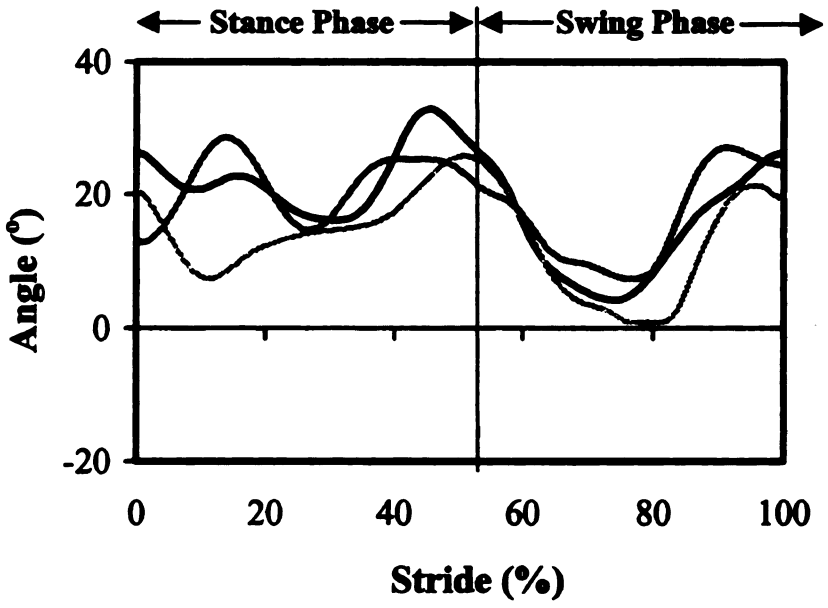

Figure A.19. Angles (°) measured between the JCS carpal flexion/extension axes and the GCS z-axis for Peruvian walking trial 1 (black line), 2 (dark gray line), and 3 (light gray line).

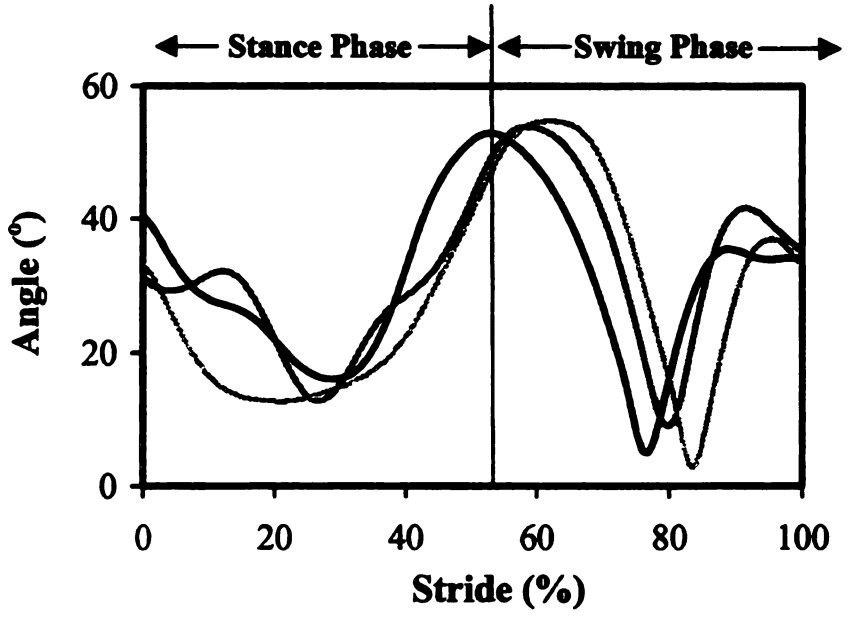

Figure A.20. Angles (°) measured between the JCS carpal adduction/abduction axes and the GCS x-axis for Peruvian walking trial 1 (black line), 2 (dark gray line), and 3 (light gray line).

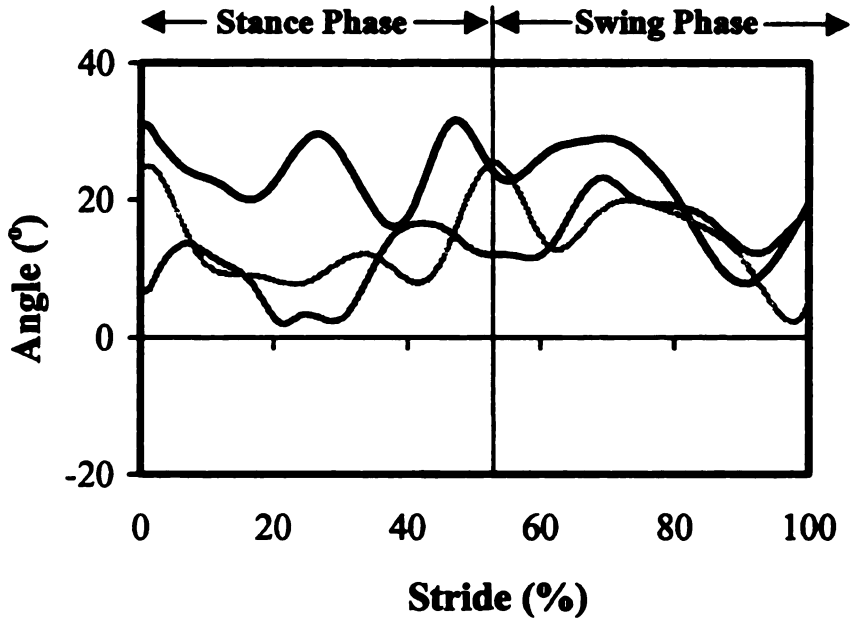

Figure A.21. Angles (°) measured between the JCS fetlock flexion/extension axes and the GCS z-axis for Peruvian walking trial 1 (black line), 2 (dark gray line), and 3 (light gray line).

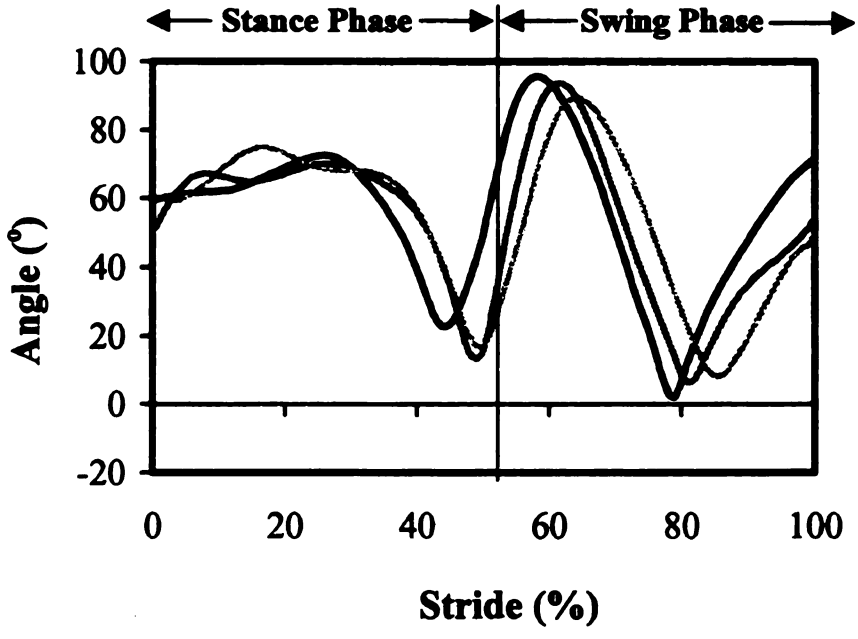

Figure A.22. Angles (°) measured between the JCS fetlock adduction/abduction axis and the GCS x-axis for Peruvian walking trial 1 (black line), 2 (dark gray line), and 3 (light gray line).

APPENDIX B: EXPERIMENT II (DERIVATION)

Adduction/Abduction Error Derivation Steps. The following illustrates and describes the derivation of the 3-D surface graph (Figure 4.16). The illustration shows the angle and orientation of two lines viewed from the side, the front, and the top before (solid line) and after (dotted line) a rotation of the top line. The angle of flexion (Θ_f) is determined from the side view by subtracting the known flexion angle between the two lines from 180°. Since the rotation is given, the rotation angle (Θ_r) is known for the top view. The angle of adduction/abduction error (Θ_e) due to the rotation is calculated in the following steps:

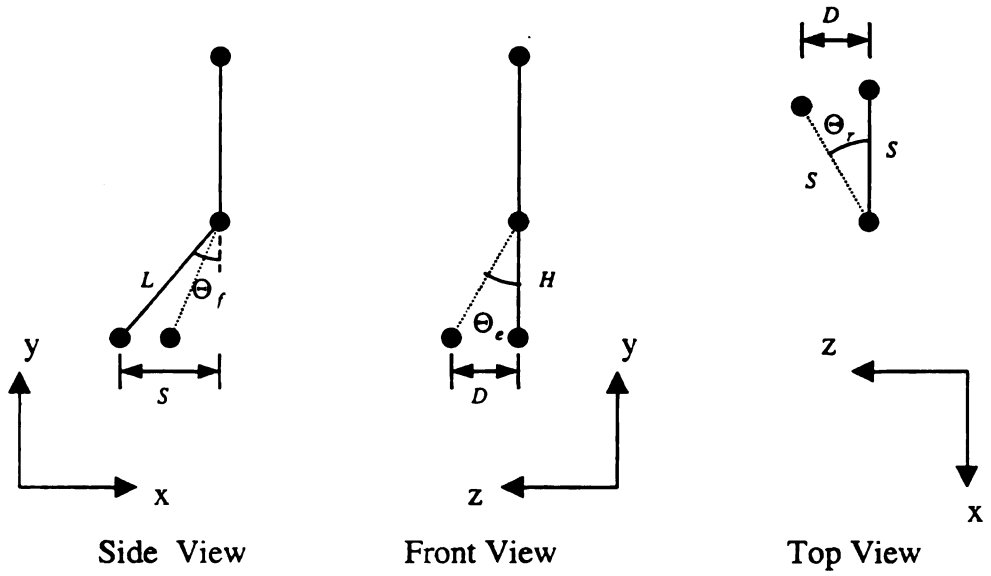

Side View Front View Top View

The length (L) of the lower line in the sagittal view is known, which is used with Θ_f to determine the distance (S) from the location of the lower line before the rotation to a line perpendicular to the ground before the rotation.

$$S = \sin\Theta_f L \tag{1}$$

This distance (S) represents the length of the lower line before and after rotation in the top view. Using the determined S value and the known rotation in the top view, the distance the line rotates (D) is calculated.

$$D = \sin\Theta_r S \tag{2}$$

When S from equation 1 is substituted into equation 2, D becomes a function of Θ_f and Θ_r.

$$D = \sin\Theta_r \sin\Theta_f L \tag{3}$$

The height (H) of the line in the front view is determined from Θ_f and the length of lower line as measured from the side view.

$$H = \cos\Theta_f L \tag{4}$$

From the determined distance (D) and the height (H), the angle of error is determined. Therefore, the angle of error is a function of the flexion and rotation angles as shown on Figure 4.15.

$$\tan\Theta_e = \frac{D}{H} \tag{5}$$

$$\tan\Theta_e = \frac{\sin\Theta_r \sin\Theta_f L}{\cos\Theta_f L} \tag{6}$$

$$\tan\Theta_e = \sin\Theta_r \tan\Theta_f \tag{7}$$

APPENDIX C: EXPERIMENT III

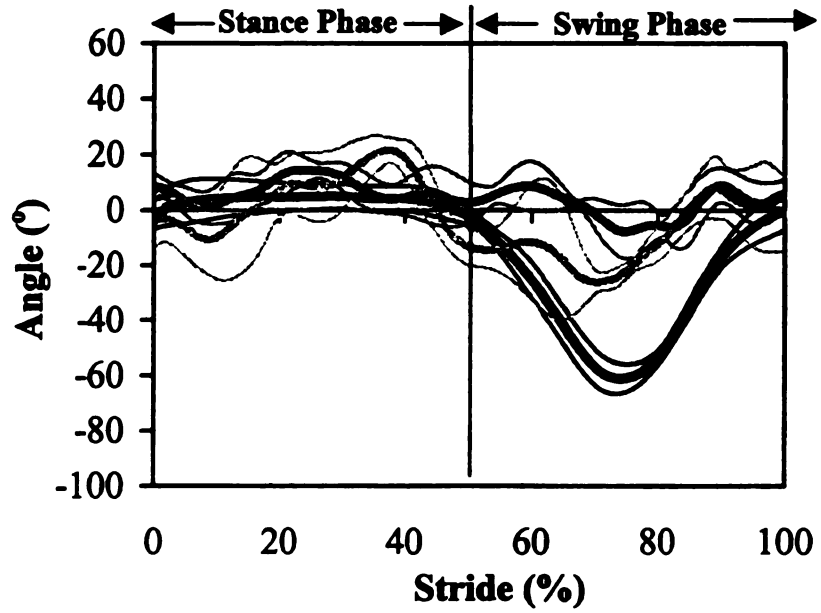

Figure C.1. Fox Trotter #1 carpal mean (thick line) and SD +/- (thin line) flexion (-)/extension (+) (black line), adduction (-)/abduction (+) (dark gray line), internal (-)/external (+) rotation (light gray line) of the flat walk.

Figure C.2. Fox Trotter #1 fetlock mean (thick line) and SD +/- (thin line) flexion (-)/extension (+) (black line), adduction (-)/abduction (+) (dark gray line), internal (-)/external (+) rotation (light gray line) of the flat walk.

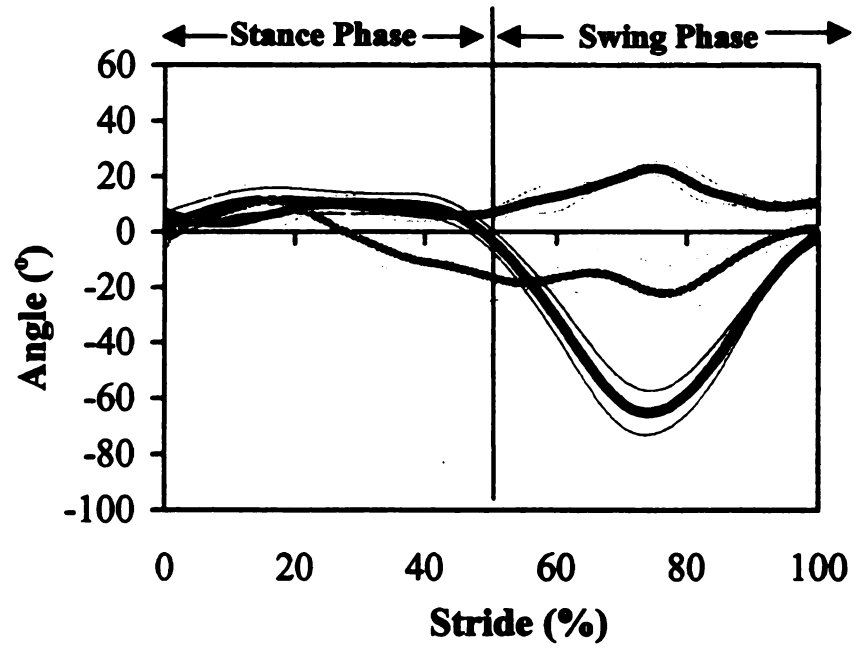

Figure C.3. Fox Trotter #1 carpal mean (thick line) and SD +/- (thin line) flexion (-)/extension (+) (black line), adduction (-)/abduction (+) (dark gray line), internal (-)/external (+) rotation (light gray line) of the fox trot.

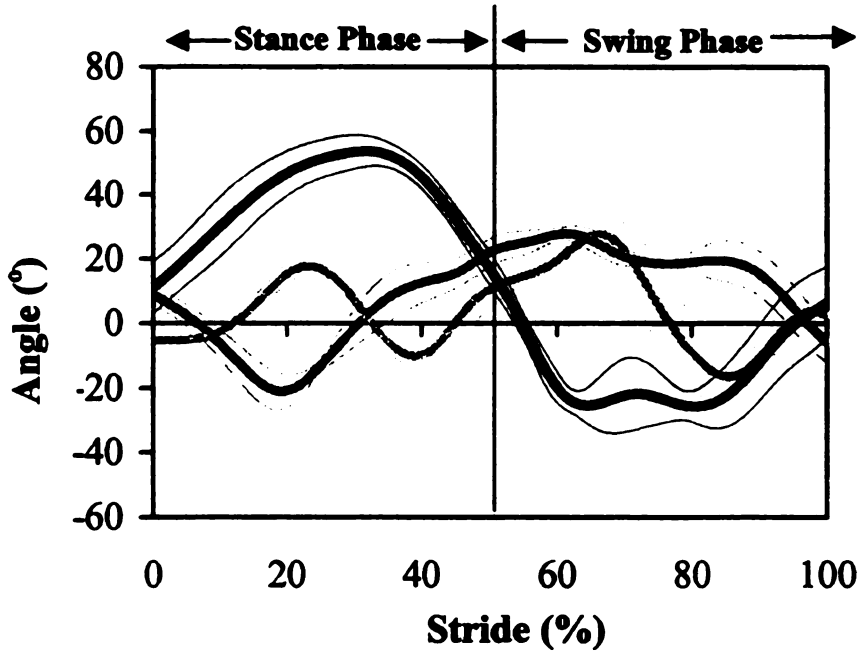

Figure C.4. Fox Trotter #1 fetlock mean (thick line) and SD +/- (thin line) flexion (-)/extension (+) (black line), adduction (-)/abduction (+) (dark gray line), internal (-)/external (+) rotation (light gray line) of the fox trot.

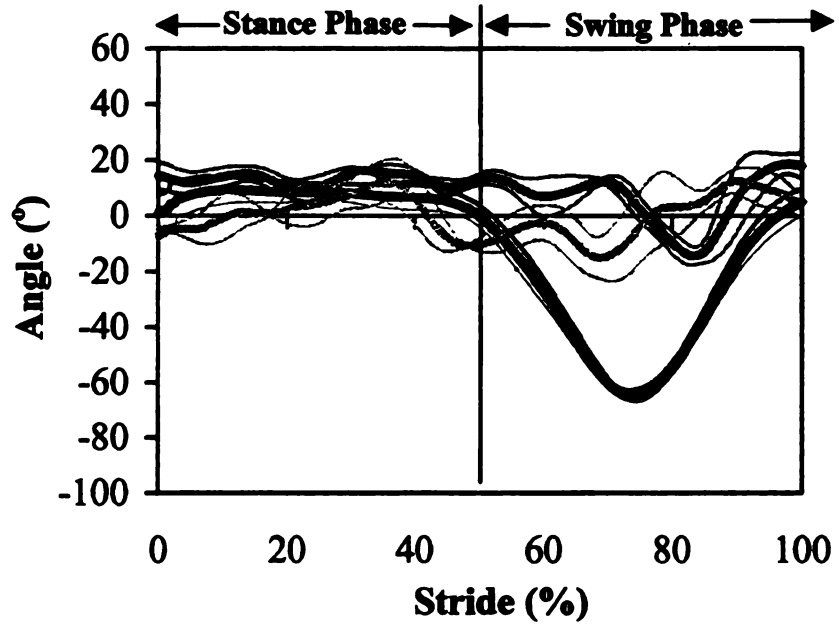

Figure C.5. Fox Trotter #2 carpal mean (thick line) and SD +/- (thin line) flexion (-)/extension (+) (black line), adduction (-)/abduction (+) (dark gray line), internal (-)/external (+) rotation (light gray line) of the flat walk.

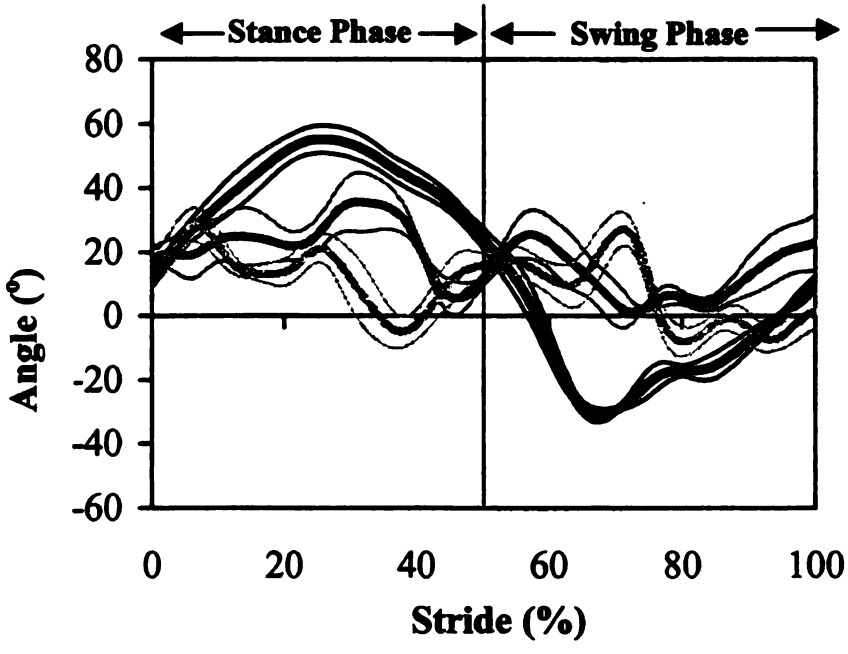

Figure C.6. Fox Trotter #2 fetlock mean (thick line) and SD +/- (thin line) flexion (-)/extension (+) (black line), adduction (-)/abduction (+) (dark gray line), internal (-)/external (+) rotation (light gray line) of the flat walk.

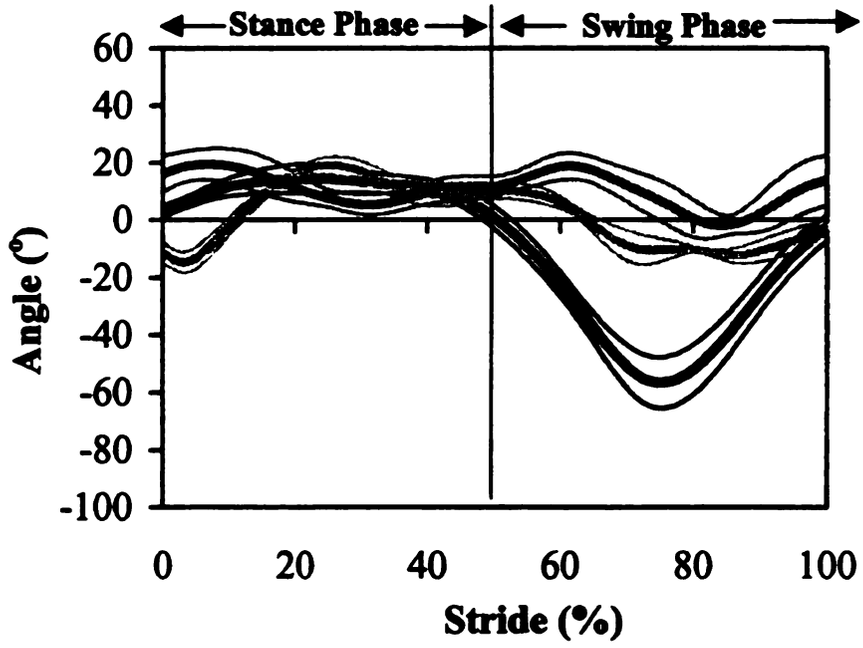

Figure C.7. Fox Trotter #2 carpal mean (thick line) and SD +/- (thin line) flexion (-)/extension (+) (black line), adduction (-)/abduction (+) (dark gray line), internal (-)/external (+) rotation (light gray line) of the fox trot.

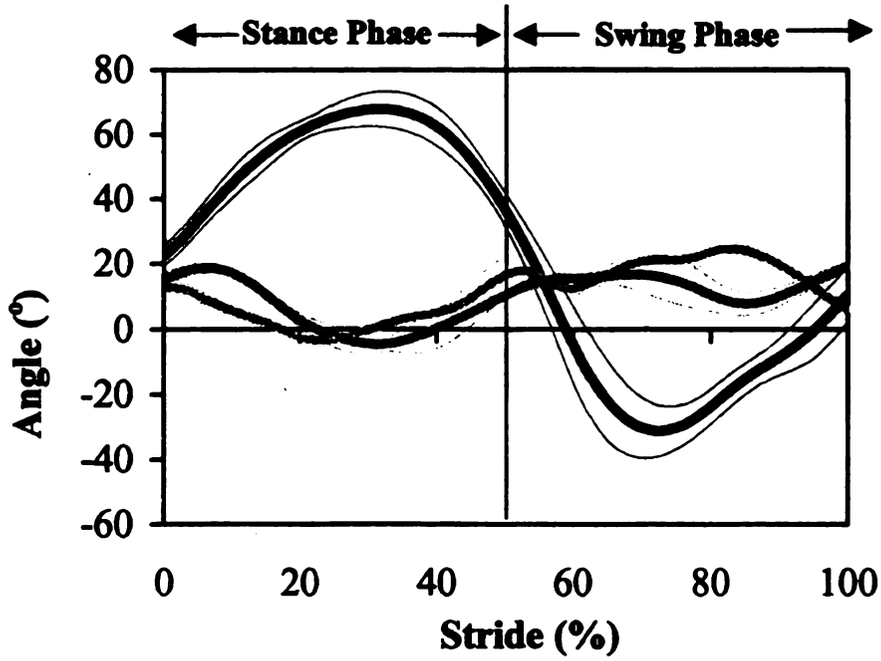

Figure C.8. Fox Trotter #2 fetlock mean (thick line) and SD +/- (thin line) flexion (-)/extension (+) (black line), adduction (-)/abduction (+) (dark gray line), internal (-)/external (+) rotation (light gray line) of the fox trot.

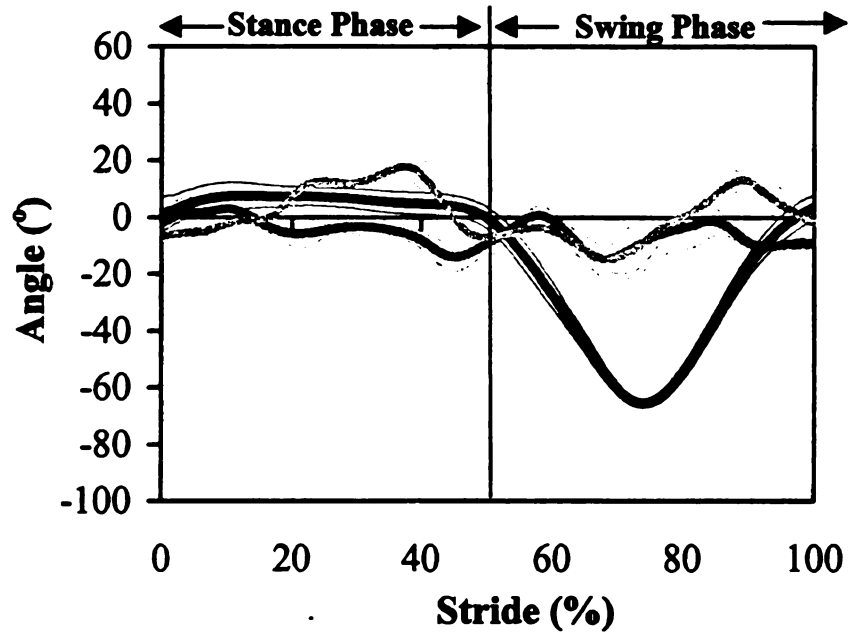

Figure C.9. Fox Trotter #3 carpal mean (thick line) and SD +/- (thin line) flexion (-)/extension (+) (black line), adduction (-)/abduction (+) (dark gray line), internal (-)/external (+) rotation (light gray line) of the flat walk.

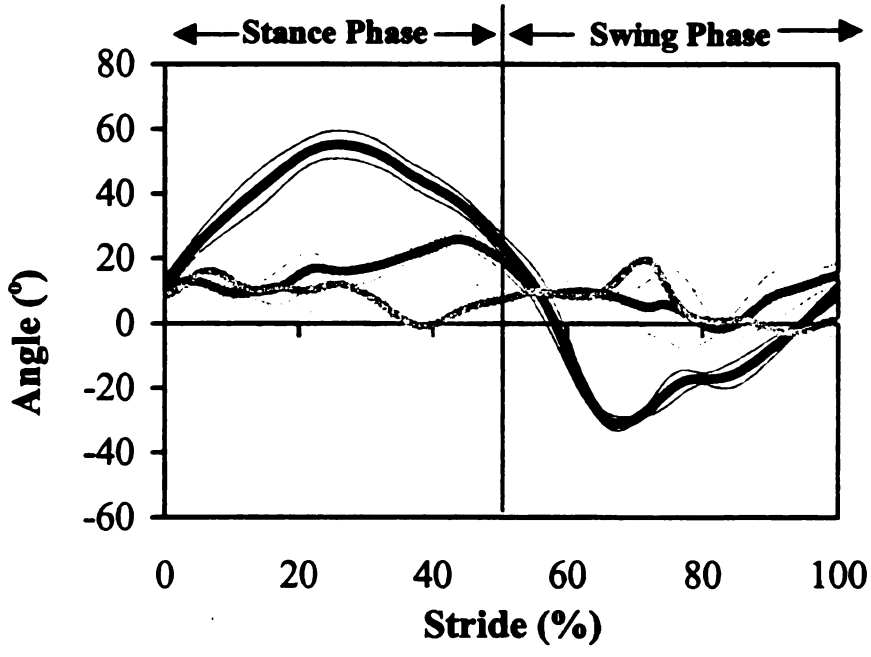

Figure C.10. Fox Trotter #3 fetlock mean (thick line) and SD +/- (thin line) flexion (-)/extension (+) (black line), adduction (-)/abduction (+) (dark gray line), internal (-)/external (+) rotation (light gray line) of the flat walk.

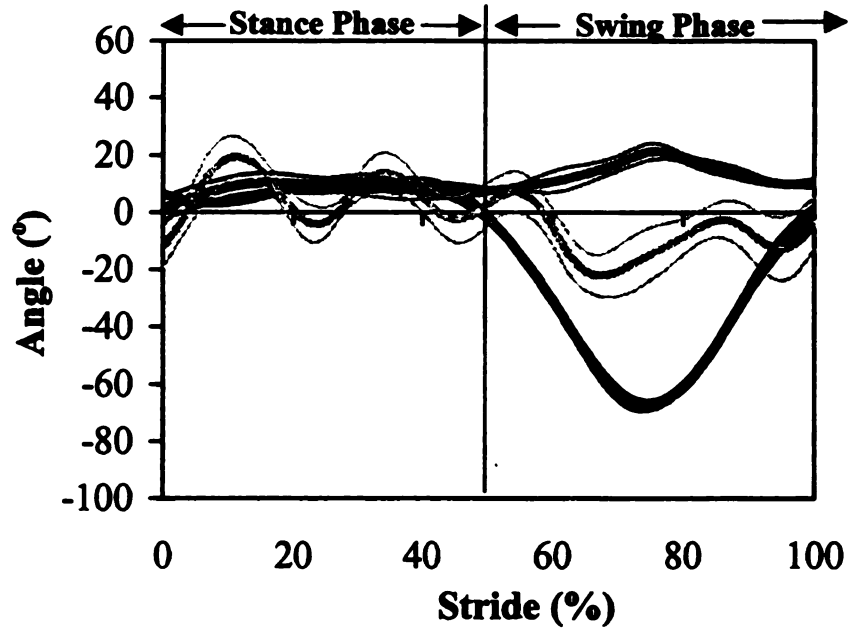

Figure C.11. Fox Trotter #3 carpal mean (thick line) and SD +/- (thin line) flexion (-)/extension (+) (black line), adduction (-)/abduction (+) (dark gray line), internal (-)/external (+) rotation (light gray line) of the fox trot.

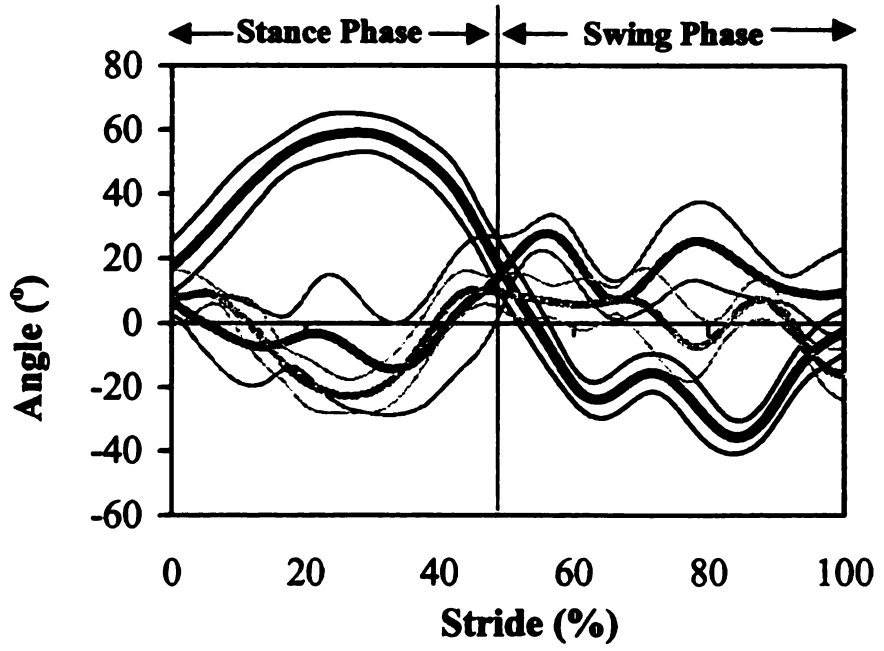

Figure C.12. Fox Trotter #3 fetlock mean (thick line) and SD +/- (thin line) flexion (-)/extension (+) (black line), adduction (-)/abduction (+) (dark gray line), internal (-)/external (+) rotation (light gray line) of the fox trot.

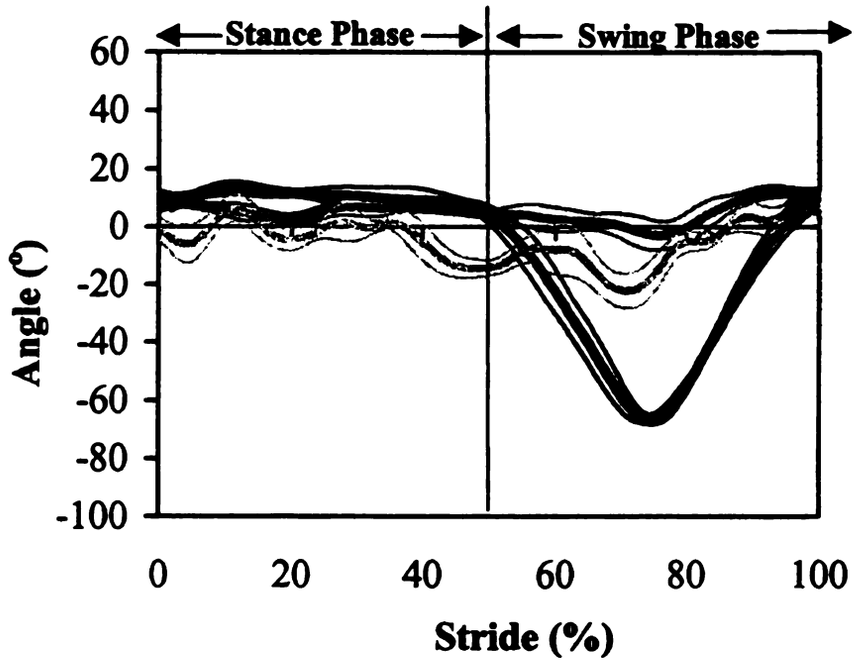

Figure C.13. Fox Trotter #4 carpal mean (thick line) and SD +/- (thin line) flexion (-)/extension (+) (black line), adduction (-)/abduction (+) (dark gray line), internal (-)/external (+) rotation (light gray line) of the flat walk.

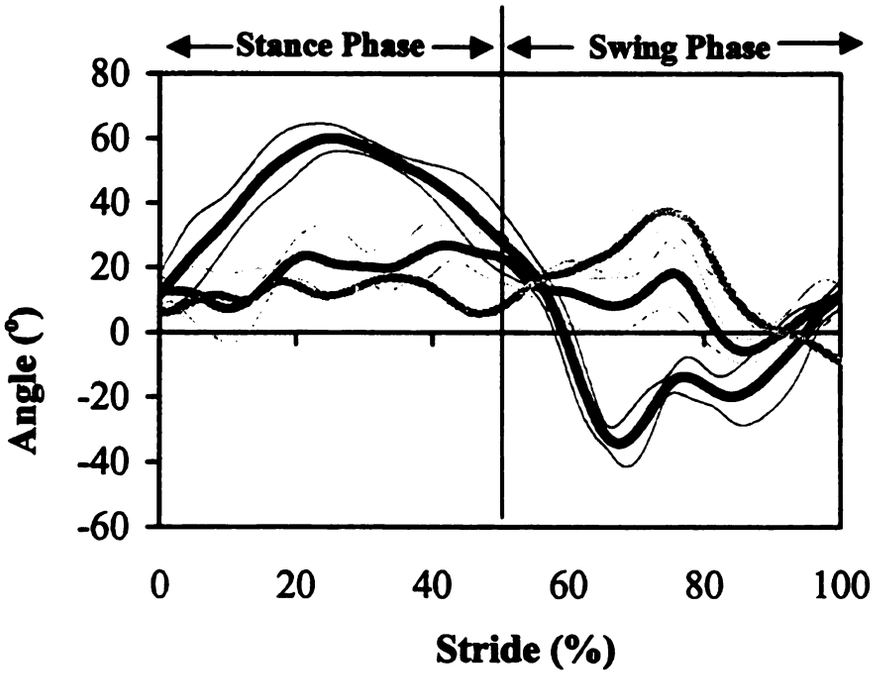

Figure C.14. Fox Trotter #4 fetlock mean (thick line) and SD +/- (thin line) flexion (-)/extension (+) (black line), adduction (-)/abduction (+) (dark gray line), internal (-)/external (+) rotation (light gray line) of the flat walk.

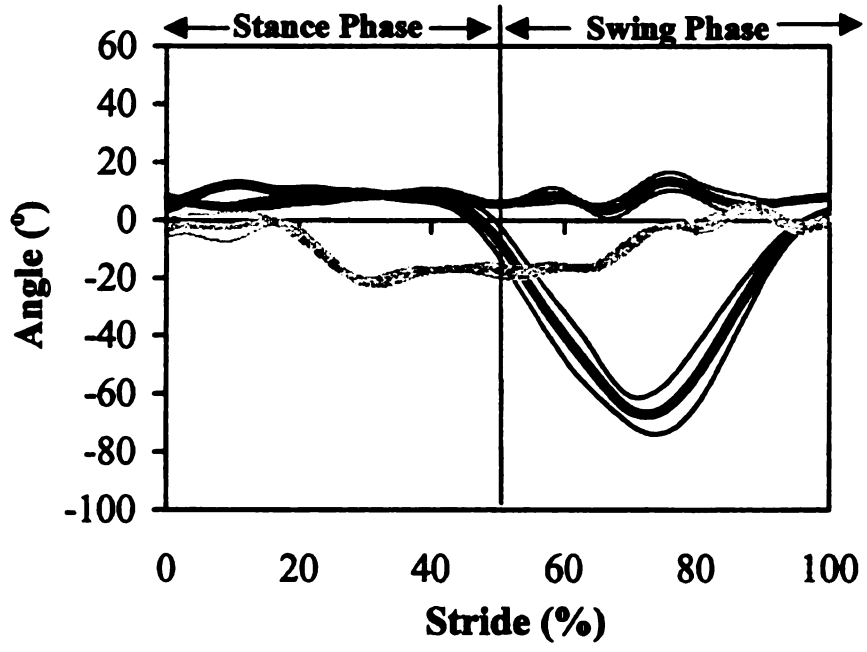

Figure C.15. Fox Trotter #4 carpal mean (thick line) and SD +/- (thin line) flexion (-)/extension (+) (black line), adduction (-)/abduction (+) (dark gray line), internal (-)/external (+) rotation (light gray line) of the fox trot.

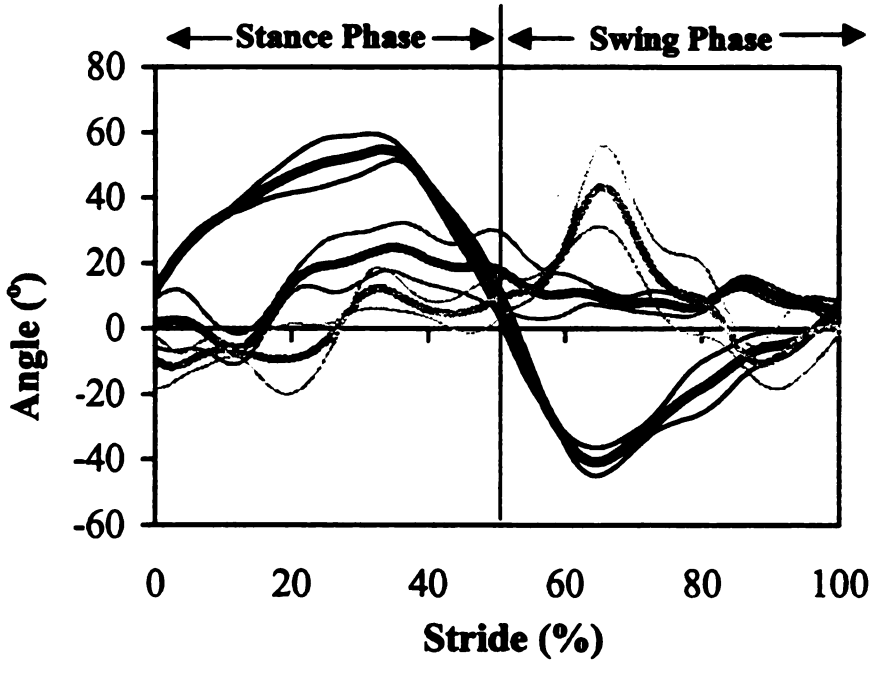

Figure C.16. Fox Trotter #4 fetlock mean (thick line) and SD +/- (thin line) flexion (-)/extension (+) (black line), adduction (-)/abduction (+) (dark gray line), internal (-)/external (+) rotation (light gray line) of the fox trot.

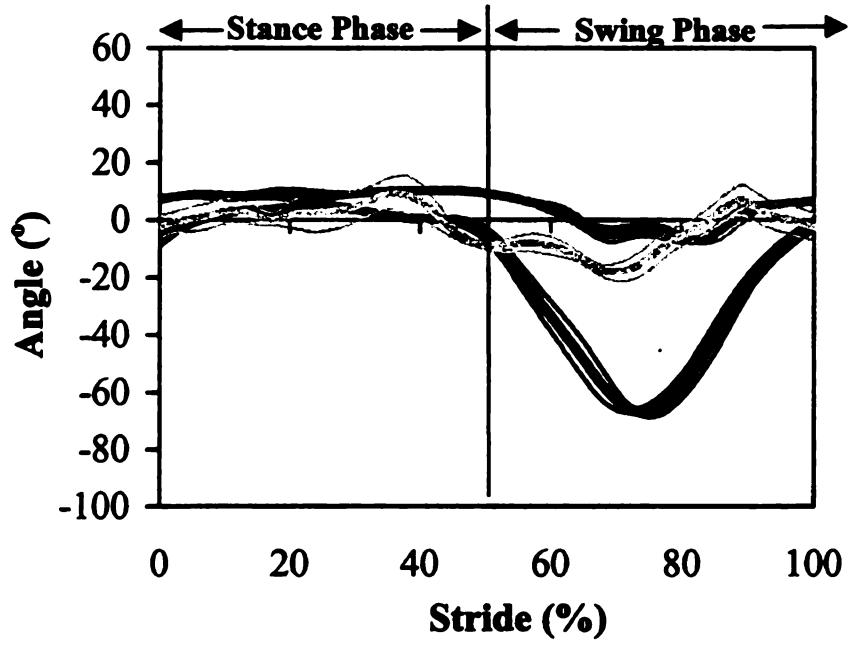

Figure C.17. Fox Trotter #5 carpal mean (thick line) and SD +/- (thin line) flexion (-)/extension (+) (black line), adduction (-)/abduction (+) (dark gray line), internal (-)/external (+) rotation (light gray line) of the flat walk.

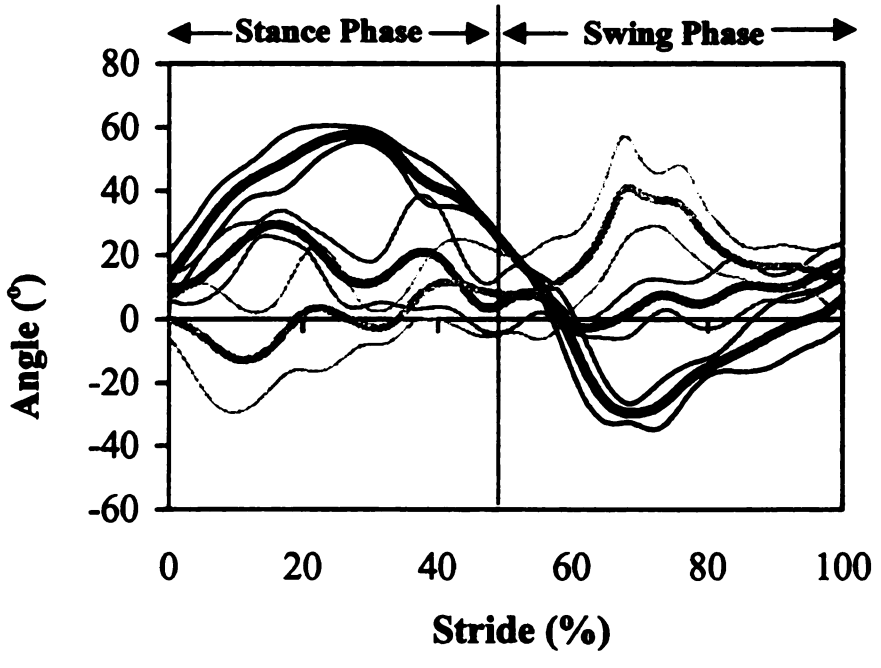

Figure C.18. Fox Trotter #5 fetlock mean (thick line) and SD +/- (thin line) flexion (-)/extension (+) (black line), adduction (-)/abduction (+) (dark gray line), internal (-)/external (+) rotation (light gray line) of the flat walk.

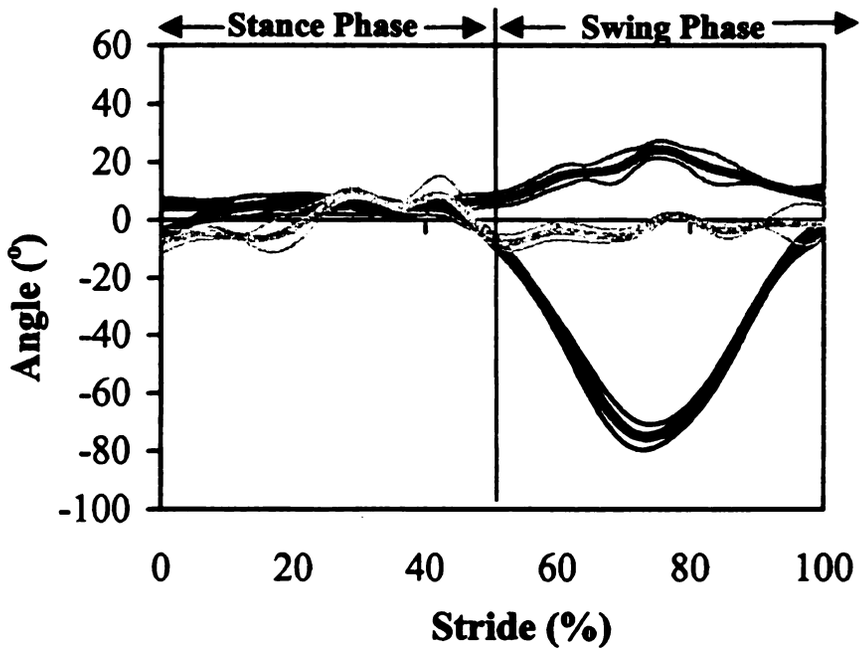

Figure C.19. Fox Trotter #5 carpal mean (thick line) and SD +/- (thin line) flexion (-)/extension (+) (black line), adduction (-)/abduction (+) (dark gray line), internal (-)/external (+) rotation (light gray line) of the fox trot.

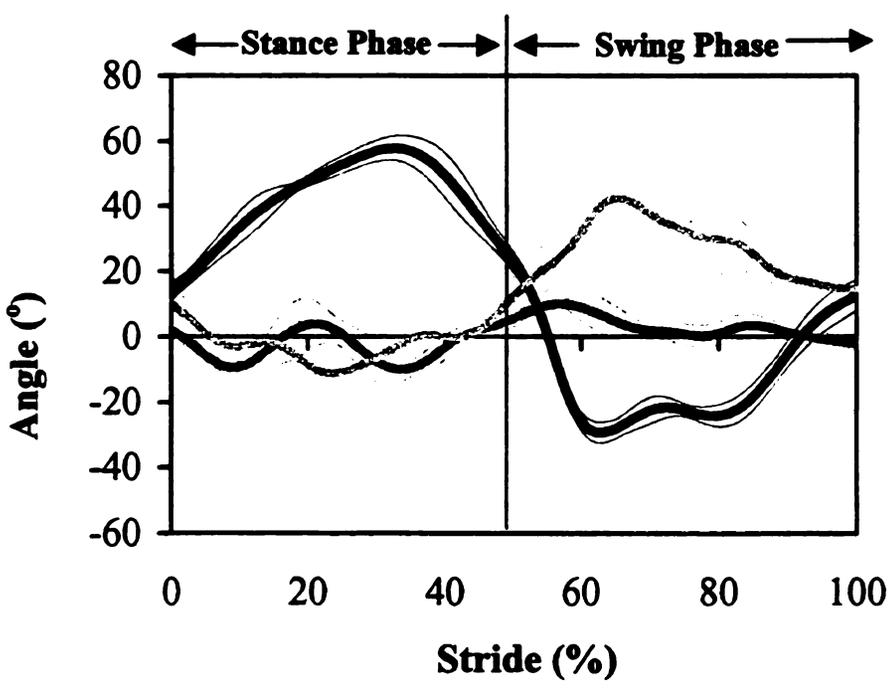

Figure C.20. Fox Trotter #5 fetlock mean (thick line) and SD +/- (thin line) flexion (-)/extension (+) (black line), adduction (-)/abduction (+) (dark gray line), internal (-)/external (+) rotation (light gray line) of the fox trot.

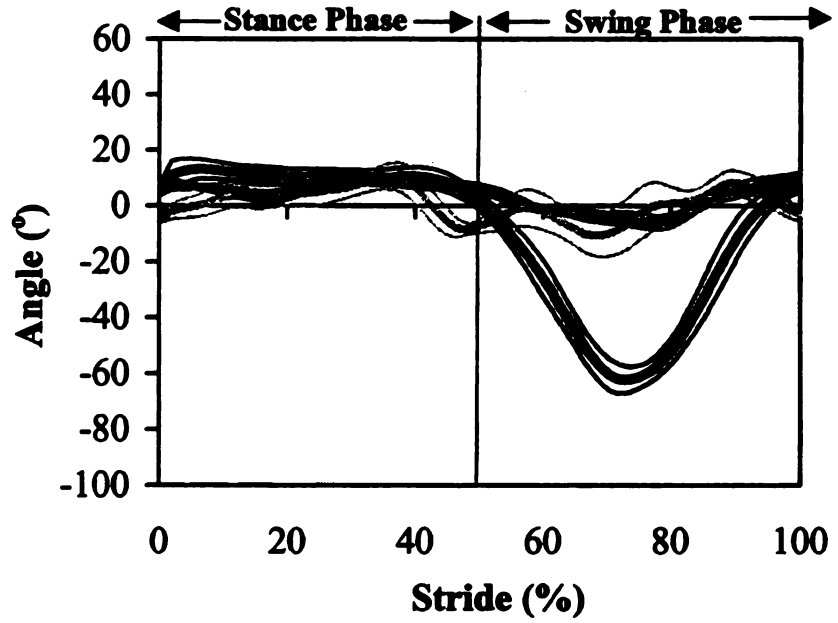

Figure C.21. Fox Trotter #6 carpal mean (thick line) and SD +/- (thin line) flexion (-)/extension (+) (black line), adduction (-)/abduction (+) (dark gray line), internal (-)/external (+) rotation (light gray line) of the flat walk.

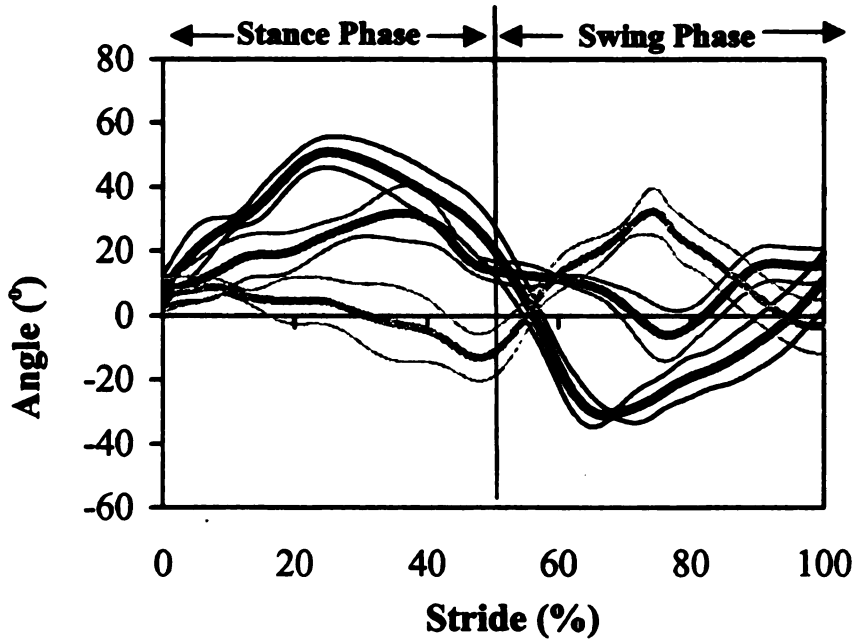

Figure C.22. Fox Trotter #6 fetlock mean (thick line) and SD +/- (thin line) flexion (-)/extension (+) (black line), adduction (-)/abduction (+) (dark gray line), internal (-)/external (+) rotation (light gray line) of the flat walk.

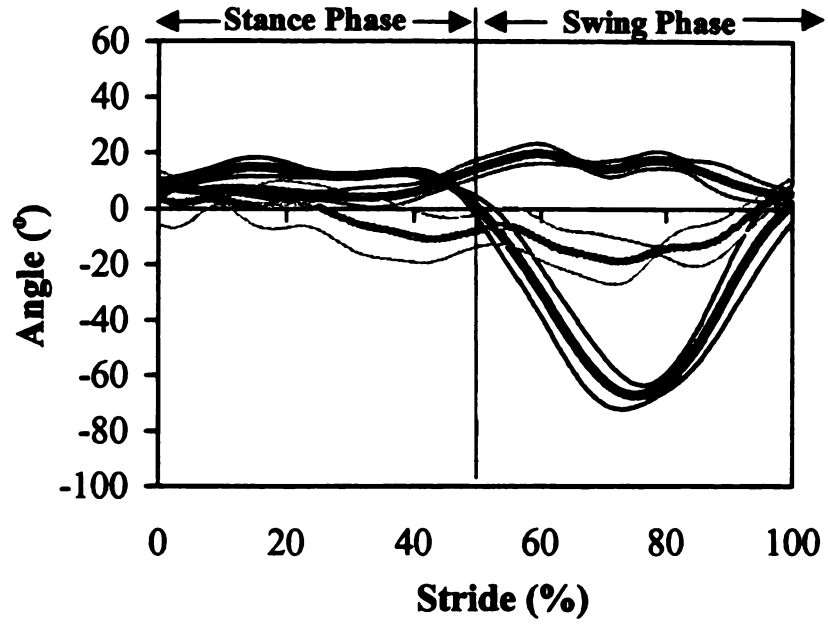

Figure C.23. Fox Trotter #6 carpal mean (thick line) and SD +/- (thin line) flexion (-)/extension (+) (black line), adduction (-)/abduction (+) (dark gray line), internal (-)/external (+) rotation (light gray line) of the fox trot.

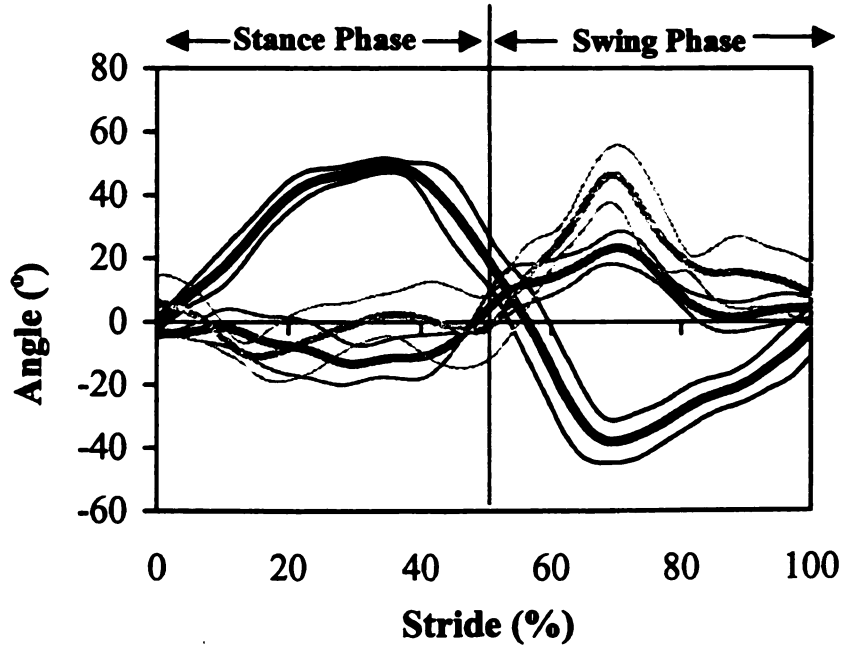

Figure C.24. Fox Trotter #6 fetlock mean (thick line) and SD +/- (thin line) flexion (-)/extension (+) (black line), adduction (-)/abduction (+) (dark gray line), internal (-)/external (+) rotation (light gray line) of the fox trot.

REFERENCES

REFERENCES

Abdel-Aziz, Y. I. and Karara, H.M. (1971) Direct linear transformation from comparator coordinates into object space coordinates into object space coordinates in close-range photogrammetry. *ASP Symposium on Close Range Photogrammetry.* American Society of Photogrammetry, Falls Church.

Adams, O.R. (1975) *Lameness in Horses*, 3rd edn. Lea & Febiger, Philadelphia. pp 331-359, 482.

Back, W., Barneveld, A., Bruin, G., Schamhardt, H.C. and Hartman, W. (1994) Kinematic detection of superior gait quality in young trotting Warmbloods. *Vet. Quart.* 16, S91-96.

Back, W., Hartman, W., Schamhardt, H.C., Bruin, G. and Barneveld, A. (1995) Kinematic response to a 70-day training period in trotting Dutch Warmbloods. *Equine vet J.* Suppl. 18, 127-131.

Back, W., Gerritsen, J., Ahne, I., Gouwerok, A., Ebell, P., Klarenbeck, A. and Koning, J.J.de. (2000) The effect of laterally wedged shoes on the sagittal and transversal plane kinematics of the shetland ponies. *Fourth International Workshop on Animal Locomotion.* 50.

Back, W., Schamhardt, H.C. and Barneveld. A. (1996) Are kinematics of the walk related to the locomotion of a warmblood horse at the trot? *Vet. Quart.* 18 Suppl 2, S71-S76.

Barrey, E., Galloux, P., Valette, J.P., Auvinet, B. and Wolter, R. (1993) Stride characteristics of overground versus treadmill locomotion in the saddle horse. *Acta Anatomica.* 146(2-3), 90-94.

Budiansky, S. (1997) *The Nature of Horses.* Simon & Schuster Macmillan Company, New York. pp 24-25.

Bush, B.M.H. and Clarac, F. (1985) *Coordination of motor behavior.* Cambridge, Cambridge University Press. pp 201-220, 221-227.

Cappozzo, A. (1991) Three-dimensional analysis of human walking: Experimental methods and associated artifacts. *Human Movement Sc.* 10, 589-602.

Cavagna, G.A. and Franzetti, P. (1981) Mechanics of competition walking. *J Physiol.* 315, 243-251.

Chao, E.Y., Laughman, R.K., Schneider, E. and Stauffer, R.N. (1983) Normative data of knee joint motion and ground reaction forces in adult level walking. *J. Biomech.* 16(3), 219-233.

Chateau, H., Degueurce, C., Pasqui-Boutard, V. and Denoix, J.M. (2000) 3D behaviour of the equine metacarpo-phalangeal joint. *Fourth International Workshop on Animal Locomotion*. 46.

Clayton, H.M. (1989) Gait analysis as a predictive tool in performance horses. *J. equine vet. Sci.* 9, 335-336.

Clayton, H.M. (1994) Comparison of the stride kinematics of the collected, working, medium and extended trot in horses. *Equine vet. J.* 26, 230-234.

Clayton, H.M. (1995) Comparison of the stride kinematics of the collected, medium and extended walks in horses. *Am. J. vet. Res.* 56, 849-852.

Clayton, H.M. (1998) The suspension is killing me! *Dressage & CT.* July, 14-16.

Clayton, H.M. and Bradbury, J.W. (1995) Temporal characteristics of the fox trot, a symmetrical equine gait. *Appl. Anim. Behavior Sc.* 42, 153-159.

Clayton, H.M., Hodson, E., Lanovaz, J.L. and Colborne, G.R. (2000a) The hind limb in walking horses: 2. Net joint moments and joint powers. *Equine vet. J.* (in press).

Clayton, H.M., Lanovaz, J.L., Schamhardt, H.C., Willemen, M.A. and Colborne, G.R. (1998) Net joint moments and powers in the equine forelimb during during the stance phase of the trot. *Equine vet. J.* 30, 384-389.

Clayton, H.M., Schamhardt, H.C., Lanovaz, J.L., Colborne, G.R. and Willemen, M.A. (2000b) Net joint moments and joint powers in horses with superficial digital flexor tendinitis. *Am. J. vet. Res.* 61, 191-196.

Clayton, H.M., Willemen, M.A., Lanovaz, J.L. and Schamhardt, H.C. (2000c) Effects of a heel wedge in horses with superficial digital flexor tendinitis. *Vet. Comp. Ortho. Traumatology.* 13, 1-8.

Colborne, G.R., Lanovaz, J.L., Sprigings, E.J., Schamhardt, H.C. and Clayton, H.M. (1997) Joint moments and power in equine gait: a preliminary study. *Equine vet. J.* Suppl. 23, 33-36.

Colborne, G.R., Lanovaz, J.L., Sprigings, E.J., Schamhardt, H.C. and Clayton, H.M. (1998) Forelimb joint movements and power during the walking stance phase of horses. *Am. J. vet. Res.* 59, 609-614.

Davids, J.R., Bagley, A. and Bryan, M. (1996) Kinematic and kinetic analysis of running in children with cerebral palsy. *Gait and Posture.* 4, 177.

Degueurce, C., Chateau, H., Pasqui-Boutard, V., Geiger, D. and Denoix, J.M. (2000) Kinematics of the proximal interphalangeal joint in the horse. *Fourth International Workshop on Animal Locomotion*. 43.

Deuel, N.R. and Lawerence, L.M. (1986) Effects of velocity on gallop limb contact variables. *J. equine vet. Sci.* 6, 143-146.

Drevemo, S., Dalin, D. and Fredricson, I. (1980) Equine locomotion: 1. The analysis of linear and temporal stride characteristics of trotting standardbreds. *Equine vet. J.* 12(2), 60-65.

Ensminger, M.E. (1977) *Horses and Horsemanship*, 5th edn. The Interstate Printers & Publishers, Inc., Danville, Illinois. pp 31-44, 363-364.

Fredricson, I. and Drevemo, S.(1971) A new method investigating equine locomotion. *Equine vet. J.* 3, 137-140.

Galisteo, A.M., Cano, M.R., Miro, F., Vivo, J., Morales, J.L. and Aguera, E. (1996) Angular joint parameters in the Andalusian horse at walk, obtained by normal videography. *J. equine vet. Sci.* 16, 73-77.

Gray, J. (1968) *Animal Locomotion*. Wiendenfeld & Nicholson, London.

Grood, E. S. and Suntay, W.J. (1983) A joint coordinate system for the clinical description of three-dimensional motions: Application to the knee. *J. Biomech.* 105, 136-144.

Harris, S.E. (1993) *Horse Gaits, The natural mechanics of balance and movement common to all breeds movement*. Simon & Schuster Macmillan Company, New York. pp 102-114.

Heleski, C. (1991) *The application of three-dimensional kinematic methodology to the equine knee and ankle joints*. Thesis. Michigan State University, East Lansing, MI.

Herring, L., Thompson, K.N. and Jarret, S. (1992) Defining normal three-dimensional kinematics of the lower forelimb in horses. *J. equine vet. Sc.* 12(3), 172-176.

Hershman, E.B. and Nicholas, J.A. (1995) *The Lower Extremity & Spine*, Vol. 1(2). Mosby, St. Louis, Missouri. pp 335-337.

Hildebrand, M. (1960) How animals run. *Sci. Am.* 202 (May), 148-157.

Hildebrand, M. (1965) Symmetrical gaits of horses. *Science*. 150, 701-708.

Hildebrand, M. (1978) The adaptive significance of tetrapod gait selection. *Annual Meeting of the American Society of Zoologists*. December, Richmond, VA. 255-267.

Hiraga, A., Yamanobe, A. and Kubo, K. (1994) Relationships between stride length, stride frequency, step length and velocity at the start dash in a racehorse. *J. equine vet. Sci.* 5(4), 127-130.

Hodson, E.F., Clayton, H.M. and Lanovaz, J.L. (1998) Temporal analysis of walk movements in the Grand Prix dressage test at the 1996 Olympic Games. *Appl. Anim. Beh. Sci.* 62, 89-97.

Hodson, E.F., Clayton, H.M. and Lanovaz, J.L. (2000) The forelimb in walking horses: 1. kinematics and ground reaction forces. *Equine vet. J.* 32(4), 287-294.

Holmstrom, M., Fredricson, I. and Drevemo, S. (1994) Biokinematic differences between riding horses judged as good and poor at the trot. *Equine vet J.* Suppl. 17, 51-56.

Hoyt, D.F. and Taylor, C.R. (1981) Gait and the energetics of locomotion in horses. *Nature.* 292, 239-240.

Imus, B. (1995) *Heavenly Gaits: The Complete Guide to Gaited Riding Horses.* CrossOver Publications, New York. pp 11-24.

Keegan, K.G., Wilson, D.A., Smith, B.K. and Wilson, D.J. (2000) Changes in kinematic variables seen with lameness induced by applying pressure to the frog and to the toe in adult horses trotting on a treadmill. *Fourth International Workshop on Animal Locomotion.* 66.

Khumsap, S., Clayton, H.M. and Lanovaz, J.L. (in press) Effect of walking velocity on ground reaction force variables in the hind limb of normal horses. *Amer. J. vet. Res.*

Khumsap, S., Clayton, H.M. and Lanovaz, J.L. (2000) Effect of walking velocity on hind limb kinetics during stance in normal horses. *Fourth International Workshop on Animal Locomotion.* 19.

Lanovaz, J.L., Clayton, H.M., Colborne, G.R., Schamhardt, H.C. (1999) Forelimb kinematics and net joint moments during the swing phase of the trot. *Equine vet. J.* Suppl. 30, 235-239.

Leach, D.H. (1990) Normal equine locomotion. *Proceedings for the Post Graduate Committee in Veterinary Science: Equine Lameness and Foot Conditions.* 25-35.

Leach, D.H. and Cymbaluk, N.F. (1986) Relationships between stride length, stride frequency, velocity, and morphometrics of foals. *Am. J. vet. Res.* 45, 888-892.

Mann, R.A. (1975) Biomechanics of the foot. In: *American Academy of Orthopedic Surgens: Atlas of Orthotics.* Mosby, St. Louis.

Mann, R.A. (1980) Running, jogging and walking: a comparative biomechanical study. In: Bateman, JE and Trot, A. (eds.): *The foot and ankle*. Theime-Stratton, New York.

Merkens, H.W., Schamhardt, H.C., Hartman, W. and Kersjes, A.W. (1985) Ground reaction force patterns of Dutch Warmblood horses at normal walk. *Equine vet. J.* 18, 207-214.

Merkins, H.W., Schamhardt, H.C., van Osch, G.J.V.M. and van den Bogert, A.J. (1993) Ground reaction force patterns of Dutch Warmblood horses at normal trot. *Equine vet. J.* 25, 134-137.

Muybridge, E. (1899) *Animal in motion*. Republished (1957) Ed: L.S. Brown. Dover Publications, Inc. New York.

Nicodemus, M.C., Lanovaz, J.L. and Clayton, H.M. (2000a) Forelimb kinematics and kinetics of the fox trot. *J. Anim. Sci.* Suppl. 1. 78, 150.

Nicodemus, M.C., Lanovaz, J.L. and Clayton, H.M. (2000b) Temporal stride variables of 4-beat square gaits. *Proceedings of the Association of Equine Sports Medicine Meetings: Equine Fitness- The Olympic Way*, 329, v.

Nicodemus, M.C., Lanovaz, J.L. and Clayton, H.M. (2000c) The effect of velocity on temporal variables of the equine walk. *Conference on Equine Sports Medicine and Science: The Elite Show Jumper*, 155.

Niki, Y, Ueda, Y, Yoshida, K and Masumitsu, H. (1982) A force plate study in equine biomechanics 2. The vertical and fore-aft components of floor reaction forces and motion of equine limbs at walk and trot. *Bull. Equine Res. Inst.* 19, 1-17.

Niki, Y, Ueda, Y, Yoshida, K and Masumitsu, H. (1984) A force plate study in equine biomechanics 3. The vertical and fore-aft components of floor reaction forces and motion of equine limbs at the canter. *Bull. Equine Res. Inst.* 21, 8-18.

Parelli, P. (2000) *In the Company of Horses*. A&E Television Documentary.

Pascoe, E. (1999) Great Gliders. *Horse & Rider*. September, 83-85.

Pasquini, C., Pasquini, S., Bahr, R. and Jann, H. (1995) *Guide to Equine Clinics: Lameness Diagnosis*, Vol. 3, Sudz Publishing, Pilot Point, Texas. pp 66-67, 142-143.

Peloso, J. G., J. A. Stick, R. W. Soutas-Little, J. P.Caron and C. E. DeCamp. (1991) Computer-assisted three-dimensional gait analysis of amphotericin-induced equine carpal lameness. *Vet. Surg.* 20(5), 344.

Pratt, G.W., Jr. (1983) Remarks on gait analysis. In: *Equine Exercise Physiology*. Snow, D.H., Persson, S.G.B. and Rose, R.J. (eds.) Granta Editions, Cambridge. 245-262.

Ridings, R.N. and Bradbury, J.W. (1976) The fox trotter, a public servant. *West. Horseman.* 41, 6.

Rooney, J.R. (1998) *The Lame Horse.* The Russell Meerdink Company, Ltd, Neenah, Wisconsin. pp 201-214.

Rubin, C.T. and Lanyon, L.E. (1982) Limb mechanics as a function of speed and gait: a study of functional strains on the radius and tibia of horse and dog. *J. Exp. Biol.* 101, 187-211.

Singleton, W.H., Lanovaz, J.L., Prades, M.L. and Clayton, H.M. (2000) Swing phase net joint moments and joint powers under different shoeing conditions. *Fourth International Workshop on Animal Locomotion.* 45.

Slade, L.M. (1993) Conformation and gait characteristics of Icelandic, Tennessee Walker and Walkony horses. *SIWAL/AESM Abstracts.* 2, 8.

Soutas-Little, R.W. (1996) The use of virtual markers in human movement analysis. *Gait and Posture.* 4, 176-177.

Soutas-Little, R. W., C. G. Beavis, M. C. Verstraete, and T. L. Markus. (1987) Analysis of foot motion during running using a joint coordinate system. *Med. Sci. Sports. Ex.* 19, 185-293.

Speirs, V.C. (1997) *Clinical Examination of Horses.* W.B. Saunders Company, Philadelphia. pp 102-103.

Taylor, C.R. (1985) What determines the cost of locomotion? A closer look at what muscles do. *Proc. 5th Annual Scientific Meeting of Assoc. for Equine Sports Medicine.* 15-30.

Weeren, P.R. van, Bogert, A.J. and Barneveld, A. (1998) Quantification of skin displacement near the carpal, tarsal and fetlock joints of the walking horse. *Equine vet. J.* 20(3), 203-208.

Weeren, P.R. van, Bogert, A.J. van den, Back, W., Bruin, G. and Barneveld, A. (1993) Kinematics of the standardbred trotter measured at 6, 7, 8 and 9 m/s on a treadmill before and after 5 months of pre-race training. *Acta Anatomica.* 146, 154-161.

Wickler, S.F. (2000) Personal communications. Sydney, Australia.

Wickler, S.F. and Hoyt, D.F. (2000) Preferred speed and the effect of weight. *Proceedings of the Association of Equine Sports Medicine Meetings: Equine Fitness- The Olympic Way*, 329, iii.

Wickler, S.F., Hoyt, D.F., Lewis, C.C., Cogger, E.A., Zarate, S., Bradley, Q. and McGuire, R. (1999) *Proc. 16th Equine Nutrition Physiol. Symp.* 24-25.

Wilson, B.D., Neal, R.J., Howard, A. and Groenendyk, S. (1988) The gait of pacers: I. Kinematics of the racing stride. *Equine vet. J.* 20, 347-351.

Winter, D.A. (1990) Kinetics: Forces and Moments of Force. In: *Biomechanics and Motor Control of Human Movement.* 2nd edn. John Wiley & Sons, New York. pp 75-102.

Winter, D.A. and Robertsons, D.G.E. (1978) Joint torque and energy patterns in normal gait. *Biol. Cybernetics.* 29, 137-147.

Woltring, H. J. (1994) 3-D attitude representation of human joints: A standardization proposal. *J. Biomech.* 27(12), 1399-1414.

Yanaghara, D., Udo, M., Kondo, I. and Yoshida, T.A. (1993) A new learning paradigm: adaptive changes in interlimb coordination during perturbed locomotion in decerebrate cats. *Neurosci. Res.* 18, 241-244.

Zatsiorky, V.M., Werner, M.S. and Kaimin, M.A. (1994) Basic kinematics of walking. *J Sports Med. Phys. Fitness.* 34(2), 109-134.

Ziegler, L. Gaits of the gaited horse. [Online] Available email: nicodem3@pilot.msu.edu from smithrider7@email.msn.com, July 26, 2000.

VITA

MOLLY CHRISTINE NICODEMUS

Department of Animal Science
Michigan State University

Birthplace: Webster, Texas
DOB: 5-29-74

HIGHLIGHTS OF PROFESSIONAL EXPERIENCE

Teaching Experience

- Three years college level teaching: Horsemanship, Dressage, Independent Study, Horse Selection and Judging, Advanced Horse Judging, Equine Exercise Physiology, and Horse Management

Intercollegiate Coaching

- Coached the MSU Intercollegiate Huntseat, Stockseat, and Dressage Teams
- Coached the MSU Horse Judging Team

Extension Experience

- Three years of adult extension presentations: MSU Adult Riding Clinic, Upper Peninsula Workshop, ANR Week, and Grand Rapids Expo
- Three years of youth extension presentations: 4-H Exploration Days, Horse Jamboree, Summer Riding Clinic, and Hoosier Horse Fair
- Extension publications: MSU Equine Extension Newsletter (Winter 1998, Spring 1999), Journal of Mo. Fox Trotter Assoc. (Mar 1998), and Equine Times (Aug 1999)

Employment History

- Mississippi State University-Department of Animal & Dairy Sciences 2000-
  Assistant Professor
- Michigan State University-Department of Animal Science 1997-2000
  Graduate Assistant
- Texas Twin Gates Farm 1995-1997
  Assistant Barn Manager/Horse Trainer
- Manes Tennessee Walking Horse Stables 1994-1995
  Assistant Horse Trainer
- Texas Lions Club Camp for Handicap Children 1993-1994
  Director of Therapeutic Riding Program

MOLLY CHRISTINE NICODEMUS

Academic Conferences: Presentations and Publications

- Agriculture and Natural Resources Research Week — March 1998
  East Lansing, Michigan
- Kentucky Equine Research Nutrition and Physiology Meetings — April 1998
  Lexington, Kentucky
- Phi Zeta Research Day: Conference on MSU Veterinary Medicine — October 1998
  East Lansing, Michigan
- Equine Nutrition and Physiology Symposium — June 1999
  Raleigh, North Carolina
- Association of Equine Sports Medicine Conference — February 2000
  Sydney, Australia
- Conference on Equine Sports Medicine and Science — May 2000
  Sicily, Italy
- International Workshop on Animal Locomotion — May 2000
  Vienna, Austria
- Annual Animal Science Meetings — July 2000
  Baltimore, Maryland

Education

Ph.D., Animal Science, Michigan State University, — Fall 2000
East Lansing, MI
Dissertation: Quantification of the Locomotion of Gaited Horses

M.S., Agricultural Sciences, Sam Houston State University, — Summer 1997
Huntsville, TX
Thesis: Stride Duration Response to Weight Training in Horses

B.S., Agricultural Communications, Southwest Missouri State University, — Summer 1995
Springfield, MO
Minor: Animal Science